NASA/CR-2008-215307

Development and Evaluation of Sensor Concepts for Ageless Aerospace Vehicles

Report 3 - Design of the Concept Demonstrator

David Abbott, Jon Ables, Adam Batten, David Carpenter, Tony Collings, Briony Doyle, John Dunlop, Graeme Edwards, Tony Farmer, Bruce Gaffney, Mark Hedley, Peter Isaacs, Mark Johnson, Bhautik Joshi, Chris Lewis, Geoff Poulton, Don Price, Mikhail Prokopenko, Torsten Reda, David Rees, Andrew Scott, Sarath Seneviratne, Philip Valencia, Peter Wang, Denis Whitnall, and John Winter
CSIRO Telecommunications & Industrial Physics, Lindfield, New South Wales, Australia

May 2008

The NASA STI Program Office . . . in Profile

Since its founding, NASA has been dedicated to the advancement of aeronautics and space science. The NASA Scientific and Technical Information (STI) Program Office plays a key part in helping NASA maintain this important role.

The NASA STI Program Office is operated by Langley Research Center, the lead center for NASA's scientific and technical information. The NASA STI Program Office provides access to the NASA STI Database, the largest collection of aeronautical and space science STI in the world. The Program Office is also NASA's institutional mechanism for disseminating the results of its research and development activities. These results are published by NASA in the NASA STI Report Series, which includes the following report types:

- TECHNICAL PUBLICATION. Reports of completed research or a major significant phase of research that present the results of NASA programs and include extensive data or theoretical analysis. Includes compilations of significant scientific and technical data and information deemed to be of continuing reference value. NASA counterpart of peer-reviewed formal professional papers, but having less stringent limitations on manuscript length and extent of graphic presentations.

- TECHNICAL MEMORANDUM. Scientific and technical findings that are preliminary or of specialized interest, e.g., quick release reports, working papers, and bibliographies that contain minimal annotation. Does not contain extensive analysis.

- CONTRACTOR REPORT. Scientific and technical findings by NASA-sponsored contractors and grantees.

- CONFERENCE PUBLICATION. Collected papers from scientific and technical conferences, symposia, seminars, or other meetings sponsored or co-sponsored by NASA.

- SPECIAL PUBLICATION. Scientific, technical, or historical information from NASA programs, projects, and missions, often concerned with subjects having substantial public interest.

- TECHNICAL TRANSLATION. English-language translations of foreign scientific and technical material pertinent to NASA's mission.

Specialized services that complement the STI Program Office's diverse offerings include creating custom thesauri, building customized databases, organizing and publishing research results ... even providing videos.

For more information about the NASA STI Program Office, see the following:

- Access the NASA STI Program Home Page at ***http://www.sti.nasa.gov***

- E-mail your question via the Internet to help@sti.nasa.gov

- Fax your question to the NASA STI Help Desk at (301) 621-0134

- Phone the NASA STI Help Desk at (301) 621-0390

- Write to:
  NASA STI Help Desk
  NASA Center for AeroSpace Information
  7115 Standard Drive
  Hanover, MD 21076-1320

NASA/CR-2008-215307

Development and Evaluation of Sensor Concepts for Ageless Aerospace Vehicles

Report 3 - Design of the Concept Demonstrator

David Abbott, Jon Ables, Adam Batten, David Carpenter, Tony Collings, Briony Doyle, John Dunlop, Graeme Edwards, Tony Farmer, Bruce Gaffney, Mark Hedley, Peter Isaacs, Mark Johnson, Bhautik Joshi, Chris Lewis, Geoff Poulton, Don Price, Mikhail Prokopenko, Torsten Reda, David Rees, Andrew Scott, Sarath Seneviratne, Philip Valencia, Peter Wang, Denis Whitnall, and John Winter
CSIRO Telecommunications & Industrial Physics, Lindfield, New South Wales, Australia

National Aeronautics and
Space Administration

Langley Research Center
Hampton, Virginia 23681-2199

Prepared for Langley Research Center
under Purchase Order L-71346D

May 2008

Available from:

NASA Center for AeroSpace Information (CASI)
7115 Standard Drive
Hanover, MD 21076-1320
(301) 621-0390

National Technical Information Service (NTIS)
5285 Port Royal Road
Springfield, VA 22161-2171
(703) 605-6000

Table of Contents

1. Introduction 5

2. Proposed General Structure of the Concept Demonstrator 9

3. Particle Impacts: Damage and Sensing 12
3.1 Damage induced by high-velocity particle impact 12
3.2 Detectable effects of impacts 14
3.3 Laboratory techniques for generating high-velocity particle impacts 16

4. Sensors and the Sensing Strategy 18
4.1 Introduction 18
4.2 Sensing requirements and strategies 18
4.3 Experimental results for piezoelectric sensors 21
4.4 Conclusions and future work 24

5. Electronics and Communications Protocols 25
5.1 Overall design and architecture of the electronic system 25
5.2 Data Acquisition Layer (DAL) 26
5.3 Network and Application Layer (NAL) 27
5.4 Current status 29

6. Computer Simulation of Self-Reconfigurable Sensor Networks in Ageless Aerospace Vehicles 31
6.1 Introduction 31
6.2 Methodology 31
6.3 Simulated cell structure and agent behaviour 32
6.4 Simulation of the AAV 33
6.5 Self-organizing impact boundaries: algorithms and simulation results 34
6.6 Self-organizing impact spanning trees: algorithms and simulation results 37
6.7 Future directions 40

7. The Concept Demonstrator Intelligent System 41

8. Summary and Conclusions 43

References 44

Appendix 1: Detailed Discussion of Sensors and Sensing 45
A1.1 Introduction 45
A1.2 Sensing requirements and strategies 45
A1.3 Experiments on sensors 51
A1.4 Further work 62
References 64

Appendix 2: Details of the Electronics and Communications Protocols 66
A2.1 Concept Demonstrator electronics requirements 66
A2.2 Overall design and architecture of the electronic system 68
A2.3 Data acquisition layer design 75
A2.4 Network and application layer 79
A2.5 Current status and ongoing plans 87
Reference 89

Appendix 3: Simulation of Self-Reconfigurable Sensor Networks in Ageless Aerospace Vehicles..... 90
A3.1 Introduction..... 90
A3.2 Methodology..... 91
A3.3 Localized algorithms for impact inspection..... 92
A3.4 Cell structure and agent architecture..... 93
A3.5 AAV Simulator..... 95
A3.6 Self-organizing impact boundaries: algorithms and simulation results..... 97
A3.7 Self-organizing impact spanning trees: algorithms and simulation results 103
A3.8 Future directions.....109
References 109

1. Introduction

Project aims

NASA's goal of ageless or robust aerospace vehicles (RAVs) requires the development of vehicles that are capable of structural self-assessment and repair. This project is concerned primarily with the self-assessment functions at this stage. These can be divided between those carried out by distributed sensors and intelligent processing and communication on the skin or within the structure, and those that could be more effectively provided by autonomous robotic NDE agents which could be deployed to monitor damage or integrity of the vehicle structure.

Critical to the success of the Ageless Vehicle program are the development of appropriate technologies for non-destructive evaluation of structures, and the development of strategies and technologies for processing NDE data, storage and communication of NDE information, and analysis of NDE data with capability for intelligent decision-making.

Previous work in this project developed and examined concepts for integrated smart sensing and communication systems that could form the distributed sensing function of a smart vehicle. This work was outlined in two earlier Reports (CTIP, 2001, CTIP, 2002). The second of these Reports (CTIP, 2002) contained a proposal for the development of a Concept Demonstrator: a combined hardware and software system capable of demonstrating principles of an intelligent vehicle health monitoring system. This Report presents design considerations for the first stage of development of this Concept Demonstrator (CD).

One of the main benefits of the CD will be to act as an experimental test-bed for results obtained from a computer simulator (CS) that is being developed in parallel with the CD. It is important to emphasize that the intention is not that the CS should simulate the operation of the CD, but rather that it be used to simulate and evaluate new concepts that may later be implemented in the CD. The CD is, of necessity, built from hardware that is currently available, and is therefore limited by the capabilities of current technology. The CS is also limited, in this case by current computing technology, but will nevertheless be capable of evaluating new strategies and concepts for intelligent communications, awareness and decision-making. In summary, the CS should lead the way in all areas that can be simulated in software, with implementation and experimental verification in the CD following when hardware technology makes this possible.

More specifically, the goals of the CD should include the evaluation of physical sensors, processing and communication strategies, and agent implementation. Computer simulation, being relatively fast and versatile, provides the opportunity to study systems with a wide variety of characteristics, from different environments, threats and sensors, to different tile configurations, communications topologies, different data processing algorithms and different characteristics of the organization and interactions of the intelligent agents. The availability of both a computer simulator and a compatible CD will provide a very powerful set of tools for studying an intelligent sensing system.

The general philosophy is to regard the development of the CD as a multi-year project, but with the development staged in such a way that significant milestones are achieved each year. Appropriate milestones will be decided, in consultation with NASA, on a year-by-year basis, depending on progress during the preceding year.

The ultimate goals for the demonstrator are to demonstrate an ability to form a concise representation (perception, awareness) of the state of the structure, to develop flexible strategies for repair of damage and mitigation of further damage, and to demonstrate an ability to learn from past experiences. The demonstrator should operate in a simple environment containing only a small number of different threats, but the frequency, severity and number of potentially damaging events may be large. The demonstrator should be as simple as possible, consistent with the stated goals. Initial objectives for it do not include development of new fabrication or miniaturization techniques, or new hardware developments.

Aims and limitations of the first stage of the Concept Demonstrator (CD)

This Report outlines what is expected to be achieved within the first 12-month stage of development of the CD and the CS. This includes the basic design of both the hardware and software systems, and initial implementation. These are both large engineering tasks, so it is necessary to limit the scope of the objectives to ensure they are achievable, while designing the structures to be sufficiently flexible that the capabilities of the systems can be readily up-graded and expanded in the future.

The purpose of the CD is to demonstrate concepts for an intelligent vehicle health monitoring system within a relatively simple environment. It was decided that, at least in the first instance, the only threats to the structure that would be considered would be from impacts by projectiles that, for a vehicle in space, might be micrometeoroids or space debris. A summary of threats associated with particle impacts, compiled from a number of sources, appears in Report 2 (in CTIP (2002), Section 5.3 and Appendix A5.1). *Thus, the aim of the initial design of the CD is only to enable the detection, location and evaluation of the effects of particle impacts.* It is expected that other threats and damage processes will be addressed in later stages of the project.

Other significant general points that influenced the initial design are as follows.

- The CD has an important function not only as a demonstration system, but also as an experimental test-bed for all aspects of the experimental hardware (including sensors, communications and processing hardware, structural materials, etc.) as well as the various concepts, strategies and algorithms used to develop intelligent responses to events and threats.

- The early stages of the development will concentrate on building a reliable, working hardware platform from current technology. There will be no attempt in the initial stage to develop new sensors or electronic hardware. It is expected that there will be novel features in the higher-level software systems that imbue the CD with a level of intelligence, but not in the hardware and lower-level software.

- The design should be highly modular to enable staged experiments and up-grades. In the initial stage, only one type of sensor and one type of skin material will be used, but subsequent stages of the development should allow for experimental trials of the following.
  - Different sensors, sensing strategies and multiple sensor types. Some possible impact sensors are listed in Appendix 1.
  - Alternative network topologies.
  - Different skin materials (e.g. composites, aluminium foam, multi-layered skins, glass or other transparent window material, …).
  - Various intelligent system strategies and algorithms.
  - Sensing and response to additional threats and damage mechanisms.

- Particle impacts can cause damage with a wide range of severities, from no damage to complete destruction of the vehicle. Damage evaluation can be a complicated task, and it will probably not be possible to carry it out in great detail during the first stage of the CD development. The aim of the initial design will therefore be to assign impact severity to the following broad categories.
  - *Light impact*. No damage (purely elastic impact) or light surface damage only.
  - *Moderate impact*. May cause significant damage to the skin of the vehicle (e.g. plastic deformation, cratering, partial penetration) but does not penetrate the skin.
  - *Serious impact*. Penetration of the skin, producing a small hole and possibly some damage to the underlying structure and/or electronics.
  - *Heavy impact*. Penetration of the skin, producing a large hole and extended damage to the underlying structure and electronics.

  A more quantitative distinction between serious and heavy impacts will be given in the next Section, when details of the proposed structural design have been outlined. The responses to each of these classes of damage will be qualitatively different, from no action apart from noting the impact and perhaps checking for accumulated surface damage for light impact, to perhaps sealing off part of the structure and initiating a major repair program for heavy impact.

Thus, the principal objectives of the initial design are reliability, flexibility and modularity. The work involved in implementing this first stage of the CD will contain a large component of hardware (mechanical and electronic) engineering design, construction and testing, and the development of a substantial amount of relatively low-level software to provide the basic infrastructure for the system.

One of the most important principles of the design, and one that distinguishes a health monitoring system from other intelligent sensing systems (or "smart spaces"), is the requirement for continued functionality in the presence of damage. A system designed to detect and evaluate damage, and ultimately initiate repair and/or other corrective action, clearly must continue to operate effectively when damage occurs, whether it is damage to the vehicle structure, damage to the sensing system, or both.

Structure of the Report

The remainder of this Report is set out as follows. The next Section outlines the proposed general structure of the CD. This is followed by a brief overview of some of the effects of high-velocity particle impacts on a structure, to provide an indication of what the CD needs to detect. Some comments on ways of producing or simulating such impacts in the laboratory are also given. Then follow Sections that outline the proposed designs, to the extent that they can be defined now, of the sensing system (Section 4), the electronics, processing and communications systems (Section 5), computer simulation and development of the intelligent multi-agent software (Section 6), and of the intelligent system to be implemented in the initial version of the CD (Section 7). A brief summary and conclusions follow.

More detailed discussions of considerations and investigations involved in the design of the sensing system, the electronics and communications system and the computer simulation are provided as Appendices. Appendices 1, 2 and 3 contain the original reports from which Sections 4, 5 and 6 respectively were extracted. It is hoped that the main body of the Report presents a concise picture of current progress towards the design and development of the CD, which can be read without reference to any of the Appendices. The Appendices contain a good deal of additional detail for the benefit of readers who wish to consult them.

It is important to emphasize that this Report makes no attempt to provide a complete design specification for the first (or any later) stage of the CD. Resolution of many of the details will require experimentation and testing as development proceeds. The Report provides general directions and details where appropriate. Its purpose is to attempt to provide a unified picture of the proposed CD development in order to elicit comments, suggestions and feedback.

2. Proposed General Structure of the Concept Demonstrator

A number of possible structures for the CD were considered, ranging from the relatively conservative (a single panel) to the more adventurous (an inflatable sphere with "stick-on" sensing patches and wireless communications). Ultimately, the requirements of reliability and flexibility and the need to have a working system within 12 months led to the adoption of a more conservative structure than might have been selected otherwise.

The structure chosen is an enclosed volume in the shape of a hexagonal prism, as shown in Figure 2.1 below. In the first stage, the six hexagonal faces will be covered by removable panels, on which sensors will be mounted. The electronics to control data acquisition, processing and communications will be mounted within the volume, so the structure must be sufficiently large that the internal volume is accessible. On the other hand it should be small enough to allow transport and demonstration overseas. It may be desirable to maintain the inner volume at a different pressure than the external ambient, so it should be possible to seal the volume.

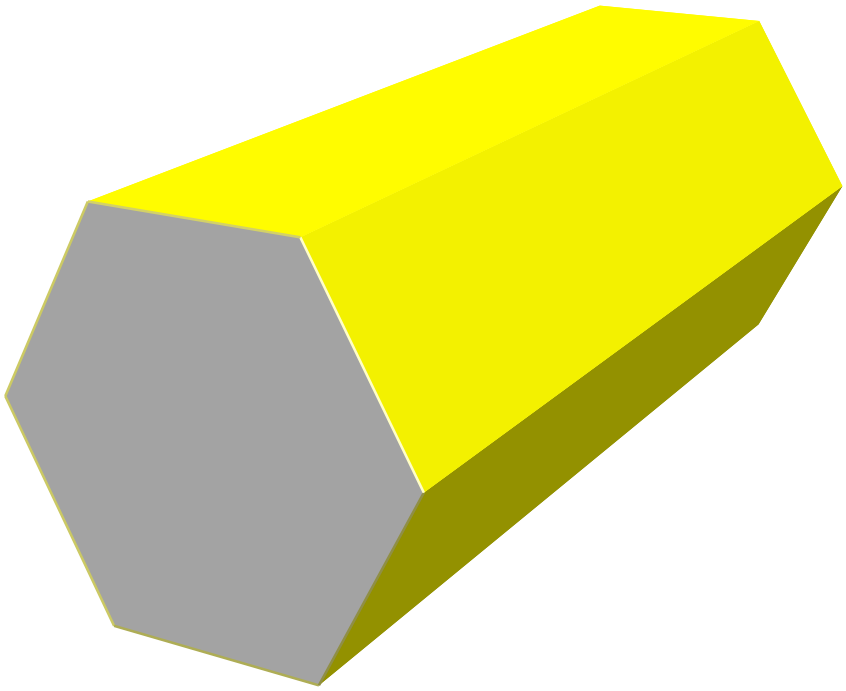

Figure 2.1: Proposed general shape of the Concept Demonstrator. The rectangular faces of the hexagonal prism will be approximately 800 mm long x 400 mm wide. The hexagonal end faces will be approximately 800 mm between opposite vertices.

Each of the rectangular faces will be considered to be composed of small regions, which will be known as cells. Each cell contains a small number of sensors, a processor to control the acquisition of data from the sensors and to control the communication of data and other information from the cell to its neighbours. *A cell is the fundamental unit of the sensing structure.* Cells may be small or large, depending

on the surface shape and complexity, and may contain different sensors or multiple sensor types, according to cell location and local requirements. However, each cell will contain a single data acquisition and processing unit, and a single communications node. These can be thought of as comprising the cell nucleus.

In the initial design CD cells will be ~ 100 mm x 100 mm in area. A cell may be square, or it may be other shapes or sizes, depending on its location on the skin. Each of the rectangular faces will, in the first instance, contain 32 cells in a regular 4 x 8 array, and will therefore be approximately 400 mm wide x 800 mm long. The widths of the hexagonal end faces, between opposite vertices, are ~ 800 mm.

The initial version of the CD will consist of a ribbed framework with 200 mm square aluminium sheet panels forming the skin, but at later stages of the development other materials will be incorporated. Likely candidates are glass (as windows), aluminium foam, carbon fibre composite, or other composite or multi-layered structures: for example, Nextel/foam/Kevlar composites have been developed as high-velocity particle shields (e.g. Christiansen et al., 1999). It is possible some parts of the initial structure will have cells or panels with skins made of other materials and/or of other shapes, but this will depend on progress. It is envisaged that the present incarnation of the CD will be subject to numerous modifications in the future, fulfilling its role as a test-bed for ideas and technologies.

In order to facilitate such modifications to the general structure of the CD, a modular system has been selected to allow a functional and easily modified construction. The Profile System of MayTec Inc. has been used to fabricate the framework of the hexagonal prism, consisting of a 20mm square cross-section of profiled extruded aluminium. This provides a light, rigid structure to support the aluminium sheets that will be used initially as the skin material, and is illustrated in Figure 2.2.

Panels of 200 mm square sheets of 1mm-thick aluminium will be attached via small brackets, and the accompanying electronics will either be supported on each panel or from the surrounding framework, depending on final weight and dimensions. Each of these panels will contain four sensor cells. Therefore there will be 48 panels monitored by 192 sensor cells. These panels will be readily removable and exchangeable to allow different materials, different sensors, different cell shapes and densities etc. to be tested.

Finally, as foreshadowed in Section 1, the cellular construction of the skin allows the distinction between serious and heavy impacts to be made as those for which impact damage is either confined to a single cell or affects many cells, respectively.

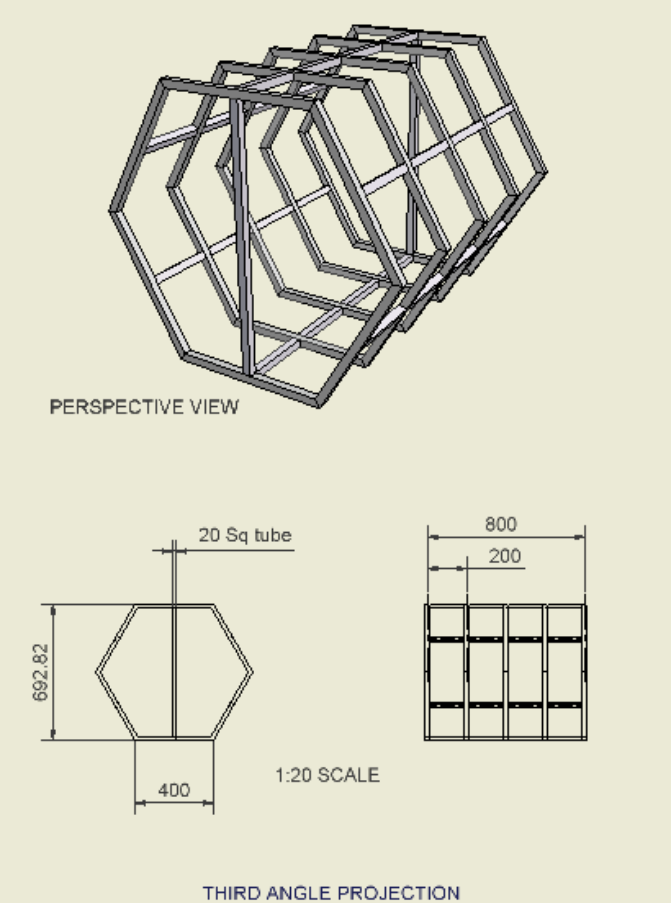

Figure 2.2: Drawing of the framework of the Concept Demonstrator

3. Particle Impacts: Damage and Sensing

This Section contains a very brief introduction to some topics that are important to the task of detecting and evaluating the effects of high-velocity particle impacts. There is no attempt to provide either rigorous or complete accounts of any of the material, but only to provide sufficient background for the following Sections of the Report. Firstly there is a general overview of the some of the damaging effects of a high-velocity particle impacting on a solid structure, following which some of the effects that could be used as a basis for impact sensing are outlined. Finally, some comments are made about possible experimental techniques for generating or simulating high-velocity particle impacts in the laboratory, since this is central to our ability to develop, test and demonstrate the required capabilities of the CD.

3.1 Damage induced by high-velocity particle impact

High velocity impacts, particularly by hard projectiles, will produce damage (i.e. inelastic effects) in the target material, as well as an elastic response. The nature of the damage depends on the materials concerned as well as on the velocity and angle of impact. It is not possible here to attempt to provide a representative review of damage mechanisms and effects in different types of materials (both particle and target), since these depend on a large number of material properties and parameters. The following few paragraphs contain very brief and incomplete descriptions of some forms of damage, simply to give an indication of the variety of effects that can occur.

Low velocity impacts (< 1 km/s)

In ductile metals, plastic deformation (of both the target and the projectile) occurs and heat is generated. The heat may be enough to produce partial melting and cratering. The figures below, reproduced from a paper on cold spraying by Dykhuizen et al. (http://sherpa.sandia.gov/9231home/pdfpapers/cold2.pdf), show some of these effects for 20 μm copper particles impacting a stainless steel substrate.

Dykhuizen et al. showed by both experiment and numerical modelling that the splat and crater dimensions scale with the diameter of the impacting particle at velocities up to ~ 700 m/s. The crater depth increases with impact velocity, but the splat diameter is relatively insensitive to it. Figure 3.1 shows a cross-section of a splat and crater.

Figure 3.1: Cross-section of a splat created by the impact of a 700 m/s copper particle (~ 20 μm diameter) onto a stainless steel substrate. Note the stainless steel that has been ejected from the crater that appears on the lower surface of the splat edge.

Figure 3.2 shows the results of calculations of the splat shapes for a 25 μm copper particle impacting a stainless steel substrate at normal incidence and various velocities from 400 m/s to 700 m/s, which is slow compared with typical particle velocities in space (~ 10 km/s). Even at these "slow" velocities, interesting damage effects can be observed. The code used (the Sandia CTH code) models the viscoplastic deformation of the materials, based on thermally-activated dislocation mechanics: it takes into account effects of isotropic strain hardening, thermal softening, strain rate dependency, and pressure-dependent shear and yield strengths. While the model is known to overestimate material temperatures, since dissipation by conduction is not included in the model, these results nevertheless show that high temperatures are developed locally in the impact region, even at these relatively low impact velocities.

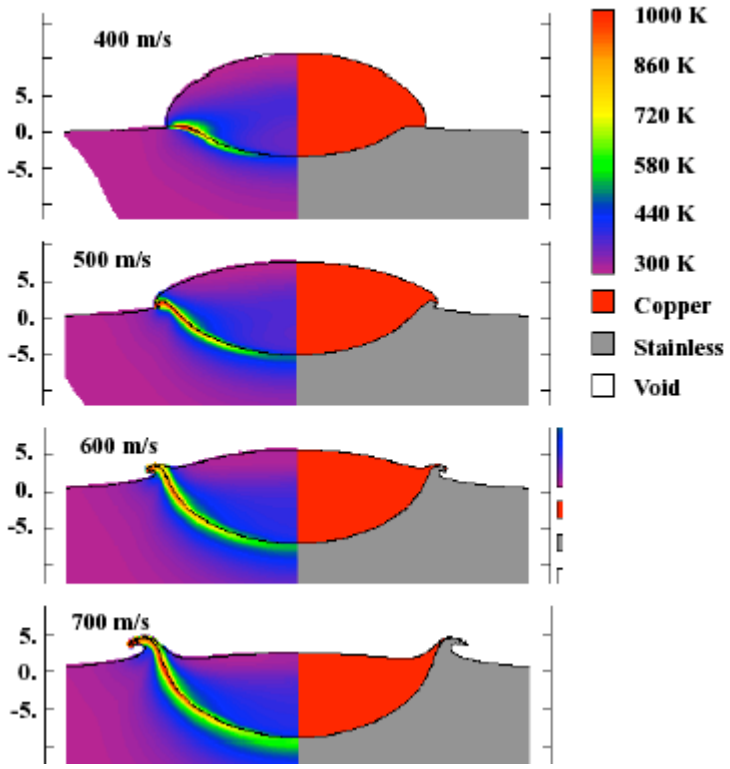

Figure 3.2: Splat shapes, calculated by Dykhuizen et al. using the Sandia code CTH, for a 25 μm copper particle impacting a stainless steel substrate at the velocities indicated. On the left-hand side, the diagrams show temperature, and material type on the right side. The original substrate surface is at zero on the left-hand scale, which is in micrometres.

Brittle materials, such as glass and ceramics, tend to crack and fracture when the stress concentration produced by an impact reaches a critical value. Cracks propagate at speeds up to the Rayleigh wave velocity in the material (~ 3.1 km/s in glass), unless the high stress is driven by a high-speed shock wave, such as may be produced by an explosion. The cracking and fracture processes will act as sources of elastic waves.

Laminated materials such as carbon fibre composites can undergo a multitude of failure mechanisms, including delamination, matrix cracking, fibre fracture, etc. There is a wealth of recent literature on impact damage in such materials.

Hypervelocity impacts

At higher velocities (~ 10 km/s and greater), the physics tends to be dominated by the kinetic energy per unit mass of the particle, i.e. the square of the velocity. The available energy per atom of the particle (in electron-volts, eV) is $E = 0.0052\ m\ v^2$ eV, where m is the mass of an atom, in atomic mass units (amu), and v is the particle velocity in kilometres/second. The atomic masses of elements that might be found in a micrometeoroid are:

Carbon:	12 amu
Oxygen:	16 amu
Silicon:	28 amu
Iron:	56 amu
Nickel:	59 amu.

At a particle velocity of 30 km/s the kinetic energy is about 4.7 eV per amu, and even for carbon this is 56 eV per atom, which is large compared with the ionization potential of ~ 11 eV. The ionization potential varies from element to element but for valence electrons a mean value of 12 eV is often quoted. Thus it is expected that the impacting particle is not simply melted or vaporized but may be highly ionized, even if only a small fraction of the collision energy goes into ionization.

The resulting extremely hot, high pressure (several megabars) plasma "fireball" expands at hypervelocity (much greater than the velocity of sound in the target material) sending a shockwave through the target, which eventually decays into an acoustic wave. A near hemispherical crater much larger than the particle is blown in the target. The momentum transferred to the target is greater than the momentum of the impacting particle due to a high velocity back spray that develops at the rim of the crater. The momentum transfer initiates elastic waves that propagate in the target, their nature depending on the target geometry.

3.2 Detectable effects of impacts

The above examples serve to illustrate the range of effects that can be produced by high-velocity particle impacts on a solid surface. These produce a number of effects that could be detected, and thus used as a means to detect and identify the location and severity of the impact. It will be assumed for the purpose of this discussion that the target material, the vehicle skin in this case, has no inherent sensing property.

Impact damage such as that described above could be detected by a number of methods. Examples include optical imaging of the surface to detect and measure impact craters, thermal imaging to detect impact-induced hot spots, thermal sensors within the skin to detect heat conducted from the impact site, etc. For higher velocity impacts, optical or rf emission from the impact-generated plasma might be feasible. However, perhaps the most generally applicable method would be to detect the elastic waves generated in the skin by the impact.

Elastic wave generation and propagation

Any impact, no matter what the mass or velocity of the particle, will transfer elastic energy to the target (the vehicle skin). When damage occurs, a substantial fraction of the incident energy may be dissipated inelastically, for example in thermal effects, plastic deformation, cracking or fracture, ionization, plasma formation, etc. However, there will always be some transfer of elastic energy to the target. This elastic energy will propagate away from the impact site according to the material and geometrical properties of the target, and according to the rate and spatial distribution of the elastic energy deposition into the target (the elastic source distribution).

The source distribution may resemble a simple surface point load for a low-energy impact by a small particle, or it could be much more complicated for a large-area impact, when wide-spread damage occurs (which may itself act as a source of elastic energy), or when a plasma-induced or particle-induced shock wave propagates in the material. Similarly, the bandwidth of the elastic disturbance will carry information about the rate of elastic energy deposition: a faster impacting particle will generally produce a broader-band elastic wave spectrum than a slower particle. Thus, the spatio-temporal spectrum of the elastic waves generated carries a great deal of information about the nature of the impact and resulting damage (but its detailed interpretation may be complicated!).

Elastic wave propagation away from the impact site may contain bulk, surface or plate waves, with longitudinal and transverse polarizations, depending on the target geometry. Propagation may be more or less lossy depending on the material properties, the geometry, and the bandwidth of the waves.

Because the skin of the CD (and many vehicles) is a thin sheet, which acts as an elastic waveguide, the elastic disturbance propagates as a dispersive guided wave (a Lamb wave or generalized Lamb wave). A source containing only low frequency components (as produced by a low-velocity impact) will excite only low frequency modes of the plate, and often the lowest frequency modes will dominate. If the skin material is homogeneous, as in this case of an aluminium sheet, the dominant low frequency mode generated is generally the zero-order antisymmetric Lamb mode, or flexural mode, designated A_0 (due to the symmetry of the impact source – the symmetry is referred to the mid-plane of the plate). For this mode, the group velocity is low for low frequency components, and tends to the Rayleigh (surface) wave speed in the material (~ 3.0 mm/μs for aluminium) at high frequencies. Thus the pulse is dispersed, with the high frequency components arriving at a remote sensor earlier than the lower frequency components. The zero-order symmetric mode, or extensional mode, (designated S_0) will not be generated by a purely antisymmetric source, but it will appear for more complex source geometries such as may be produced by material damage accompanying an impact. This mode propagates faster than the flexural mode at low frequencies, and is also dispersive.

A wide bandwidth source, such as expected from a higher velocity impact, may generate many more than the zero-order Lamb modes. The behaviour of the group velocities of the higher-order modes as functions of frequency is more complicated (but readily calculable for a homogeneous plate), so the simple dispersion behaviour described above will no longer apply. However, the linear group velocity is always

less than the longitudinal bulk velocity in the material (~ 6.4 mm/μs for aluminium). Higher-order modes generally suffer higher attenuation than their lower-order counterparts, but, for a low-attenuation material like aluminium, this should not necessarily preclude their observation if they are generated efficiently.

A final comment about pulse dispersion is that, for isotropic skin material, dispersion is a function of the product *fd*, where *f* is the frequency and *d* the plate thickness. The dispersive behaviour therefore scales with the thickness of the skin. In the low frequency, or thin plate (i.e. small *fd*) limit, the only modes that exist are A_0, which has linear dispersion, and S_0, which has constant velocity (dispersionless).

Elastic wave propagation is also influenced by the extent (and shape) of the impact source, and, of course, by reflections from boundaries or other reflecting structures. For the situations of interest in this work, it can probably be assumed that the source is smaller than the wavelength of the highest frequency waves that will be detected, so that propagation away from the source region will be approximately omnidirectional. This may not be true when the impact produces damage, but, in the absence of shock wave generation, this will probably be true for the initial elastic response.

Low frequency components of elastic disturbances can be detected by sensitive accelerometers, and this is done (though not necessarily for impact detection) in NASA space vehicles by "micro-gravity monitors": instruments such as SAMS, the Space Acceleration Measurement System on the International Space Station, and OARE, the Orbital Acceleration Research Experiment on the STS-107 shuttle mission (http://microgravity.grc.nasa.gov/MSD/MSD_htmls/acceleration.html). Higher frequency components are commonly detected using piezoelectric acoustic emission (AE) sensors. This will be discussed further in the next Section and in Appendix 1.

3.3 Laboratory techniques for generating high-velocity particle impacts

An issue of some concern for the present work concerns the generation of high-velocity small particles for experimental and demonstration purposes. It would be desirable to have particles of various materials, in the range 10 μm to 1 mm in diameter, with velocities up to several km/s, in order to produce damage ranging from zero (purely elastic collision) up to penetration of the skin. This is not a trivial requirement. There is certainly no suitable facility within CSIRO, and, as far as we have been able to ascertain, within Australia.

High-velocity and hypervelocity (so-called when the impact velocity exceeds the longitudinal sound velocities in the both the target and the projectile, i.e. a few km/s) particles may be obtained in the laboratory using light gas guns, which are usually multi-stage devices that utilize an explosive charge (gun powder) and a compressed gas tube. Figure 3.3 is a highly stylized diagram of a light gas gun to show the basic principles behind its operation.

We are presently investigating the possibility of acquiring a light gas gun facility within CSIRO, or initially the first stage of one. However, the process of approval,

acquisition, installation and commissioning will take some time. It may be advantageous for some preliminary measurements to be undertaken at an existing facility, possibly within NASA or elsewhere.

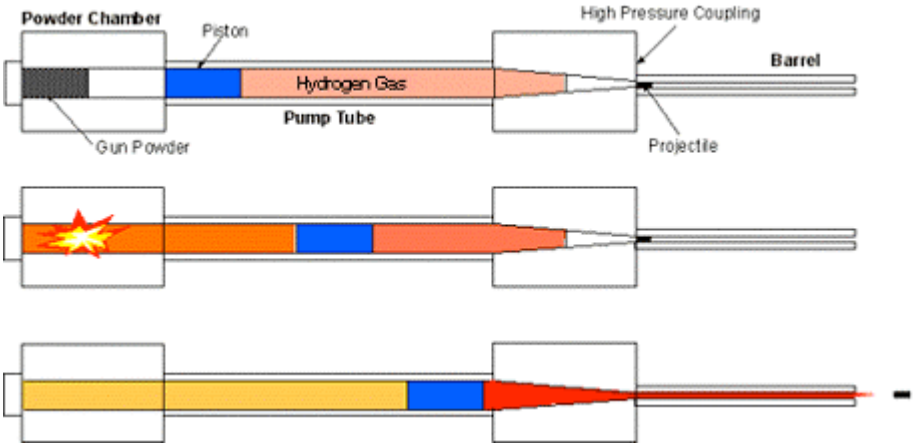

Figure 3.3: A highly stylized diagram of a light gas gun, to show the basic principles of its operation. This diagram, along with a general description of the gas gun operation, is from a NASA Johnson Space Center website (http://ares.jsc.nasa.gov/Education/websites/craters/lgg.htm).

Laser pulse simulation of impacts

In the absence of a source of fast particles, particle impacts are being simulated using a 500 mJ, 8 ns FWHM pulse from a Q-switched Nd:YAG laser (wavelength 1.06 μm). If such a pulse is focused onto an aluminium surface, the absorbed energy density is significantly greater than that required to produce ablation of the material. The elastic reaction to the material ablation provides a useful simulation of a particle impact, within certain bounds. These limitations include the following.

Firstly, it is only capable of simulating normal incidence impacts, unless some complex structuring of the incident beam was undertaken. Secondly, it is capable of simulating impacts only over a restricted energy range: it is not, for example, expected to be capable of adequately simulating an impact that penetrates the skin. We would like eventually to be able to achieve both oblique incidence and skin-penetrating impacts. When operated in air, the focused laser beam induces ionization (breakdown) in the air near the metal surface. This produces a shock wave in the gas, which also impinges on the metal surface, complicating the elastic source distribution. Furthermore, both the ionized gas and ablated material attenuate the incident laser beam, thereby limiting the energy that is deposited on the metal surface. A detailed discussion of laser generation of elastic waves in metals may be found in the book by Scruby and Drain (1990).

Nevertheless, the use of laser pulses has provided a valuable and useful means of obtaining preliminary results in our investigations of sensors. All of the experimental measurements reported here (Section 4 and Appendix 1) were carried out using the laser pulse to simulate a particle impact. Further details of the experimental arrangement are given in Appendix 1.

4. Sensors and the Sensing Strategy

4.1 Introduction

The initial aim of the Concept Demonstrator (CD) is to develop an operational experimental platform and demonstrator, in which high-velocity particle impacts generate signals that may be processed intelligently in order to provide information about the location, severity and consequences of impacts. The particles of interest may be anything from sub-micron dust or ice grains upwards – micrometeoroids, meteoroids or orbital debris. Typical impact velocities may be of the order of 10-20 km/s, with a range from zero to ~ 100 km/s.

This Section discusses the sensors and sensing strategy that is proposed for initial implementation of the CD. A more detailed version of this discussion is contained in Appendix 1. It should be emphasized that it is not the aim of this stage of the project to develop new sensors, but rather to take existing technology and use it in an appropriate way to produce a reliable platform for further development at a later stage.

The basic sensing requirements and strategies that have been adopted are described below, followed by a report on experiments using various sensors detecting simulated impacts and a discussion of the implications of these results. To conclude, experiments in progress and the immediate future research will be outlined.

4.2 Sensing requirements and strategies

Sensors for detecting particle impacts

There are a significant number of sensor types, utilizing different physical principles, which can and have been used to detect particle impacts. Some of these, direct detectors, require the detector itself to be directly struck by the particle, while others detect secondary effects of the impact and do not necessarily require a direct hit, generally relying instead on radiation or conduction of elastic or thermal energy, from the impact site. Further details of some of these sensor types are given in Appendix 1.

Direct sensors have some advantages over indirect sensors: interpretation of the sensor output is generally simpler and requires minimal signal processing, and spatial resolution is usually determined directly by the sensor dimensions. On the other hand, direct detection sensors would need to form a quasi-continuous layer on the outer surface of the vehicle skin, and in many cases may therefore be more susceptible to damage than the skin itself. It is difficult to see how redundancy can be easily built into a system of direct detection sensors, or how the system could be readily reconfigured to compensate for damage to or failure of a sensor.

Therefore, despite the attractions of direct sensing, it is proposed that the initial development of the CD should utilize indirect impact detection, and the use of piezoelectric acoustic emission (AE) sensors has been chosen for reasons listed in Appendix 1. However, there are also disadvantages related to the use of AE sensors, which need to be addressed in the development of a strategy for their use. The main

one is complexity of signal processing, particularly in the presence of background structural noise and elastic wave reflections from structural boundaries. Another is the huge dynamic range required to take full advantage of the potential functional flexibility of these sensors.

It is envisaged that the CD will be used in the future to test other sensor types and sensing strategies.

Proposed sensing strategy and sensor geometry

One of the goals of the proposed sensing strategy is to reduce the processing and data acquisition requirements for the cell processor, to reduce complexity and cost, and to increase reliability (see Section 5). Thus, the objectives of the sensing strategy are:

- to detect and locate impacts and to evaluate damage as indicated in Section 1;
- to detect penetration of the skin by the impact; and
- to minimize processor and processing requirements, by minimizing the analogue to digital conversion (ADC) speed requirement and simplifying data processing.

To achieve these objectives it is proposed that a dual piezoelectric film sensor be used, as is shown schematically in Figure 4.1 below for a square cell. It consists of a sheet of piezoelectric film, bonded to and covering almost the entire inner surface of the skin within the cell boundary, along with (say) four small sensors that can be used for acoustic emission sensing. The small sensors may be produced by patterning of the electrodes of the large sheet as illustrated in Figure 4.1, or they could be separate sensors bonded to the large sensor.

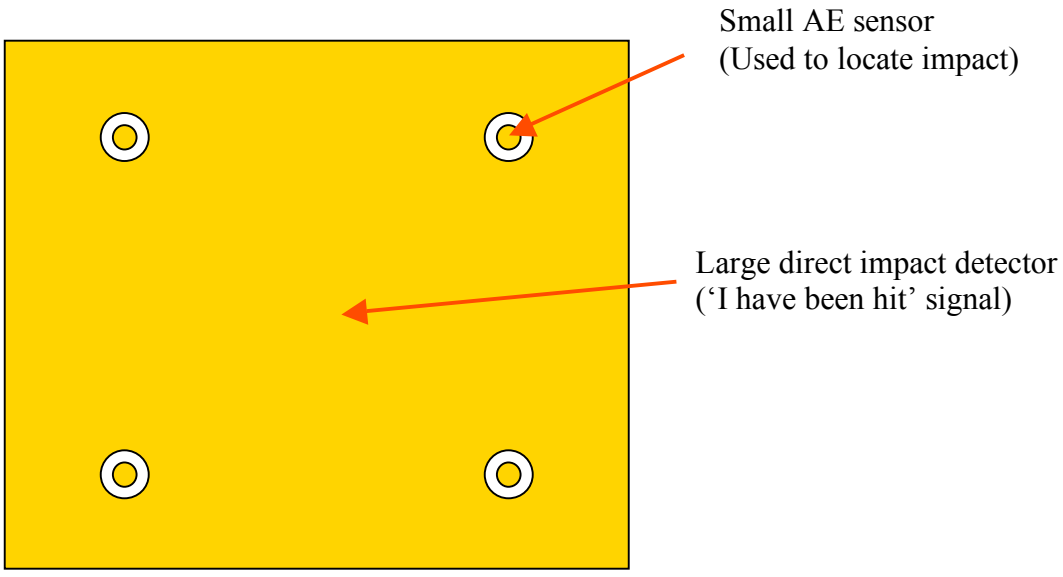

Figure 4.1: Proposed sensing cell structure for piezoelectric sensing. The cell could equally well be triangular, pentagonal, hexagonal, or some less regular shape.

The purpose of the large sensor is to detect impacts and provide a direct indication that the cell has been hit, i.e. it localizes the impact to within the cell. The position of the impact within the cell may then be determined from the small-sensor signals by

relatively simple signal processing, assuming that the skin of the cell is reasonably homogeneous. Straightforward triangulation is used, but this must take account of the dispersive nature of the elastic wave propagation from the impact point to the sensors.

Detection of penetration

The system must also be capable of detecting penetration of the skin by a particle, so a strategy for achieving this must be developed. There would appear to be (at least) four possible ways by which the piezoelectric film sensors outlined above could be used to detect penetration (puncturing) of the skin by an impacting particle. However, while these methods should be sensitive to skin penetration in principle, their practical feasibility is somewhat speculative and has not yet been tested experimentally. Further discussion of this point may be found in Appendix 1. Experiments will be carried out when access to high-velocity particles is available.

Sensor failure

The system is required to remain operative and functional in the event of a sensor failure, or other functional failure of a cell, whether these failures are the result of a previous particle impact, or have occurred for other reasons. In principle, the small AE sensors on neighbouring cells can be used to detect the elastic waves that emanate from the impact site, as long as the cells are not isolated acoustically from each other.

Sensor deployment in the initial design

As described in Section 2, each rectangular face of the hexagonal prism structure is covered by eight (in a 2 x 4 array) 200 mm x 200 mm panels, each of which contains four sensing cells. Therefore there will be 48 panels monitored by 192 sensor cells, incorporating 192 large-area sensors (one each cell) and 768 (four each cell) small, integrated sensors for precise location of the impacts. The general arrangement of sensors on each panel is shown schematically in Figure 4.2. It is expected that this relatively large number of cells and sensors will allow the study of communication protocols, intelligent processing and any complex or emergent behaviour that may result from such large numbers of interacting agents.

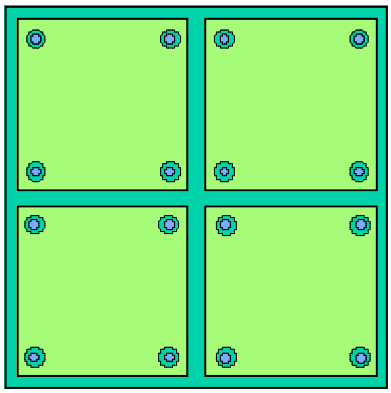

Figure 4.2: Schematic layout of sensors on a 200 mm x 200 mm panel, showing four 90 mm square 'direct impact' sensors, each of which has four small sensors to allow determination of the impact location and a measure of the elastic energy emanating from the impact.

4.3 Experimental results for piezoelectric sensors

A number of experiments have been carried out to evaluate aspects of the design of the piezoelectric sensors described above. This program is not yet complete, and further experiments are required. In the absence of a high-velocity particle launcher, all experiments carried out so far have employed a 500 mJ Nd:YAG laser pulse, with an energy density above the threshold required to produce ablation of the aluminium skin, to simulate particle impacts. When the laser beam is focused to a point on the skin surface, the pulse is expected to simulate quite well some of the broad features of elastic wave generation by normal impact by a small particle with energy less than that required for penetration of the skin. Some experiments were done in this configuration, and some with the laser beam unfocused and approximately 5 mm in diameter. It is unlikely that the unfocused beam experiments provide a close simulation of particle impact, but they were done for comparison with the focused beam measurements. Appendix 1 contains details of the experimental technique.

The experiments conducted so far have been designed to evaluate various aspects of the utility of PVDF film sensors, epoxy-bonded to 1 mm aluminium sheet, for use as the large direct impact and small AE sensors shown in Figure 4.1. Only brief summaries of these experiments and their results will be reported here: further details are available in Appendix 1.

Comparison of small sensors

Some comparative measurements were made to confirm the fidelity and sensitivity of the PVDF film sensors. Figure 4.3 shows the signals generated by a conical PZT transducer, 1.6 mm in diameter where it contacts the skin surface, based on a NIST design (see Appendix 1), those received from a 1.8 mm diameter "patch" of 52 μm PVDF film, and two signals acquired using a 0.5" commercial PZT transducer by Prosser et al. (1999).

It is apparent that the signals produced by the PVDF sensor carry essentially the same information as do the other signals. It therefore appears that the small PVDF sensors would be suitable for use as AE sensors in the present context.

Sensor size

Measurements were made to study the dependence of direct impact signals on sensor dimensions, to determine the practicality of using large direct impact sensors. A number of square PVDF sensors of differing sizes (5, 15, 32, 45, 48 and 90 mm square) were fabricated and bonded to the rear (non-impacted) side of a 1 mm-thick aluminium sheet. Both focused and unfocused laser pulses were directed at the front surface of the aluminium sheet, directly opposite the sensor being studied.

There were two clear results. Firstly, for a particular sensor size, the received signal (voltage) amplitude was always approximately an order of magnitude larger for the unfocused laser beam than for the focused beam. Secondly, within the range of sensor sizes used, the signal amplitude is always greater for smaller sensors than for larger ones. These results are summarized in Figure 4.4, with sensor area converted to nominal capacitance.

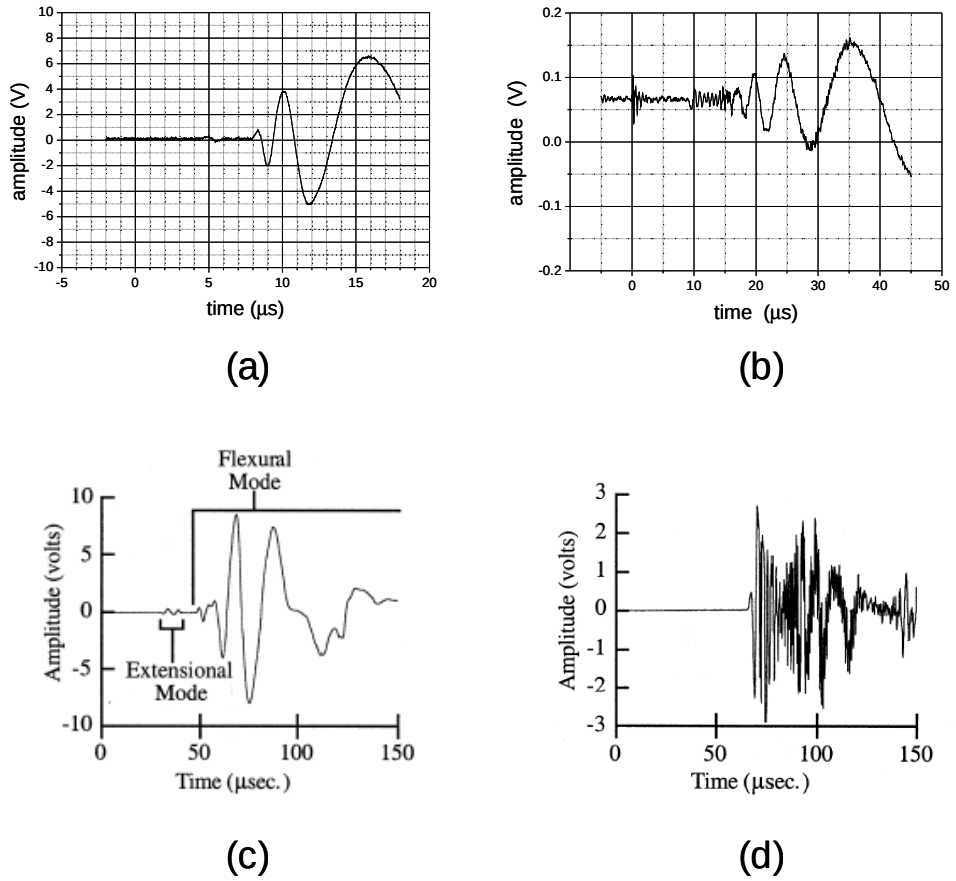

Figure 4.3: Comparison of signals from different (small) transducers. (a) Conical PZT transducer output resulting from elastic waves in 1 mm aluminium sheet caused by a laser pulse on the opposite side of the sheet, 25 mm from the centre of the sensor ($\Delta x = 25$ mm). (b) 1.8 mm diameter PVDF sensor output under similar conditions to (a) but with $\Delta x = 50$ mm. (c) Signal from 12.7 mm diameter PZT transducer due to low-velocity impact on 3.175 mm-thick aluminium sheet, $\Delta x = 152$ mm (Prosser et al., 1999). (d) Signal from a 12.7 mm diameter PZT transducer due to high-velocity impact on 3.175 mm-thick aluminium sheet, $\Delta x = 147$ mm (Prosser et al., 1999).

It is apparent from Figure 4.4 that the signals can be interpreted in terms of a constant charge amplitude being developed in the PVDF capacitance, which is ~ 9 nC for an unfocused laser pulse and ~ 0.7 nC for the focused pulse. It is perhaps not surprising that the signal amplitude produced by a laser pulse, which is a displacement charge for a piezoelectric sensor, is independent of the sensor dimensions within the size range used here. The impact area is smaller than all the sensors used, and the direct impact signal should be generated only within the impact region.

It is not quite so obvious why the signals should be approximately an order of magnitude smaller for the focused laser beam than for the unfocused. There may be at least two contributing factors. Firstly, the energy density at the focal spot is sufficiently high that ablated material will shield the skin surface from the laser radiation (i.e. the pulse energy reaching the skin surface may be significantly less for the focused than the unfocused pulse). Secondly, the nature of the elastic wave source produced by the unfocused pulse is quite different to that of the focused pulse. Depending on the details of the polarization of the PVDF, this may induce a larger signal. Source and elastic wave modelling may shed some light on this issue.

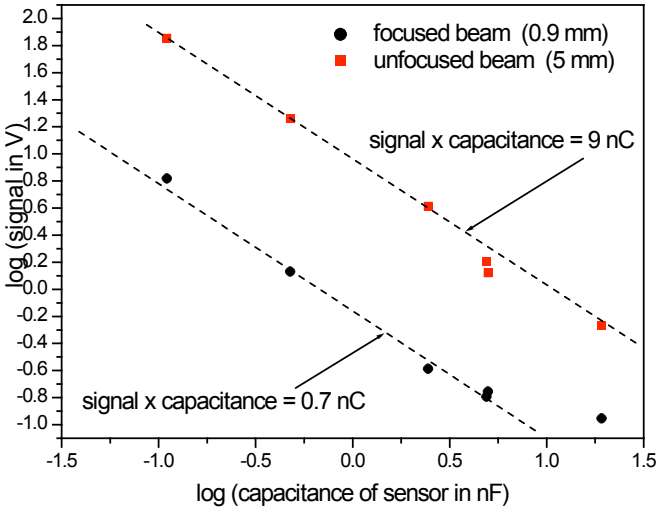

Figure 4.4: Maximum peak-to-peak direct 'impact' signal, as a function of nominal PVDF sensor capacitance, for both focused and unfocused laser beam 'impacts'.

It can be seen in Figure 4.4 that large sensors produce small voltage signals, and thus show reduced sensitivity. One way of overcoming this problem is to divide the large sensor into a number of smaller sensors that can be connected in series. This results in a large area sensor with a smaller effective capacitance, which produces an increased voltage output signal. Another solution is to use a broadband charge amplifier. Initial investigations of these approaches are described in Appendix 1.

Dependence of the direct impact sensor signal on impact location

The purpose of these experiments was to determine how effectively a large area sensor could provide a clear indication that its cell has been hit. In other words, how readily can the direct impact signal from a large area PVDF sensor be used to distinguish impacts that occur on the skin surface directly opposite the sensor ('on-sensor' impact, $\Delta x < 0$) from those that occur further from the sensor ('off-sensor' impact, $\Delta x > 0$), where Δx is the distance of the impact site from the edge of the sensor.

A medium sized PVDF sensor (32 mm square) was selected for these measurements to ensure a high signal-to-noise ratio, and its output signal was measured as the 'impact' site, the point where the focused laser beam pulse was incident, was moved from on-sensor to off-sensor in 1 mm increments. The results are shown in Figure 4.5.

The results indicate a qualitative change in the nature of the signal within a region ~ 2 mm wide as the impact site is moved across the edge of the sensor. When the impact is on-sensor, the first detected signal, produced by the direct impact, is a sharp narrow pulse with centre frequency ~ 21 MHz, which is the thickness resonance of the 52 μm sensor film. When the impact site is ~ 2 mm or more beyond the edge of the sensor, the first detected signal is produced by a propagating Lamb wave, and contains only lower frequency components. Thus, without taking absolute amplitudes

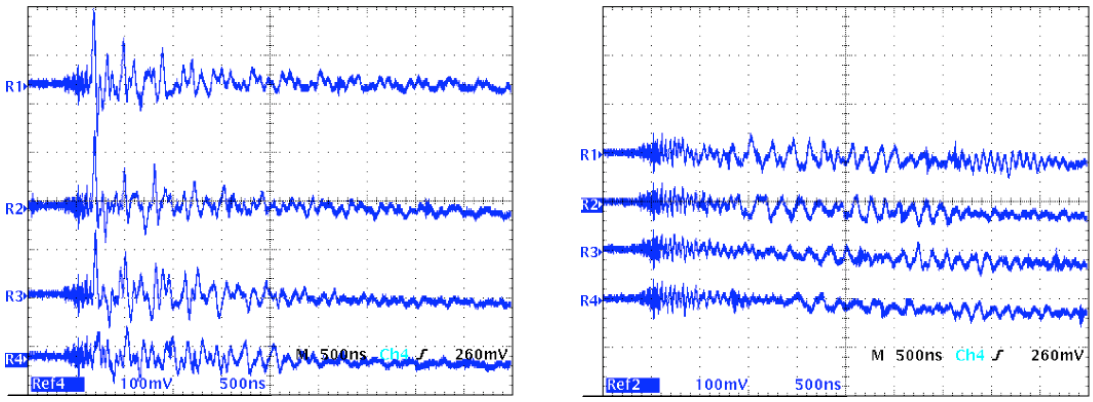

Figure 4.5: Signals received from a 32 mm square PVDF sensor as the 'impact' site of a focused laser beam is moved from 'on-sensor' to 'off-sensor'. The oscilloscope traces on the left correspond to Δx = -2, -1, 0 and +1 mm from top to bottom respectively, while those on the right correspond to Δx = +2, +3, +4 and +5 mm from top to bottom, respectively.

into account, there is a clear basis for distinguishing between 'on-sensor' and 'off-sensor' impacts.

Further details of these and other measurements, including measurements of the dependence of the signal received by a small (1.8 mm diameter) PVDF sensor on the distance of the 'impact' from the sensor, are contained in Appendix 1.

4.4 Conclusions and future work

A novel sensing strategy has been proposed to detect and locate particle impacts on the surface of the CD. The results obtained so far provide grounds for optimism that it can be implemented successfully. However, a number of issues remain to be clarified. Perhaps the issue of most concern to the ultimate success of the proposed strategy is that of sensitivity of the large area sensors to electromagnetic interference (EMI). Early measurements (Appendix 1) showed deleterious effects of coherent noise emanating from the pulsed laser, unless very careful shielding of the sensors and connecting cables was effected. When implemented on the CD, the sensors will be enclosed within the conducting structure, which should provide a degree of shielding from externally generated EMI. However, also enclosed within the CD will be a number of fast digital processors operating in close proximity to the sensors (see next Section). It remains to be seen how effectively the sensor signals can be rendered immune from switching noise from these processors.

In order to investigate some other issues, access to a source of high-velocity particles is necessary. Such issues include detection of penetration of the skin by particles, the detection and identification of oblique particle impacts, and a more quantitative investigation of the utility of simulating particle impacts with laser pulses. We are currently looking at ways to address these issues (see Section 3 above).

Sensor manufacture and connection to the processing electronics are important issues. A final decision on an appropriate design for the initial cell implementation will be made in conjunction with a procedure for fabrication compatible with the production of hundreds of these sensor cells (see Appendix 1).

5. Electronics and Communications Protocols

This Section outlines the requirements for and proposed implementation of the electronic hardware in the CD. Broadly, the electronics are responsible for acquiring data from the sensors, processing the data, communicating information around the system, providing a platform for the software that will imbue the system with intelligence and, ultimately, enabling the system to take actions in response to decisions it makes. The electronic and communications systems therefore provide the platform, or essential infrastructure, for the cells to work together as a single intelligent system. There is therefore a very broad range of requirements of the electronic system. An expanded version of this Section is provided as Appendix 2.

It is essential that the CD be designed for as high a degree of operational flexibility as possible (within cost constraints). This particularly applies to data sampling rates, where full-waveform capture of some AE sensors might require sampling rates up to ~ 50 MSPS (megasamples/second), computational power, where ultimate requirements can only be guessed at, and communication data rates. At this stage the philosophy has been to maximize these capabilities, within cost constraints, at the expense of considerations of economy, power consumption, etc. The general architecture and functionality of the system are described in this Section, with a more detailed discussion appearing in Appendix 2.

5.1 Overall design and architecture of the electronic system

A conceptual view of the physical and logical structure of a cell is of a seven-layer structure. Thus, the total CD system may be viewed as a pseudo-planar array of ~ 200 cells, each seven functional layers deep. These layers may be delineated as follows.

1. The physical outer skin. This is protective, and may be structural as well.
2. The sensor layer as described in Section 4 above.
3. Conditioning electronics. This layer converts the signals from the sensors to a form suitable for analogue to digital conversion (ADC).
4. Sampling and data pre-processing. This includes ADC, retaining any relevant digital signals and time stamps, calibration and other data corrections, and interpretation/reduction of data based on purely local considerations.
5. Data analysis and system processing functions. Further interpretation of the information passed from layer 4, taking into account information from other cells, previous trends and patterns, etc. This is the layer in which the agent-based software will run, and is the source of the system "intelligence" and adaptability.
6. Inter-cell communications functions. Enables communication with neighbouring cells, to enable information sharing, mutual function checking, regional or global interpretation of data, sharing of processor resources, etc. This allows the cell to cooperate with its neighbours, and the collection of cells to behave as an entity.
7. Inter-cell physical connections. Permits transfer of information and power between the individual cells of the array.

A schematic diagram of the layer structure is shown in Figure 5.1, which shows two adjacent cells. Below the sensor layer, the layers are grouped into two: the Data Acquisition Layer (DAL), comprising layers 3 and 4, and the Network and Applications Layer (NAL), comprising layers 5 to 7. These will be discussed further below. To facilitate flexibility and adaptability of the structure, and to increase available computing power, there will be separate processors in the DAL and NAL.

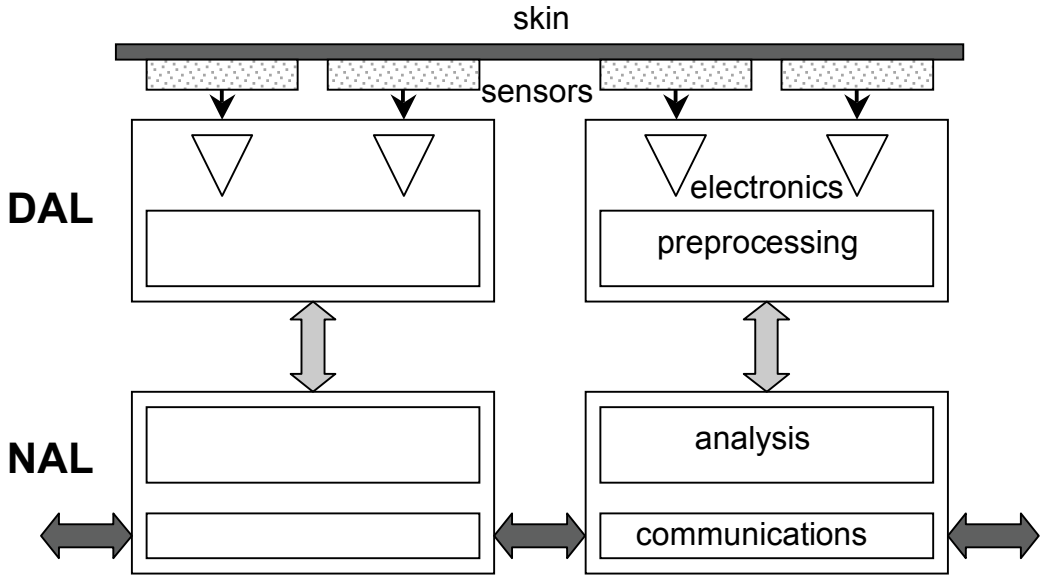

Figure 5.1: The conceptual layer structure for two adjacent cells of the CD.

The main purpose of this conceptual division between a DAL and an NAL is to split the responsibilities for the sensors and data acquisition (DAL) and the intelligent system and communications (NAL).

5.2 Data Acquisition Layer (DAL)

The purpose of the DAL is to condition, acquire and process data from the sensors, and to provide information derived from the sensor data to the NAL. Thus, its detailed function and performance requirements are strongly dependent on the types of sensor interfaced to it, and on the way the sensed data is to be used.

The main purposes of a processor within the DAL, to be referred to as the Data Acquisition Processor (DAP), are firstly to provide a flexible interface between the particular set of sensors embedded in the cell, and the higher-level intelligent processing and communications of the network, and secondly to provide information to the NAL that is more concise than the sensor data: an output "Impact of severity S at position (X,Y)" is much more directly useful than 4 or 5 sampled signal sequences.

Based on the sensing strategy outlined in Section 4, the requirements for the DAP are:

- multiple (five +) high-speed (few MSPS) analogue sampling channels;
- built-in FLASH memory to store code for data pre-processing; and
- a standard high-performance communication link to the NAL to allow data transfer and inter-processor communications.

The processor selected is the Texas Instruments TMS320F2810/2812, which has the following capabilities:

- 150 MHz, 150 MIPS (million instructions/second) processor, which allows for quite complex pre-processing.
- 64/128 kword FLASH memory (2810/2812), providing a reasonable amount of space for software without the need for external memory.
- 16 multiplexed analogue input channels sharing 2 sample and hold circuits and a single 12 bit, 16.6 MSPS, pipelined ADC.
- High-speed serial (McBSP[1]) interface, to allow rapid communications throughput to the NAL.
- Many other memory, timer and interface facilities, which permit the system to run with very little additional logic.

Perhaps the greatest potential limitation is that the ADC sampling rate is a little low, given that it must be shared by five inputs. The resulting 3.3 MSPS average per input is expected to be acceptable. A more minor limitation is that only two of the inputs can be sampled at the same time, as there are only 2 sample and hold circuits. This will have to be compensated for, either by the external electronics and digital "time-of-arrival" detection, or by time-delay compensation in the processing of the interleaved data samples.

At this stage the link between the DAP and the NAL is a point-to-point link, but one attractive option is the ability to attach multiple DAPs to the same McBSP bus. This would allow the DAL to support additional sampling bandwidth, via multiple DAPs.

5.3 Network and Application Layer (NAL)

Inter-cellular communications: physical links

For the initial implementation of the CD, with its requirements for system reliability and short development time, only radio broadcast and wired electrical links were seriously considered as options for the inter-cellular communications. However, later developments might employ more than one type of communication link, with appropriate media being employed for specific communication requirements, as is the case in, for example, the human body.

For various reasons, mostly related to uncertainties in bandwidth requirements, and complications associated with sharing of space and bandwidth, it was decided to implement a nearest-neighbour point-to-point direct-wired link system. The arguments are outlined in Appendix 2. Thus, in the initial CD implementation, each cell will have a direct communications link to its four immediate neighbours[2]. While

[1] One of the attractive features of some of the TMS family of DSP devices is the use of a flexible high-speed serial bus known as the Multichannel Buffered Serial Port (McBSP). This bus can support up to 75 Mb/s data rates, as well as allowing multiple devices to share the bus. The presence of a McBSP controller on both the DAP and the NAL processor greatly simplifies the design of inter-processor communications.

[2] Later developments of the CD might incorporate structures with different cell shapes and different numbers of immediate neighbours with which a cell will communicate directly.

the physical connectivity will be hard-wired, the logical connectivity is limited only by the network protocols and the communications latency, a function of the protocol and link speed. Therefore, appropriate design of the network protocols (see below) will allow evaluation of different network topologies other than the simple regular array topology.

Functions and processing

The main requirements of the NAL are communication with the DAL via the McBSP bus, communication with the NALs in neighbouring cells, and the high-level processing of sensed information required for the formulation of intelligent responses to detected events. The NAL in each cell contains a processor (Network and Application Processor, NAP) whose ideal characteristics should include the following.

- Processing capability in hundreds of MIPS.
- FLASH memory of at least a few hundred kbytes, from which the processor boots. This does not need to contain all NAP software, but sufficient to enable the processor to obtain the rest of its software using the network.
- Fast RAM of at least a couple of Mbytes for software and data. This is too large to be found in the processor, so it is desirable that the processor supports a glueless interface to external memory.
- NAL communications hardware supporting four general-purpose I/O ports (UARTs) with data rates of at least 1 Mbps.
- Hardware supporting a standard high-speed serial interface for communication with the DAL.

No affordable processors containing four homogeneous high-speed serial communications ports were available, so external UARTs will be required. The processor most closely matching the remaining requirements, and which has been selected, is the Texas Instruments TMS320C5509, whose capabilities are listed in Appendix 2.

Inter-cellular communications requirements

The NAL communications software must implement not only communications to each port, but it should also act as a multi-port router for transmission of data between other NAPs. This must be done in a flexible manner so the CD can be used to experiment with networking protocols. The types of communications required are as follows.

- Initialization. Code and data need to be sent to each NAP using the NAL, stored and then executed.
- Diagnostics. As the CD will be used as an experimental tool, it will be useful to have the ability to obtain diagnostic information that is not otherwise used.
- Agent Communication. This is the communication between software agents running on the processors. There may be frequent changes to operational communications protocols, so a capability for updating software during initialization is required. Communications between different types of software agents may require multiple protocols to be running simultaneously.
- Packet Routing. Where agent communication is not just between adjacent processors with a direct communication path, there will be a need for routing of communications packets. Different protocols, or experiments with different network topologies, may also require different routing algorithms.

Communications software architecture

The architecture of the communications software required to satisfy these requirements will take the form of a layered communications stack. A schematic diagram of its structure is given in Figure 5.2. Further details of the stack architecture, and of the protocols that have been designed so far, are provided in Appendix 2.

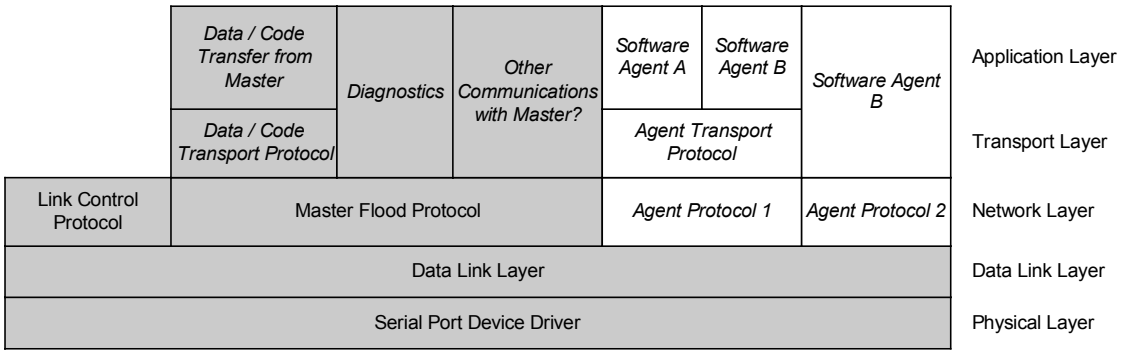

Figure 5.2: The communications stack to be implemented on the concept demonstrator. The protocols in italics are indicative only and have not yet been defined. The protocols with a grey background will be implemented in the NAP FLASH memory, while the others may be downloaded at initialization.

At the bottom of the stack is the serial port driver, which is responsible for controlling the physical communications hardware, and the Data Link Layer (DLL) passes data through the serial port driver. The DLL controls communications between two processors across a physical link and forms the next lowest level in the stack. The DLL protocol is fixed and it is not intended that it be changed.

In the next level are the network protocols, and the data link protocol can support multiple simultaneous network protocols. To allow network protocols downloaded during initialization to be used, the data link uses the concept of registering a network protocol. Therefore, some network protocols (e.g. for initialization) must reside in the processor FLASH memory, and some may be downloaded during initialization (e.g. agent communication).

From the network layer up, the stack is not fixed, as new protocols can be transferred through the network and registered with the DLL. The transport layer (like TCP for the internet) provides reliable end-to-end communications based on the unreliable transport of packets at the network layer, but it is not needed for all applications. The agent protocols are indicative only of what could be done, and will not be further described in this document.

5.4 Current status

Details of other aspects of the design of the electronic system, including power distribution, physical interconnections, UART selection, the possibility of a synchronizing clock distribution, etc. are contained in Appendix 2. Design work is well advanced with the exception of some aspects that require further investigation,

such as the processing required for interpretation of the sensor data (see also Section 4 and Appendix 1). Development of NAL communications software has commenced, some functions (the Data Link Layer and Link Control Protocol, see Figure 5.2) have been successfully implemented, and test hardware for implementation of the NAL communications ports has been built.

A significant issue still to be investigated concerns the influence of EMI, particularly that generated by the processors and communications hardware, on the sensor outputs, and means for providing adequate shielding.

6. Computer Simulation of Self-Reconfigurable Sensor Networks in Ageless Aerospace Vehicles

6.1 Introduction

This Section, and an expanded version provided as Appendix 3, describes the underlying principles, methodology, preliminary results, and future directions for modeling and simulating a multi-agent system made of units that will be referred to as "cells". Initially, these cells will form a physical shell for an aerospace vehicle, and will also have embedded sensors, logic, and communications. Later implementations may contain cells that are mobile, carrying their physical and logical capabilities to wherever they are needed, perhaps performing active measurements using in-built sensors, or other functions. Single cells may need to make fast and automatic responses to sudden damage, while collections of cells may solve more complex tasks, such as creating the boundary of an impact-damaged region.

The present work is aimed at investigating the use of a non-hierarchical system of agents, from which a global response emerges from purely local information and interactions. Such a system contains no supervisor and no central intelligence to direct agents' behaviour and responses. Major benefits of this approach in the context of an ageless vehicle are that there is no single point of vulnerability, and no requirement for explicitly provided redundancy. The inherent redundancy of a multi-agent system is utilized to enable the system to continue operating when individual agents are damaged.

This Section describes the development, within the Simulator, of two algorithms that will form the basis of the intelligent response of the initial stage of development of the CD. These two algorithms embody the following strategies.

1. A strategy appropriate to situations where major damage is inflicted on one or more cells by one or more impacts. This would include damage in which the skin is penetrated and/or the functionality of the cell is impaired. The initial aim of this strategy is the formation of "impact boundaries" that enclose critically damaged areas.
2. A strategy appropriate for the case of minor damage to the vehicle skin produced by one or more impacts. This would include impacts that did not penetrate the skin and resulted in no damage to the cell functionality. Such impacts may require repair of skin damage, but even when repair is not required, the system needs to be aware of the occurrence, rate and spatial clustering of impacts.

It is intended that a hybrid version of these algorithms will be implemented in the initial development stage of the CD (see Section 7), while further development and evaluation of these algorithms and others will continue using the computer simulator.

6.2 Methodology

The primary principle on which this work is based is that a *global response emerges* as a result of local interactions involving transfer of purely local information. The major reason for adopting this approach is to increase reliability in the presence of

damage or failure. The second important principle is *economy of information* – the behaviour of each cell should be as simple as possible, in terms of both its internal logic and communication strategies. Economy of information should result in a simpler cell, which in turn should make it easier to manufacture new cells and to repair or replace damaged cells.

Recent advances in sensor networks and micro-electro-mechanical systems (MEMS) and devices led to the idea of localized algorithms, by which a desired global objective is achieved from simple behaviours of network nodes (agents) that communicate only within a restricted neighbourhood (Estrin et al., 1999). However, despite some progress, there is a lack of a unifying methodology for the design of localized algorithms. Major problems include how to constrain the emergent behaviour to that which is desirable, and how to systematically transform the global task to individual behaviour models. Thus, the problem of global response engineering in multi-agent networks is of central importance to this project.

The proposed methodology for this work is based on an iterative process including the following steps:

a) forward simulation (for a class of localized algorithms dealing with impacts of various strengths), leading to observation of emergent behaviour;
b) measurement of emergent behaviour (based on information-theoretic metrics for bounded emergent behaviour);
c) evolutionary modeling of the desired global emergent behaviour, where the fitness functions correspond to the metrics obtained at step (b).

This Section reports work that is part of step (a).

6.3 Simulated cell structure and agent behaviour

The fundamental components of an autonomous agent (or cell) are:

- structure – the physical shape of the cell;
- sensors – to obtain data readings from the environment;
- logic and memory – to process sensed data, interpret the data (to the extent local interpretation is possible), make decisions and perform useful tasks;
- communications – to read and write messages for interaction with neighbouring cells;
- energy – to enable the cell to perform all its tasks; and
- mobility – actuators enabling movement (changing surface shape, movement of mobile cells, cell replacement, etc.) within the environment.

Figure 6.1 shows a square planar cell containing these components, except for the mobility unit.

When impact damage occurs, the cell's physical functionality can be impaired and any or all of its components may be damaged. Thus, damage may affect sensors (no readings or increased noise levels), the logic unit, the communications ports (possibly affecting communications in either or both directions), the energy unit (reducing or eliminating available energy), or the mobility unit.

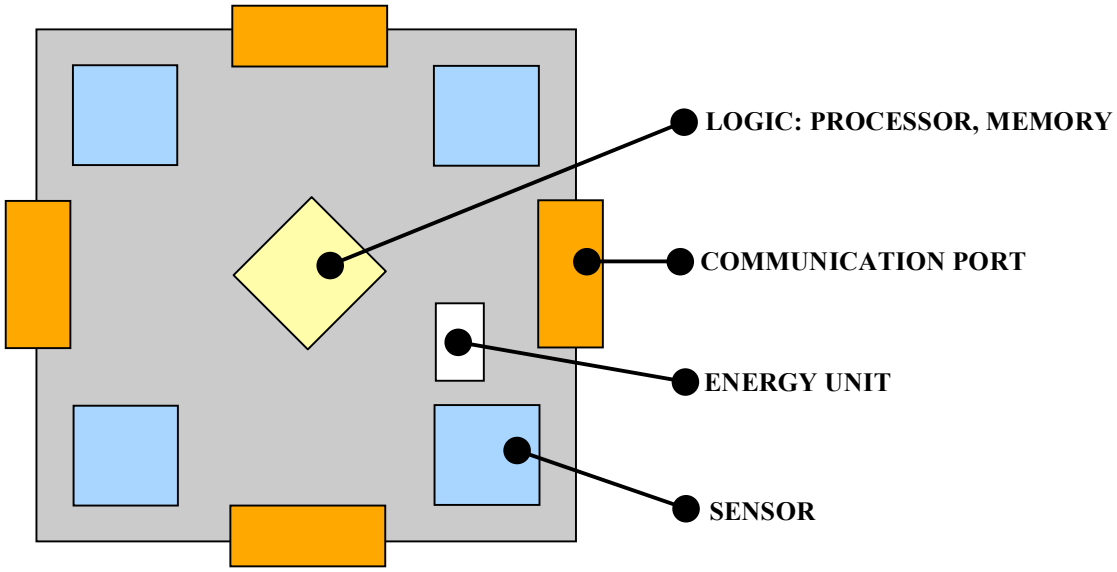

Figure 6.1: A square cell with 4 communication ports.

Cells may have a range of reactive behaviours embedded in their logic unit. The Deep Behaviour Projection (DBP) framework (Prokopenko et al., 2001; Prokopenko and Wang, 2002) has been adopted to represent increasing levels of agent reasoning abilities, where every new level can be projected onto a deeper (more basic) behaviour. DBP behaviour can be present in the architecture in two forms: implicit (emergent) and explicit (embedded). What the DBP approach suggests in particular is that the reactive/cognitive distinction is always relative in a hierarchical architecture. The behaviour produced by the level $\mathbf{l}_k$ may appear reactive with respect to the level $\mathbf{l}_{k-1}$ but, at the same time, may look deliberate with respect to the level $\mathbf{l}_{k+1}$. This can be illustrated by the following three behaviour levels:

- tropistic behaviour: Sensing → Response,
- hysteretic behaviour: Sensing & Memory → Response,
- tactical behaviour: Sensing & Memory & Task → Response.

Hysteretic behaviour is generally more reactive than tactical behaviour, because the latter uses the task states in determining a response. However, by contrast with very basic tropistic behaviour, the hysteresis provided by (internal) memory states ensures a *degree* of cognition: the hysteretic behaviour involves lagging of an effect behind its cause, providing a (temporary) resistance to change. For example, hysteretic behaviour is able to distinguish a persistent communication failure with an adjacent cell from an occasional noise-induced miscommunication. This ability is embedded explicitly by specifying a filter length.

6.4 Simulation of the AAV

A flexible architecture was developed for simulating the modular surface or skin of the vehicle, comprising the cells described above. At this stage, all cells are identical. Furthermore, the simulator has the ability to simulate simple environmental effects, such as the incidence of small impacts. The initial aim of the simulator is to study the

effects produced by different communications strategies and locally embedded behaviours.

In general, many events may occur in parallel, so the simulation has a (non-real time) clock, and all events have a defined duration. The simulation is essentially a state machine that sweeps through the elements (cells) of the system and updates their current state $\mathbf{S_i(t)}$ at time point **t** on a regular basis. Cells are represented as (mobile) objects (polygons) on a two-dimensional plane (Figure 6.2), where they interact with their immediate neighbours through connected (geometrically overlapping) communication ports.

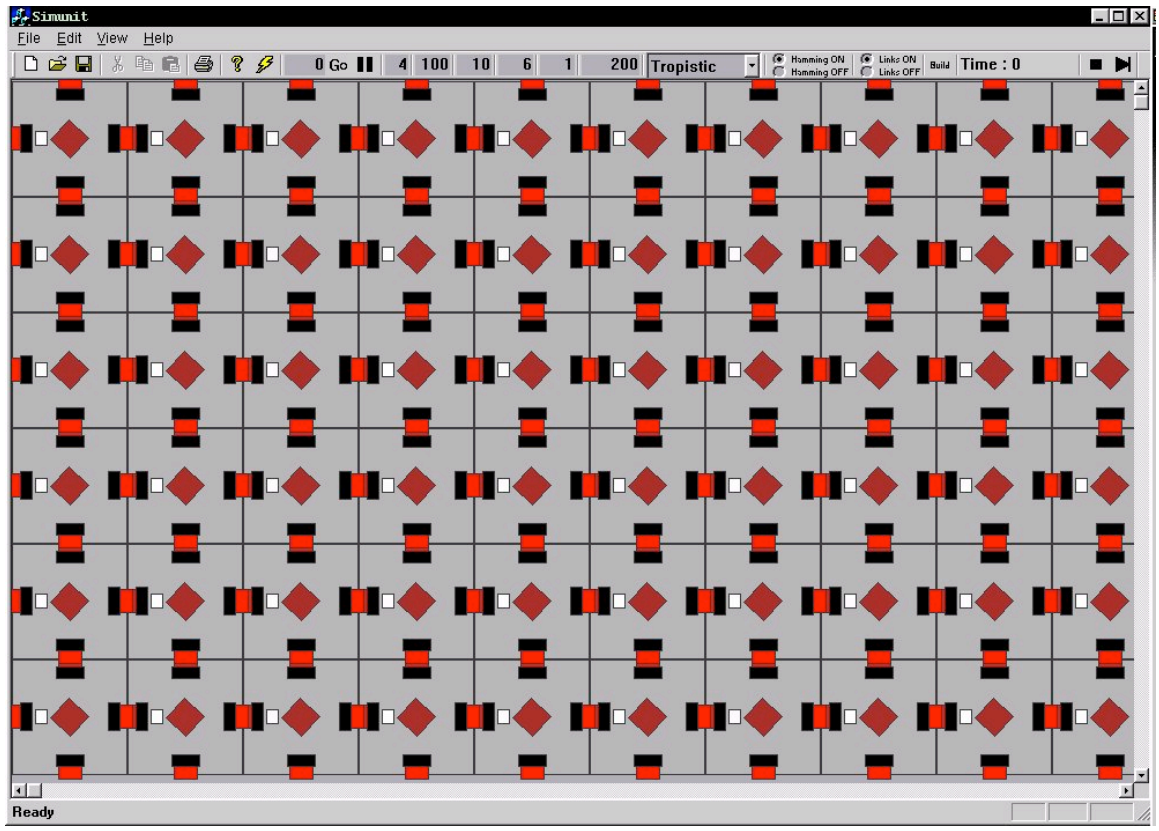

Figure 6.2: An initial configuration of 10x6 square cells.

The next state is, generally, dependent only upon the current state and current inputs, so the next state is a result of interactions with immediate neighbours. The decision about what is the next state of each element depends upon an algorithm, which could be quite complicated, embedded in the cell logic.

6.5 Self-organizing impact boundaries: algorithms and simulation results

This sub-section describes the development and performance of an algorithm for the creation of self-organizing impact boundaries, to apply to situations where critical (disabling) damage to the structure and functionality of one or more cells is produced by one or more impacts. An incremental approach was followed in studying

conditions leading to robust, stable and regular self-organizing impact boundaries: the aim was to keep the algorithm simple by imposing as few requirements as possible. It is assumed that, for a critical impact, the impact energy may be dissipated through a number of neighbouring cells, destroying or disabling those close to the point of the impact and possibly damaging other cells. Communications are likely to be affected by this energy dissipation. Communication damage is simulated by a "bit-by-bit" corruption, by assigning a probability of a bit error that depends on the proximity of the affected communication port to the impact epicentre.

Frame boundary

The first objective was formation of a boundary that is not necessarily continuously connected as a closed circuit, but which separates cells that have suffered unrecoverable communication damage (including those that were completely destroyed) from those that are able to communicate normally. Such a preliminary border, it was hoped, would form a "frame" for the desired closed boundary, regardless of cell shape (triangular or square). Steps investigated in the development of a suitable algorithm are outlined in Appendix 3.

Four possible states are defined for each cell: the cell is destroyed or disabled; the cell is damaged or is surrounded by damaged cells (referred to as a "scaffolding" state); the cell has some good and some damaged neighbours (a frame boundary state); and the normal, fully functional state. The successful strategy resulted in a stable self-organizing boundary around the damaged area. An example is shown in Figure 6.3.

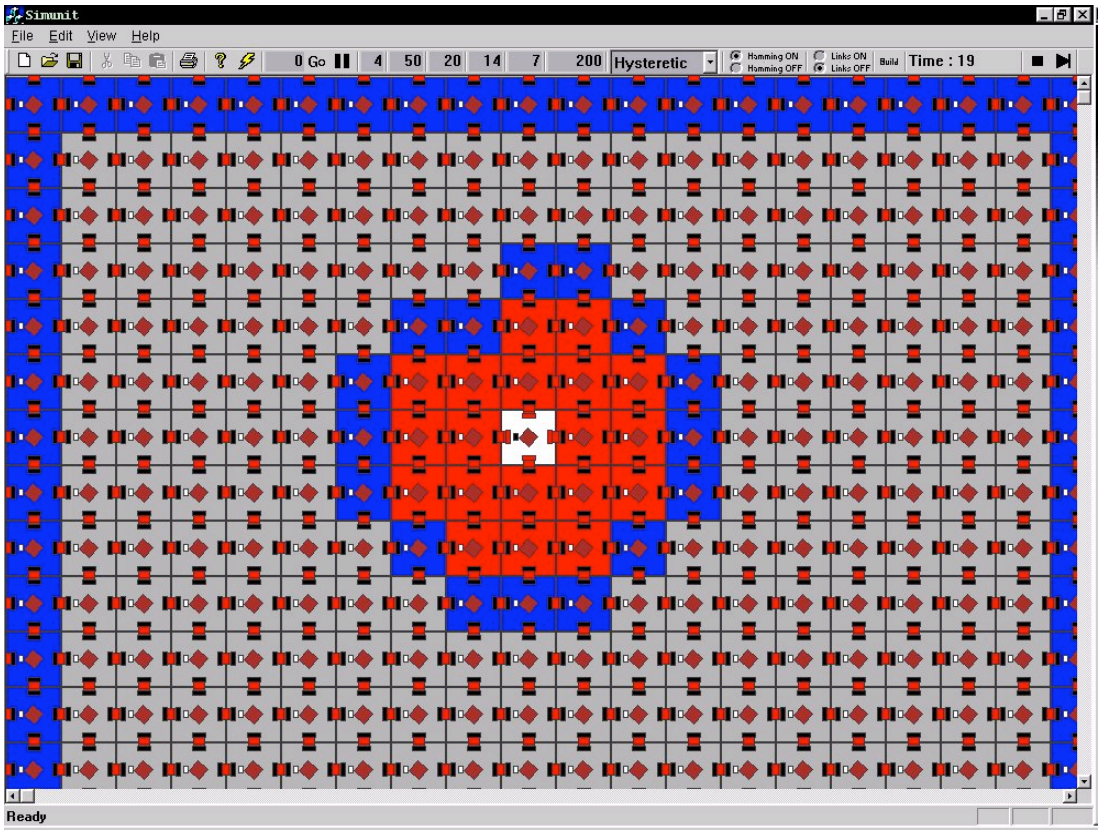

Figure 6.3: A regular frame boundary produced by the strategy devised in this work (see Appendix 3). Normal cells are light grey, cells in the frame boundary state are blue, those in the scaffolding state are red, and destroyed or disabled cells are white.

Closed boundary

Creation of the frame boundary is the first stage leading to the desired continuously connected (closed) boundaries that would clearly delineate damaged areas. In order to generate links between disconnected cells on the frame boundary, it was necessary to introduce some additional rules. The additional communication rules required to generate a closed boundary around the impact region are a little more complicated than those for the frame boundary. They are described in detail in Appendix 3.

The strategy adopted, which includes the frame boundary rules and adds some more, achieves the desired robustness and continuity of self-organizing impact boundaries for a variety of cell shapes, impact energy dissipation profiles and communication damage probability models. An example of triangular cells with hysteretic behaviour is shown in Figure 6.4. Triangular cells are shown in this example because for this case convergence was more difficult than for square cells.

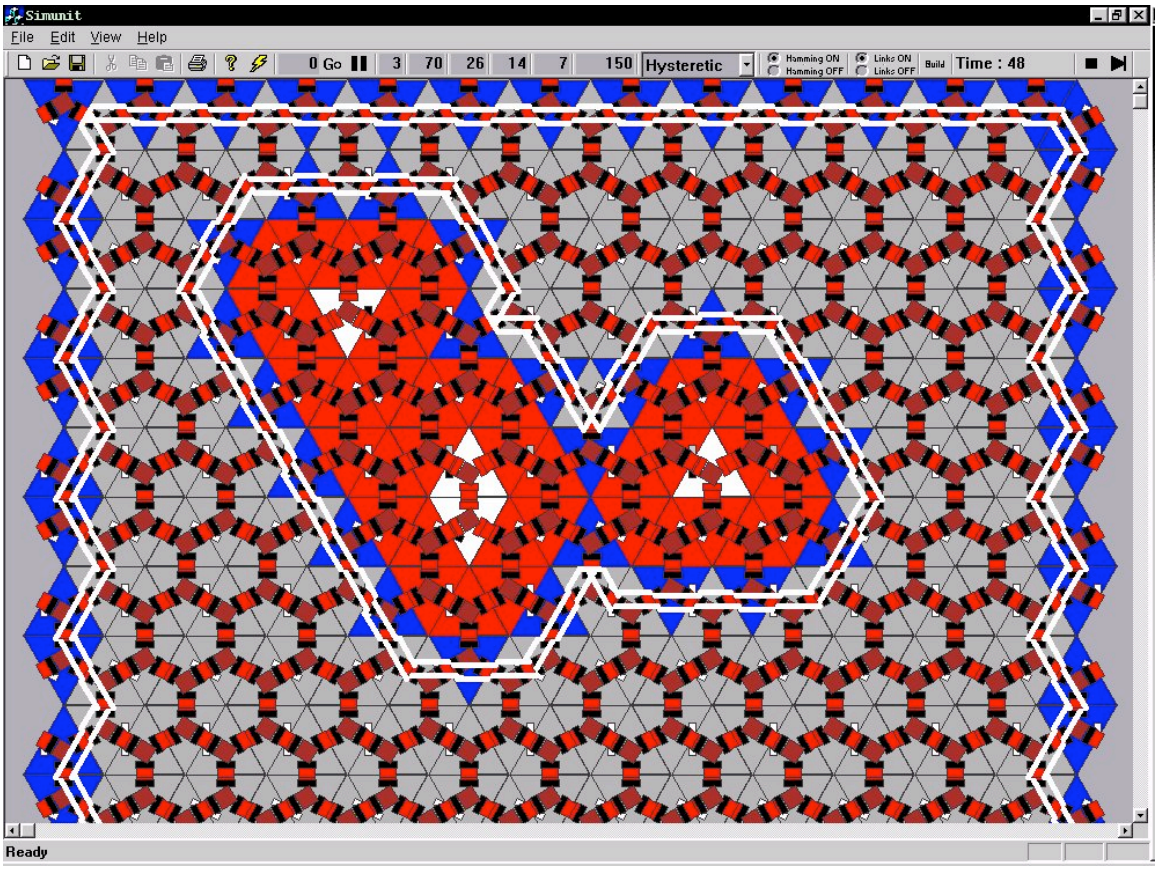

Figure 6.4: A robust emergent closed boundary formed on a skin of triangular cells, with hysteretic behaviour. The double white lines are the closed impact boundary.

Figure 6.4 demonstrates the result of a strategy for constructing a stable, closed boundary around a damaged region using only the local information obtained by the cells on the boundary from their immediate neighbours. It is a structure that emerges from the local interactions between the cells, and requires no hierarchical overview. It is a genuinely emergent response to the detected impact damage.

6.6 Self-organizing impact spanning trees: algorithms and simulation results

The self-organizing impact boundaries described above are useful when cells at or close to the impact points are destroyed, when communication links between cells in the neighbourhood of an impact, or other cell functions, are damaged. However, when dealing with non-critical impacts, which may damage the skin but not affect the functionality of the cell, it is possible to obtain information directly from the cells that register the impact. In these cases the communication links between the cells that are close to the impact point are likely to remain intact. This suggests the use of the impact points (detected by the individual cells) as nodes in an *impact network*, in which direct linking paths connect impact sites. Such impact networks may be needed to conduct a rapid inspection of the impact area, to determine impact densities and/or to route the repair resources.

The concept of the impact network introduced here makes it possible to apply some fairly well-known algorithms, such as Ant Colony Systems (ACS) algorithms proposed by Dorigo et al. (1991), to the problem of impact analysis in the AAV. ACS algorithms use the ability of agents to indirectly interact through changes in their environment by depositing pheromones and forming a pheromone trail. They also employ a form of autocatalytic behaviour – the probability with which an ant chooses a trail increases with the number of ants that chose the same path in the past.

However, the AAV simulation presents significant challenges to the direct application of ACS algorithms, due to the fact that impact sites are not known in advance, and that they may appear rapidly: the impact networks are highly dynamic. Furthermore, it would be impractical to employ a measure based on knowledge of the distance between two impacts because individual cells have no record of their absolute coordinates. These issues are detailed in Appendix 3.

The hybrid method of establishing impact networks proposed in this report is based on a single *impact gradient field (IGF)*, used to complement the autocatalytic behaviour of ant-like agents. This gradient field is created by *all* impacts in a given spatio-temporal neighbourhood. Obviously, by superimposing the effects of all impacts, we lose optimal routes between an individual cell and a given impact node, but we gain in economy of information: each cell keeps only a single IGF value. The IGF values are initialized to infinity and then established by propagating messages from impact nodes.

The strategy employed (Appendix 3) establishes a single IGF because each cell minimizes gradients to all impact nodes. The minimization scheme approximates vector superposition used in gravity field calculations. An important aspect of the strategy is that propagation of IGF values from each impact node does not result in message flooding: eventually the propagation waves meet each other and stop along the ridge regions, which are said to correspond to regions of "weightlessness" in a gravity field (Figure 6.5). The IGF is up-dated regularly, or when new impacts occur.

The general principle is that each impact node generates a number of exploring ants, which seek to establish direct paths to other impact nodes. The ants are implemented as communication message packets in this case, but could equally well be mobile

inspection or repair agents. The IGF helps to guide ant-like agents, especially during the initial exploration phase: rather than explore the area randomly the agents may ascend along the gradient until they reach a ridge region, and only then switch to random exploration.

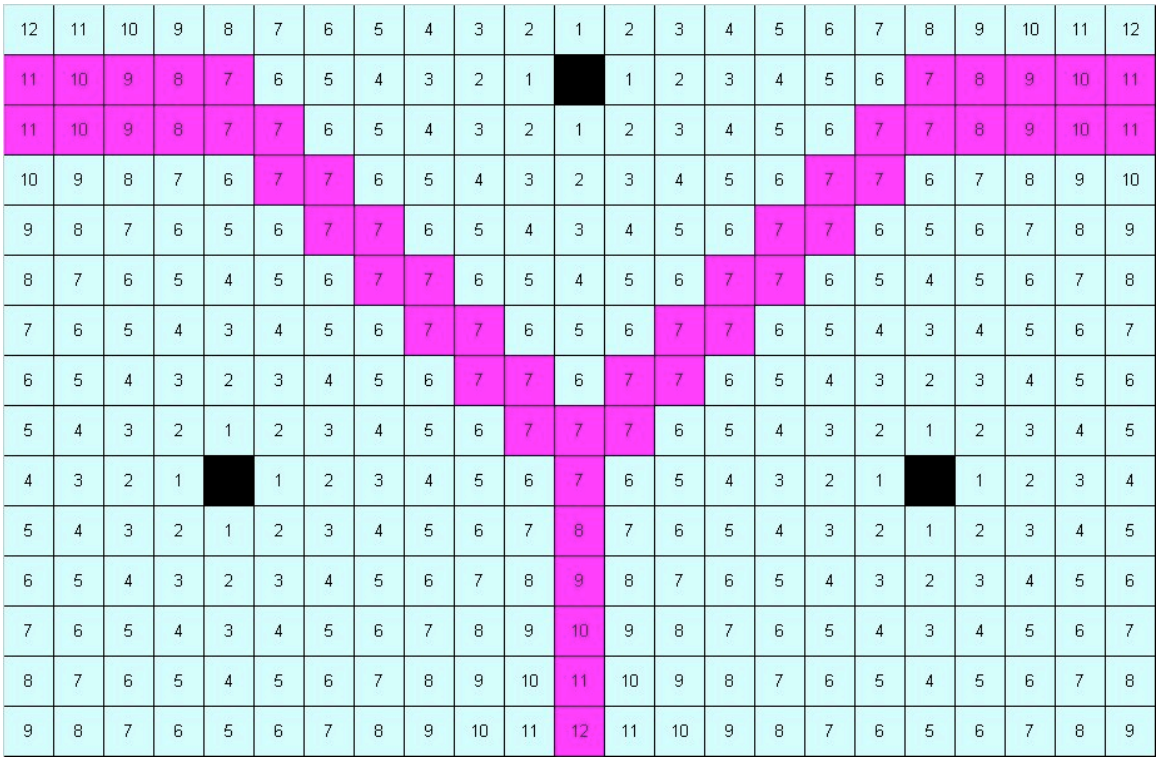

Figure 6.5: An example of an Impact Gradient Field: black cells are impact nodes; purple (dark) cells form the ridge (weightless) region.

When an exploring ant/agent reaches another impact node, it seeks to return to its home node using a dead reckoning scheme. In general, ants proceeding along a shorter return path deposit more pheromone than ants that selected a longer path, simply because the deposited amount is inversely proportional to the traversed distance. A higher quantity of pheromone attracts more ants, producing a positive reinforcement. Eventually, the shortest trail is established between the pair of impact nodes. It is important to note that for any such pair of nodes, both impact nodes generate exploring ants that potentially find the other impact node and return back. The shortest trail is therefore reinforced by returning ants going in opposite directions.

Detailed rules for the ants' movements are given in Appendix 3. An example of a simple impact network developed in this way is shown in Figure 6.6.

Obstacles caused by damaged cells

Because the ants are implemented as message packets, their movement strategies are implemented via appropriate message passing in which the cells are responsible for unpacking the packets, interpreting them, and propagating updated packets according to the strategy rules. Thus, ants cannot move into the cells with damaged (or shut-down) communication links. Therefore, the regions enclosed by self-organizing impact boundaries described in the previous sub-section form obstacles, and the ants

are supposed to find the shortest paths around them using positively reinforced pheromone trails.

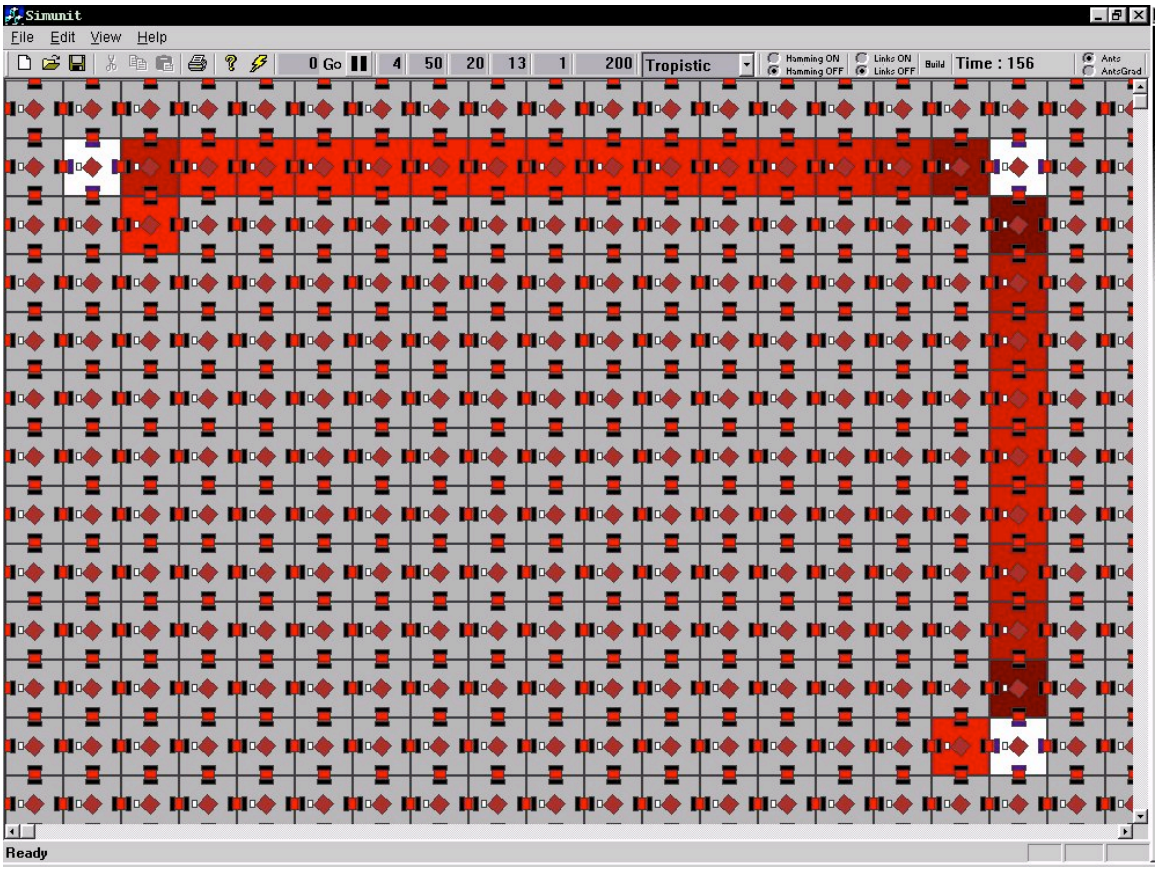

Figure 6.6: An example of a spanning tree in a simple impact network. The impact nodes are the white cells. Different shades of red (dark) colour represent the trail intensity, which is greater for darker cells. A diagonal trail is also present but is much weaker: its trail intensity is below a visualization threshold.

Similar ant movement strategies are followed in this case, except that an ant cannot enter a damaged region. When it reaches an impact boundary it can move one way or the other along the boundary, depending on the impact gradient, on the strength of an existing pheromone trail, or by random selection. Again, pheromone deposits from returning ants will reinforce a shorter trail around an obstacle. An example of such a self-organized path around an obstacle is shown in Figure 6.7.

At this stage two strategies have been investigated. The first did not employ an IGF at all, with the ants relying on random exploration and pre-existing paths to locate impact nodes, while the second used all the IGF rules presented in Appendix 3. The strategies were investigated with the aim of observing the emergence of shortest paths and spanning trees in impact networks (e.g. Figure 6.6). The second (IGF) strategy performed better, as expected, but only a formal evaluation that will be carried out later will show if its benefits are worth the additional time cost.

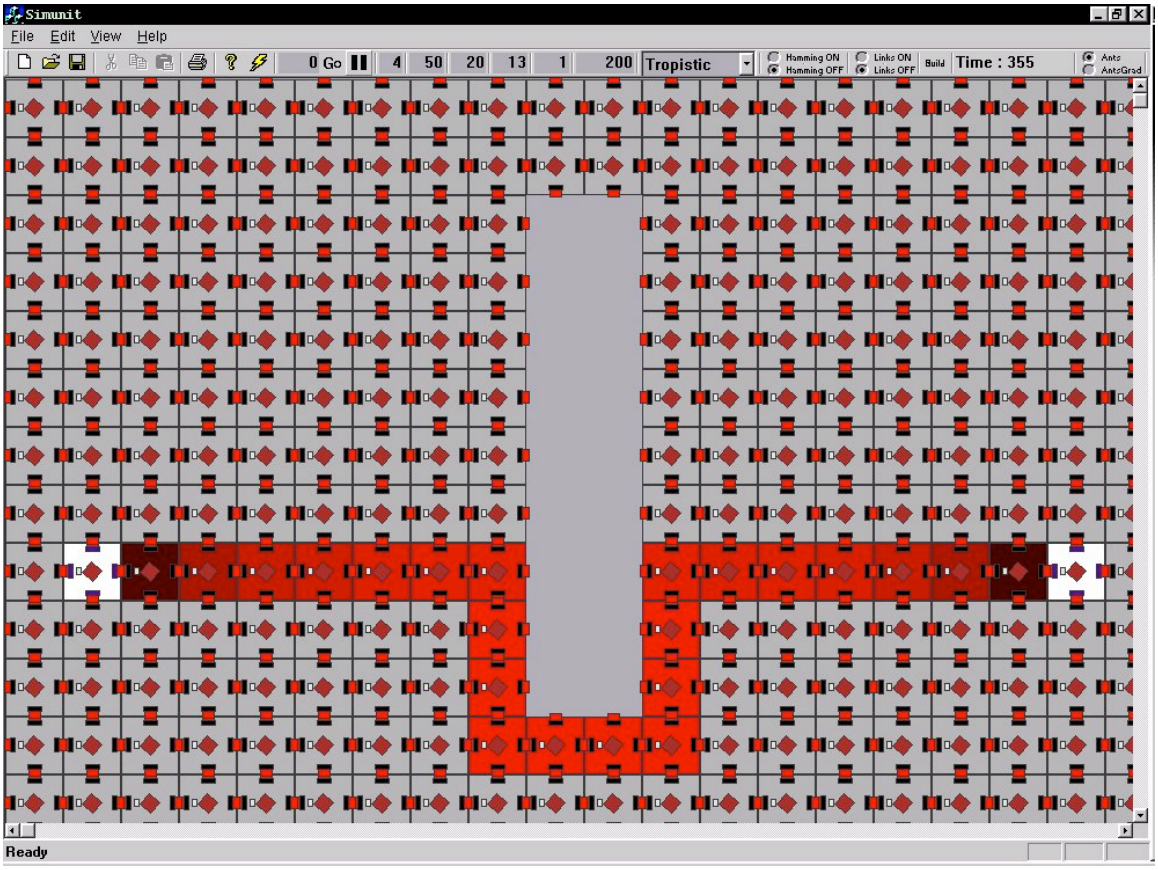

Figure 6.7: An example of a shortest path between two impact nodes (white cells) around an obstacle. Different shades of red (dark) colour represent the trail intensity, which is greater for darker cells.

6.7 Future directions

The described communication strategies, behaviours and emergent patterns of impact boundaries and impact networks demonstrate the potential of self-organizing multi-agent networks for detecting and containing critically damaged sections of the modular multi-cellular aerospace vehicle skin.

The main challenge in the immediate future will be to investigate the information-theoretic complexity of various communication strategies, and relate it to the coordination of the agents.

7. The Concept Demonstrator Intelligent System

The software and hardware that enables the Concept Demonstrator (CD) to respond intelligently to impacts or other threats or events is expected to be developed over a number of years, following the development and testing of concepts and strategies in the Computer Simulator (CS) described in the previous Section. Experimental testing of this software cannot begin until the construction and basic functional testing of the CD is largely complete. This is expected to take a large proportion of the time available for the first stage of development, so it is expected that the level of intelligence that can be demonstrated by the CD at this stage will be relatively limited.

The initial aim is to implement in the CD the impact boundaries and impact networks algorithms described in the previous Section. This will enable the CD to deduce the extent of critically damaged areas using self-organized boundaries, and to form a network of impact sites. The only response planned at this stage is to display this information graphically on a remote computer screen.

The display system will be run from a remote computer that collects information from the distributed processors in the CD via (at least in the first instance) a cable. Details of the interface between the CD processors (agents) and the display computer have not yet been worked out, but it is important to emphasize that the display computer will simply be displaying information it receives from the distributed system that is the CD. It will not be acting as a supervisor, or a "master computer" in any sense, but more like a slave that enables the CD to provide a visual summary of its aggregated information for the benefit of human observers.

There are still a number of issues to be considered and resolved, including the following.

1. Should the multi-agent algorithms run synchronously, as they do at present in the simulator, or asynchronously? Synchronous operation would require a synchronizing clock signal to be supplied to all processors. Advantages and difficulties of providing such a signal have been canvassed in Section 5 (and Appendix 2). Asynchronous operation would seem preferable from the points of view of flexibility and reliability.

2. Amalgamation of the impact boundaries and impact network algorithms. How this should be done will depend on the priority given to locating boundaries of critical impacts relative to mapping the network of non-critical impacts.

3. Detection of critical damage caused by impact, and distinguishing it from electronic failure on a cell. Functional (electronic) failure of a cell can be detected by regular polling of the communications ports by neighbouring cells (e.g. by sending a message and requesting an acknowledgement). If a cell is damaged to an extent that prevents it communicating with its neighbours, the only immediate indication of whether this was caused by impact rather than electronic failure may be the detection of impact signals by sensors on neighbouring cells. Therefore cells may need to be monitored for impact on neighbouring cells.

4. Code implementation of algorithms for CD processors.

5. Details of the hardware and software interface between CD processors and display. How does each cell send a packet of information describing its state to the display processor, and when? One (extreme) solution is a dedicated communication line from each processor to the display, which may also be useful for initial debugging of the system. However it is a somewhat heavy-handed and inelegant solution. Perhaps a set of software agents (ants) can collect and transmit information for the display processor.

6. Coding of the display infrastructure.

While high-level design objectives for this important aspect of the CD are clear, there are still a number of quite complex problems to be solved. However, sensible resolution of these issues cannot be completed without further work in the sensors, electronics, communications and simulation areas. This will be a continuing priority in the immediate future.

8. Summary and Conclusions

This Report provides an outline of the essential features of the Concept Demonstrator that will be constructed during the next eight months. It has been emphasized throughout that the design cannot be considered to be complete, and that design work will continue in parallel with construction and testing. A major advantage of the modular design is that small modules of the system can be developed, tested and modified before a commitment is made to full system development.

It has also been emphasized that the CD is expected to develop and evolve for a number of years after its initial construction. This first stage will, of necessity, be relatively simple and have limited capabilities. Later developments will improve all aspects of the functionality of the system, including sensing, processing, communications, intelligence and response. The various Sections of the Report indicate some of the directions this later development will take.

References

Christiansen, E. L., Kerr, J. H., De La Fuente, H. M. and Schneider, W. C., (1999) "Flexible and deployable meteoroid/debris shielding for spacecraft", Int. J. Impact Engng., **23**, 125-136.

CTIP (2001) *Development and Evaluation of Sensor Concepts for Ageless Aerospace Vehicles, Report 1: Threats and Measurands*. CSIRO Telecommunications and Industrial Physics. Confidential Report No. TIPP 1516. December 2001. Also published as NASA technical report NASA/CR-2002-211772, Langley Research Center, Hampton, Virginia.

CTIP (2002). *Development and Evaluation of Sensor Concepts for Ageless Aerospace Vehicles. Development of Concepts for an Intelligent Sensing System.* CSIRO Telecommunications and Industrial Physics. Confidential Report No. TIPP 1517. May 2002. Also published as NASA technical report NASA/CR-2002-211773, Langley Research Center, Hampton, Virginia.

Dorigo M., Maniezzo, V. and Colorni, A. (1991). "The Ant System: An Autocatalytic Optimizing Process." *Technical Report No. 91-016 Revised*, Politecnico di Milano, Italy.

Estrin, D., Govindan, R., Heidemann, J. and Kumar, S. (1999). "Next Century Challenges: Scalable Coordination in Sensor Networks." In Proceedings of the Fifth Annual International Conference on Mobile Computing and Networks (MobiCOM '99), August 1999, Seattle, Washington (Mobicom'99), Seattle, USA.

Prokopenko, M. and Wang, P. (2002). "Relating the Entropy of Joint Beliefs to Multi-Agent Coordination." In Proceedings of the 6th International Symposium on RoboCup, 2002.

Prokopenko, M., Wang, P. and Howard, T. (2001). "Cyberoos '01: 'Deep Behaviour Projection' Agent Architecture." In RoboCup-2001: Robot Soccer World Cup V, Springer, 2001.

Prosser, W. H., Gorman, M. R. and Humes, D. H., (1999) "Acoustic Emission Signals in Thin Plates Produced by Impact Damage", J. Acoust. Emission, **17** (1-2), 29-36.

Scruby, C.B and Drain. L. E., (1990) **Laser Ultrasonics, Techniques and Applications**, Adam Hilger, Bristol.

Appendix 1: Detailed Discussion of Sensors and Sensing

A1.1 Introduction

This Appendix outlines progress made towards developing smart sensors for the Concept Demonstrator. It amplifies and adds detail to the material presented in Section 4. It should be made clear that it is not the aim of this stage of the project to develop new sensors, but rather take existing technology and use it in an appropriate way to produce a reliable platform for further development at a later stage. The primary aim is to develop an operational demonstrator in which impacts generate signals that may be processed intelligently and communicated parsimoniously, and to link such systems with a simulation of impact and communication events in order to obtain the location, severity and consequences of impacts.

The basic sensing requirements and strategies that have been adopted are delineated below, followed by a description of the structure under construction, a report on experiments using various sensors detecting simulated impacts and a discussion of the implications of these results. To conclude, experiments in progress and the immediate future research will be outlined.

A1.2 Sensing requirements and strategies

Sensors for detecting particle impacts

There are a number of sensor types that can and have been used to detect particle impacts. A number of space missions have carried meteoroid and orbital debris detection and counting experiments. Examples are the OMDC (Orbital Meteoroid and Debris Counting Experiment) on the Clementine spacecraft, and the Cosmic Dust Analyzer (CDA) on the Cassini-Huygens mission, but there have been others such as VEGA, Giotto, Galileo and Ulysses. The sensors used in these missions can all be categorized as direct detectors, in the sense that the particle impacts the sensor directly, generally producing some level of damage in the sensor.

Some types of sensors that could be used to detect impacts directly include the following.

- Semiconductor detectors. These consist of a semiconductor wafer with a bias voltage applied using electrodes on the two flat surfaces. An impacting particle penetrates the wafer and produces ionization, which is detected as a current pulse. Sensors of this type have been flown on NASA missions such as the OMDC on the Clementine spacecraft to detect and quantify the particle (meteoroid and space debris) flux in earth orbit (see, e.g. http://setas-www.larc.nasa.gov/CLEM/whk_pub.html).
- Ferroelectric polymer detectors. These operate on a similar principle to the semiconductor detectors, but employ a permanently poled ferroelectric film and detect the depolarization signals generated by the passage of an impacting particle through the polarized polymer. The Cassini Cosmic Dust Analyzer contained examples of this type of sensor (see, e.g. http://saturn.jpl.nasa.gov/spacecraft/instruments-cassini-cda.cfm).

- Photoelastic detectors. For suitable (transparent) materials (e.g. Perspex) internal strain fields produced by an impact could be detected optically using polarized light.
- Triboluminescent detectors. Many solids show the phenomenon of triboluminescence, the emission of light when the material is crushed, fractured or rubbed. The phenomenon has been known for many years, but only recently has been studied with a view to damage sensing (e.g. Sweeting (http://www.towson.edu/~sweeting/wg/candywww.htm), Sage et al.(1999, 2001)). A thin film of a triboluminescent material could be coated on the outer surface of the vehicle skin, and emitted light pulses detected optically.

There are other detection methods, classified as indirect detection techniques, which detect the effect of an impact on the vehicle skin. In such cases the detector may be less prone to damage from the impact than are direct detectors. Indirect sensors may include the following.

- Elastic wave detection sensors. Detection of elastic waves generated in the skin and surrounding structure by the impact, and which propagate away from the impact site. This is generally referred to as acoustic emission (AE). AE sensors are commonly piezoelectric, either bonded to or in pressure contact with the skin surface. However, other types of sensors can also be used for AE detection, such as optical (interferometric), electromagnetic acoustic sensors (EMATs), capacitive sensors, etc. Piezoelectric sensors will be discussed further below.
- Temperature or IR radiation sensors. Detection of the heat generated by an impact, either indirectly by detecting the heat conducted through the skin to an array of temperature sensors, or directly by imaging the IR radiation emitted from the impact site.
- Accelerometers. Detect momentum transfer to skin or to vehicle by means of remote accelerometers, possibly located on the inside surface of the skin. Could be developed as MEMS devices.
- Acoustic sensors (for airborne sound). Sensing of the sound emitted by the impact, preferably from inside the vehicle (since outside may be a vacuum).
- Optical imaging of surface deformation. Use of interferometric, shearographic or holographic imaging techniques to detect surface deformations (transient or static) produced by an impact.

Direct detection sensors are attractive because they sense directly, and require minimal signal processing to obtain spatial information about an impact. The sensor dimensions determine spatial resolution. In the long term, it seems likely that a sensory material would detect impacts and impact damage directly, so use of direct detection sensors may be more consistent with the eventual long-term solution.

On the other hand, direct detection sensors would need to form a quasi-continuous layer on the outer surface of the vehicle skin. In many cases they may be more susceptible to damage than the skin itself, which would reduce the effective durability of the skin. To compound this problem, it is difficult to see how redundancy can be easily built into a system of direct detection sensors, and the system cannot be reconfigured to compensate for damage to or failure of a sensor.

One of the initial aims of the present work is to detect impacts indirectly, so that the sensor is less prone to being damaged by the impact than is the skin. Possible means of achieving this include detection of the elastic waves generated in the skin by the impact, or detection of thermal or optical emission produced by the impact. Most effort so far has centred on the use of acoustic emission sensors for impact detection. This is attractive for a number of reasons, including the following.

- A relatively small number of sensors can be used to obtain a given spatial resolution for locating the impact site.
- The sensors can be mounted on the back (inside) surface of the skin.
- The system can be built with redundancy of sensors, and the ability to reconfigure to compensate for damage or failure.
- The functional flexibility of AE sensors, which can also be used to detect the emission from a number of other damage-related events, such as crack (or microcrack) formation and/or propagation, delamination, gas or liquid leaks, various catastrophic events, etc.
- Piezoelectric AE sensors can be used reciprocally to transmit signals, to allow active interrogation of damage or for self-test purposes.

However, there are also disadvantages related to the use of AE sensors. The main one is the complexity of signal processing, particularly in the presence of background structural noise and elastic wave reflections from structural boundaries. Another is the huge dynamic range required to take full advantage of the potential functional flexibility of these sensors. It is therefore desirable that a strategy is developed for using these sensors, which reduces the effects of these disadvantages.

It is envisaged that the CD will be used in the future to test other sensor types and sensing strategies.

Piezoelectric sensors

The proposed sensing strategy is based on the use of piezoelectric film sensors bonded to the back (inside) surface of the skin. In more advanced structures the films may be laminated on or within the material of the skin. Initial experiments are being carried out with PVDF film bonded to the aluminium sheet skin.

In this situation, the use of acoustic emission (AE) techniques requires a number of small piezoelectric sensors to be deployed on the inner surface of the skin, and the received signals processed to provide information concerning impact location and severity. Acoustic emission signals contain a great deal of information, but the processing required can be very complicated if the structure contains discontinuities (such as edges, holes, ribs, supports, stiffeners, etc.) that reflect elastic waves, if damage mechanisms are complex, and if there are multiple impacts. For high-velocity particle impacts, the generated elastic waves will contain quite high frequency components (> 10 MHz), since the bandwidth will increase with the rate of elastic energy transfer to the skin. These signals must be digitally acquired by the processor(s), so use of this high frequency information would require very fast data acquisition capability. Thus, standard acoustic emission techniques, which require a detailed knowledge of the geometry and material properties of the structure concerned, are complicated to apply to the monitoring and analysis of a complex structure with a large number of sensors distributed over it. The processing

requirements and communications strategies may be too demanding and complex for rapid assessment of the effects of multiple impacts.

Proposed sensing strategy and sensor geometry

One of the goals of the proposed sensing strategy is to reduce the processing and data acquisition requirements for the cell processor, both to reduce complexity and cost, and to increase reliability. The objectives of the sensing strategy are, therefore:

- to detect and locate impacts and to evaluate damage as indicated in Section 1;
- to detect penetration of the skin by the impact; and
- to minimize processor and processing requirements, by minimizing the analogue to digital conversion (ADC) speed requirement and simplifying data processing.

To achieve these objectives it is proposed that a dual piezoelectric film sensor be used, as is shown schematically in Figure A1 below for a square cell. It consists of a sheet of piezoelectric film, bonded to and covering the entire inner surface of the skin within the cell boundary, along with (say) 4 small sensors that can be used for acoustic emission sensing. The small sensors may be produced by patterning of the electrodes of the large sheet as illustrated in Figure A1, or they could be separate sensors bonded to the large sensor.

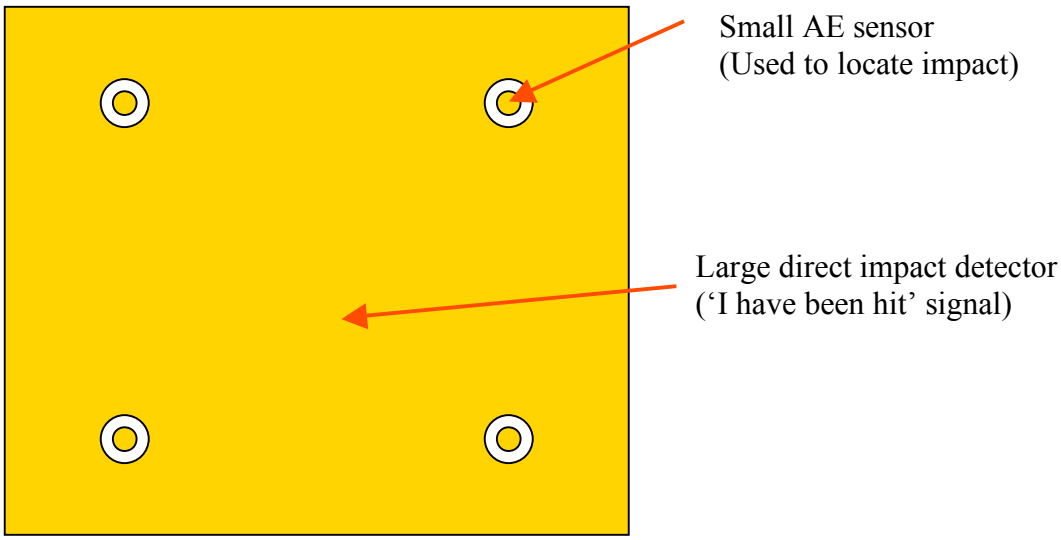

Figure A1: Proposed sensing cell structure for piezoelectric sensing. The cell could equally well be triangular, pentagonal, hexagonal, or some less regular shape.

The purpose of the large sensor is to detect impacts and provide a direct indication that the cell has been hit, i.e. it localizes the impact to within the cell. Experiments using a focused laser pulse (with energy density greater than the ablation threshold) to simulate a particle impact show a clear distinction between the signals produced by pulses that are incident on the aluminium sheet immediately opposite the large sensor, and those that strike the skin even 1 or 2 mm beyond the edge of the sensor. It therefore seems feasible that the large sensor can be used as a direct impact or 'This cell has been hit' sensor.

The position of the impact within the cell may then be determined from the small-sensor signals by relatively simple signal processing, assuming that the skin of the cell is reasonably homogeneous. Straightforward triangulation is used, but this must take account of the dispersive nature of the elastic wave propagation from the impact point to the sensors. We are planning to investigate the following two techniques for carrying out the triangulation. They both depend on the skin material within the cell being uniform and homogeneous.

- Time-of-flight of a single frequency component. A single frequency component of the broadband signal can be isolated using a narrow-band filter. The relative times of arrival at the small sensors can then be determined by cross-correlation techniques, and the triangulation carried out.
- Distance measurement using dispersion. The distance from the impact site to a small sensor is evidenced in the dispersion of the signal reaching the sensor. This can be estimated if two frequency components are isolated using narrow-band filters. The time difference between the arrivals of each component is proportional to the distance over which the signal has propagated, and can be used for triangulation.

Evaluation of these techniques will be undertaken shortly.

Detection of penetration

Additionally, the sensing requirements above require the system to be capable of detecting penetration of the skin by a particle/micro-meteoroid, so a strategy for achieving this must be developed. Can it be done using the piezoelectric film sensors, or are additional sensors of some type required? There would appear to be (at least) four possible ways by which the piezoelectric film sensors outlined above could be used to detect penetration (puncturing) of the skin by an impacting particle. However, while these methods should be sensitive to skin penetration in principle, their practical feasibility is somewhat speculative and has not yet been tested experimentally.

The first method involves detecting the local depolarization of the PVDF film when a particle passes through it. This principle has been used in dust detector systems flown on a number of space missions, including Galileo, Ulysses, Cassini and Stardust (see, e.g. The Cassini Cosmic Dust Detector). These sensors were developed and refined by Simpson and Tuzzolino at the University of Chicago in the 1980s and ‘90s. In these cases, a free-standing film, isolated from acoustic disturbances in the structure, was used to detect incident dust particles, whereas here the film is bonded to the inside surface of the skin. In principle, penetration of the ferroelectric sensor film by a particle should result in the generation of a charge pulse resulting from the local depolarization. In practice, the magnitude of this charge pulse may be small, and it may be difficult or impossible to distinguish it from the acoustic signal that will inevitably accompany the impact. There may be a wide range of effects depending on the particle size, velocity, angle of incidence and composition, and on whether and how it fragments on passing through the skin. In all cases an acoustic signal will accompany the impact. Experiments using high-velocity particles are needed.

A second method might employ either the large or small piezoelectric film sensors to detect the acoustic signals that accompany a pressure leak from the punctured skin of the cell, at least for cases where a pressure differential exists across the skin. Such flow-induced signals should persist long after the reverberations produced by the

impact have decayed. However, experiments are required to test the feasibility of this approach.

Thirdly, the elastic signature of skin penetration could be obtained from analysis of the signals from the large and small sensors. This would require detailed analysis of the signal waveforms, which we prefer to avoid, but the option will be kept open until a decision is made on the best approach to penetration detection.

Fourthly, active inspection techniques could be used to detect penetration following a substantial impact. Possibilities that could be investigated include active ultrasonic inspection using the small, embedded sensors as both transmitters and receivers, or acoustic or optical inspection by autonomous mobile agents.

Sensor failure

It should be noted that the system is required to remain operative and functional in the event of a sensor failure, or a processor (cell) failure, whether these failures are the result of a previous particle impact, or have occurred for other reasons. In principle, the small (acoustic emission) sensors on neighbouring cells can be used to detect the elastic waves that emanate from the impact site, as long as the cells are not isolated acoustically from each other. Triangulation to determine the impact location will follow, and may require data from more than one neighbouring cell. How readily this can be done in practice will depend on the physical structure of the skin.

Sensor deployment in the initial design

As described in Sections 2 and 4, each rectangular face of the hexagonal prism structure is covered by eight (in a 2 x 4 array) 200 mm x 200 mm panels, each of which contains 4 sensing cells. Therefore there will be 48 panels monitored by 192 sensor cells, incorporating 192 large-area sensors (one each cell) and 768 (four each cell) small, integrated sensors for precise location of the impacts. The general arrangement of sensors on each panel is shown schematically in Figure A2; more details of their fabrication are given below. It is expected that this relatively large number of cells and sensors will allow the study of communication protocols, intelligent processing and any complex or emergent behaviour that may result from such large numbers of interacting agents.

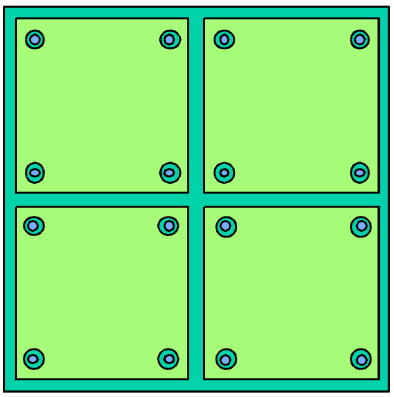

Figure A2: Schematic layout of sensors on a 200 mm x 200 mm panel, showing four 90 mm x 90 mm 'direct impact' sensors, each of which has a further four small-area sensors to determine the impact location and a measure of the elastic energy emanating from the impact.

A1.3 Experiments on sensors

Laser pulse experiments

In order to evaluate the response of different sensors to impact, the beam of a Q-switched Nd:YAG laser (wavelength 1.06 μm) was directed towards a 1 mm-thick aluminium sheet to simulate impacts of high-velocity particles. Sensors were attached to the reverse side of the sheet. For most of the experiments parameters were chosen so the laser beam interaction with the aluminium surface was in the ablative region; only the lowest pulse energies in an unfocused beam realized a purely thermoelastic interaction. The laser pulses were 8 ns FWHM (full width at half maximum), up to 500 mJ per pulse, in an unfocused beam diameter of about 5 mm, but a lens (focal length 100 mm, giving a focal spot size about 100 μm in diameter) was used in some of the experiments to minimize the interaction zone, thereby simulating smaller particle impacts. In the experiments reported below, therefore, the laser was used to generate a (near) point source of elastic energy, and for the purposes of these initial tests represented a reasonable and highly convenient simulation of high-velocity particle impact. Further discussion of this is provided below, where a comparison is made between present results and those of some previous experiments with particle impact at NASA.

The experimental arrangement is shown in Figure A3. A half-wave plate in a mount capable of rotation about the optic axis was placed in the beam path, and combined with a transparent plate set at Brewster's angle enabled the energy in the beam incident on the aluminium plate to be changed conveniently and quickly. (Some changes in the spatial distribution of energy in the beam resulted, but were largely immaterial to these experiments.) A small fraction of the beam reflected from the Brewster plate was directed towards a fast photodiode, the signal from which was used to trigger an oscilloscope, which also measured the output from the sensors attached to the sheet, thereby providing a time reference. In the results shown below the laser was incident on the aluminium sheet at time t = 0. Experiments were performed with and without a focusing lens.

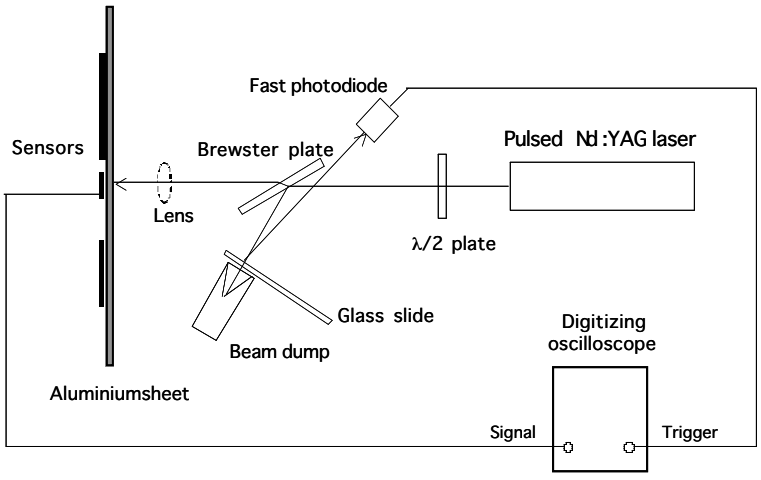

Figure A3: Experimental arrangement for the measurement of sensor responses to simulated impacts using Q-switched laser pulses.

Laser pulse 'impacts' are described below as being either 'on-sensor' or 'off-sensor', according to whether the position on the front side of the aluminium sheet where the laser beam was incident was or was not (respectively) directly opposite a sensor on the back side of the sheet. As many of the sensors were significantly larger in area than the irradiated zone, the distance an incident beam was 'off-sensor', Δx, was measured to the nearest edge of the sensor. For large sensors a negative value of Δx meant that the laser beam was 'on-sensor', and in from the nearest edge of the sensor by the absolute value of Δx. Measurements have been made of sensor output for different sensor types and sizes as functions of Δx and laser pulse energy.

Sensor comparison

In order to arrive at the proposed sensor geometries several experiments were performed. Although no particular type of sensor has been ruled out of consideration for implementation, it was thought that PVDF (or similar copolymer) film sensors would probably provide the most functional sensor for the early experiments. Such films are light, flexible, and have excellent sensitivity as detectors. While PZT and similar ceramic materials are generally considered better transmitters, their primary disadvantage in the present application is the difficulty of fabricating large-area, low-weight thin-film sensors. At present, tape-cast PZT, even when encased in polymeric materials, is not nearly as flexible as PVDF (the latter's compliance is ten times that of PZT), nor as mechanically tough. It is doubtful such PZT detectors would remain operational if cracked or holed.

In order to establish some comparison between these two sensor types, preliminary experiments were performed that compared the 'on-sensor' output of three types of sensor: a standard, unbacked 0.5″ diameter disc of PZT, 1 mm in thickness, with fired-on silver electrodes; a conical PZT transducer with similar electrodes (2.5 mm in thickness, with an included angle of 60° and a tip diameter of 1.6 mm), with a large brass backing (of the type pioneered by researchers at NBS, now NIST; see Proctor (1982), Greenspan (1987), Hamstad and Fortunko (1995), and Fortunko and Boltz (1996)); and a small piece of PVDF, 52 μm in thickness with an active area of 5 mm x 5 mm coated with silver ink on both faces. The PVDF sensor was glued to the back side of the aluminium sheet using Epotek[3] epoxy (as were all subsequent PVDF sensors), as was the PZT disc. The conical transducer was held against the sheet using a compressive spring. The output of the large PZT disc was dominated by resonance frequencies of the unbacked disc that persisted for more than 100 μs after impact. The conical PZT transducer's response, while known to be reasonably flat over a wide frequency range from a few kiloHertz, declined significantly above about 1 MHz. The PVDF sensor had adequate sensitivity and frequency response up to nearly 100 MHz, based on FFTs of the transient responses.

There have been a number of researchers who have studied the use of different sensors to detect elastic waves in plates generated by laser pulses, pencil breaks and particle impact. Dewhurst et al. (1987) used a Q-switched laser to generate Lamb waves in thin metal sheet, and employed a laser interferometer as the detector. Dewhurst and Al'Rubai (1989) used a 9 μm-thick PVDF sensor as a detector for compressive waves in various thicknesses of duraluminium sheet, and also compared

[3] Selected for its low viscosity, which allows more effective de-gassing.

the output of these sensors with laser interferometer measurements. They concluded that, as the wavelength of the components of the detected pulse were significantly larger than the film's thickness, the PVDF was acting as a velocity rather than a displacement sensor. The same will be true in the present experiments, although interpretation of our measurements will be complicated by effects resulting from the large area of the sensor. Buttle and Scruby (1990) measured acoustic emission from impacts of small dust particles (53 μm to 90 μm) at low velocities (< 7.1 m s^{-1}) on steel and aluminium targets, using both capacitance and PZT transducers.

To further confirm the suitability of both the PVDF sensors and the use of a fast laser pulse for impact simulation, a comparison was made between the 'off-sensor' responses of the conical transducer and a small-area (diameter 1.8 mm) PVDF sensor, both employing laser pulses as the excitation source, with the results of Prosser et al. (1999b, 1999c) who studied the acoustic emission signals from a 12.7 mm diameter commercial PZT transducer resulting from slow and fast particle impacts. It is understood that penetration did not occur for any of these impacts. Figure A4 shows the signals from four different experiments: (a) output from the conical PZT transducer with $\Delta x = 25$ mm; (b) output from the 1.8 mm PVDF transducer with $\Delta x = 50$ mm; (c) Prosser et al.'s (1999b) AE signals produced by a low-velocity impact on an aluminium plate (3.175 mm thickness, 12.7 mm diameter transducer, $\Delta x = 152$ mm); (d) Prosser et al.'s (1999b) AE signals produced by a high-velocity impact on an aluminium plate (3.175 mm thickness, 12.7 mm diameter transducer, $\Delta x = 147$ mm). In cases (a) to (c) the impact was at time $t = 0$; in case (d) a difference in trigger timing was evident. It is clear from Figure A4(a) that the conical PZT transducer is limited in its frequency response, but nevertheless registers the arrival of the S_0 extensional mode at around 5 μs as a result of the Q-switched laser pulse incident on the aluminium sheet (thickness 1 mm) at $t = 0$, and the lower frequency components of the flexural mode for $t \geq 8$ μs. Both these modes are dispersive.

For similar laser pulse excitation, a more detailed picture of the arrival of various dispersive modes is given by the small PVDF sensor (Figure A4(b)), which clearly shows the arrival of the extensional mode (at around 10μs), the lower frequencies arriving earlier, and then the flexural mode (at around 15μs), the higher frequencies arriving earlier. Such transient signals are in good agreement with the results of Prosser et al. (1999a, 1999b, 1999c), who used pencil breaks as well as particle impacts. If these signals are compared with signals resulting from low-velocity impacts (see Figure A4(c)) it may be seen that while the general form of the signals are the same, there are very few high-frequency components in the low-velocity impact signals. For high-velocity impacts (Figure A4(d)) not only are much higher frequencies present, but also there is a much larger extensional mode component present.

Having established that the PVDF sensors render a consistent picture of the AE signals generated in plates, and that laser excitation as a source of elastic waves is similar to at least medium velocity particle impacts, a characterization of the outputs from PVDF sensors of a range of sizes as a result of 'on-sensor' excitation was undertaken. For the largest and smallest of these sensors the dependence of the signals on Δx was measured. These experiments were aimed at establishing the appropriate dimensions for the direct impact sensor and the smaller AE sensors.

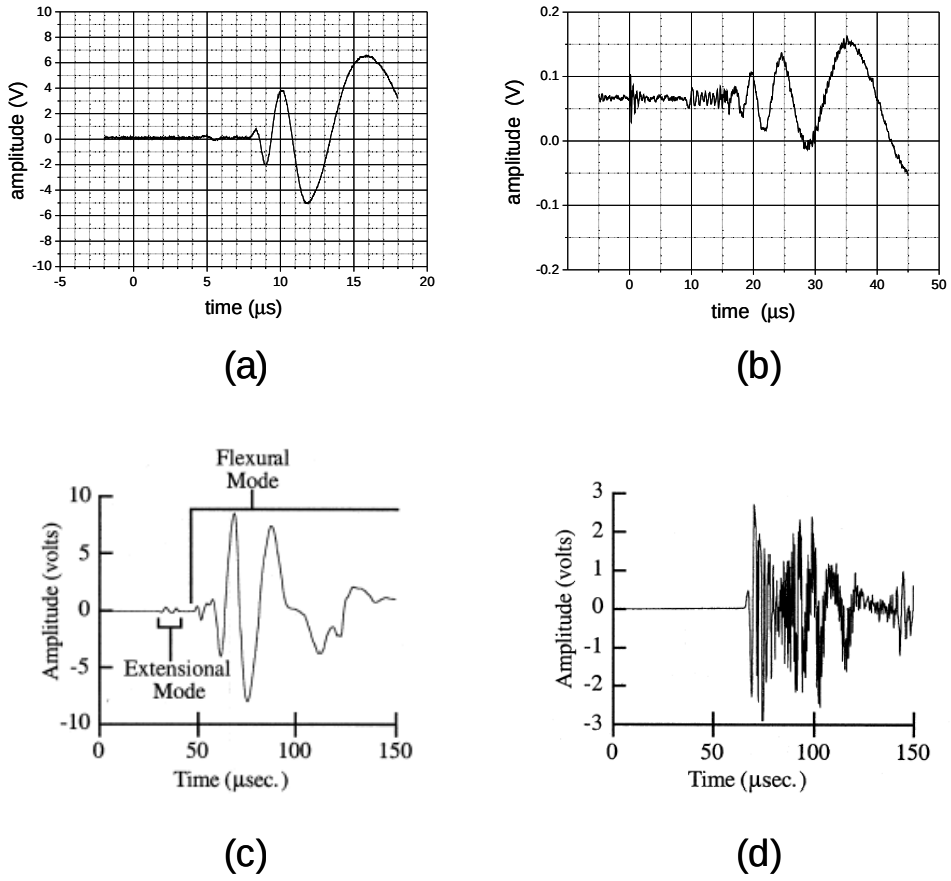

Figure A4: Comparison of signals from different transducers. (a) Conical PZT transducer output resulting from elastic waves in 1 mm aluminium sheet caused by a laser pulse on the opposite side of the sheet, Δx = 25 mm. (b) 1.8 mm diameter PVDF sensor output under similar conditions to (a) but with Δx = 50 mm. (c) Signal from 12.7 mm dia. PZT transducer due to low-velocity impact on 3.175 mm-thick aluminium sheet, Δx = 152 mm (Prosser et al., 1999b). (d) Signal from 12.7 mm dia. PZT transducer due to high-velocity impact on 3.175 mm-thick aluminium sheet, Δx = 147 mm (Prosser et al., 1999b).

Sensor size

When the laser beam was incident on the Al surface directly opposite a PVDF sensor (i.e. 'on-sensor'), the signal consisted of a series of short-pulse responses separated by about 315 μs, the reverberation time through the 1 mm aluminium sheet[4]. These pulses were typically one to two cycles at a centre frequency of about 21 MHz, the thickness resonance frequency of the PVDF sheet itself[5]. The peak-to-peak amplitude of these pulses decayed roughly exponentially. Figure A5 shows examples of the responses of one such PVDF sensor (5 mm x 5 mm) to both unfocused (beam diameter about 5 mm) and focused (beam diameter about 0.1 mm) laser beams 'on sensor'.

[4] i.e. twice the Al thickness divided by the longitudinal wave velocity in Al, 2 mm / 6350 ms^{-1}.
[5] with v = 2200 ms^{-1} and $\lambda/2$ = PVDF thickness = 52 μm.

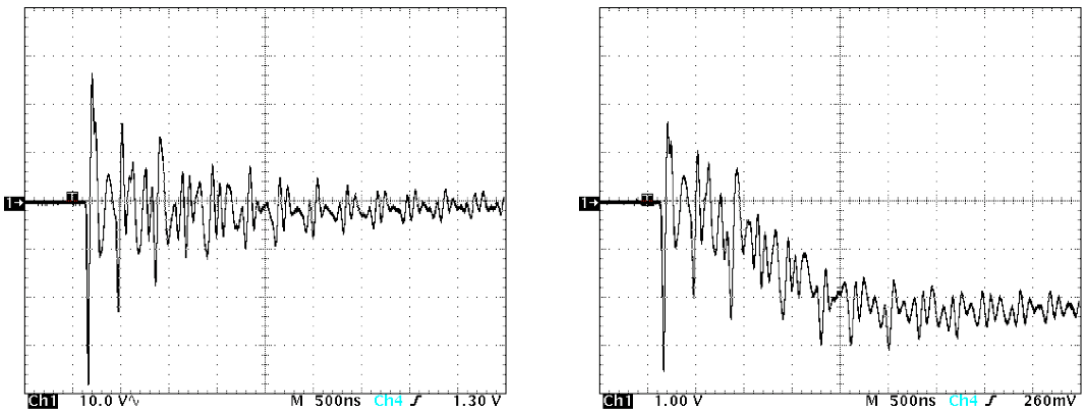

Figure A5: Response of 5 mm x 5 mm PVDF sensor to 'on-sensor' laser pulse using an unfocused laser beam (left), vertical scale 10 V/division, and a focused laser beam (right), vertical scale 1 V/division. The horizontal scale for both is 500 ns/division.

A number of square PVDF sensors of differing sizes (5, 15, 32, 45, 48 and 90 mm square) were fabricated and glued with Epotek epoxy to the rear (non-impacted) side of a 1 mm-thick aluminium sheet. Although the PVDF was glued to the aluminium sheet with an insulating epoxy there was invariably an electrical connection made between the glued-on electrode and the aluminium sheet during the gluing process, as small slivers of the electrode material from the edges of the sensors penetrated the epoxy as it was pressed onto the aluminium sheet.

The maximum (first) peak-to-peak amplitude was measured and plotted as a function of the nominal capacitance of the PVDF film, calculated from $C = \kappa\varepsilon_0 A/d$ (where κ = 12.5 for PVDF, the film thickness d = 52 μm, and A is the area of the sensor). There was very little dependence of these signals on the position 'on-sensor', provided the 'impact' was wholly on the sensor. These measurements were made using both a focused laser beam and an unfocused beam, both with 500 mJ pulse energy. The results are shown in Figure A6.

These results show that the maximum signal decreases for increasing sensor capacitance. Further, the signals measured when the laser beam is focused are about an order of magnitude lower than when the beam is unfocused. After fitting a straight line to each set of results (on a log-log plot), application of Q = CV indicated that the charge generated in the PVDF films using an unfocused laser beam is approximately 9 nC, whereas for the focused beam the charge is only about 0.7 nC. Other than to say that significantly less charge, and therefore a smaller voltage signal, results from a smaller 'impact' size a quantitative comparison is not straightforward. The difference in generated charge by the focused and unfocused beams may be due to a difference in efficiency of elastic wave generation (the focused beam produces breakdown in the air near the aluminium surface, and it also causes ablation of material from the surface, both of which tend to shield the surface from the optical radiation), and a difference in the nature of the waves generated (for the unfocused beam the generation region is larger and the proportion of thermoelastically generated elastic energy higher than for the focused beam).

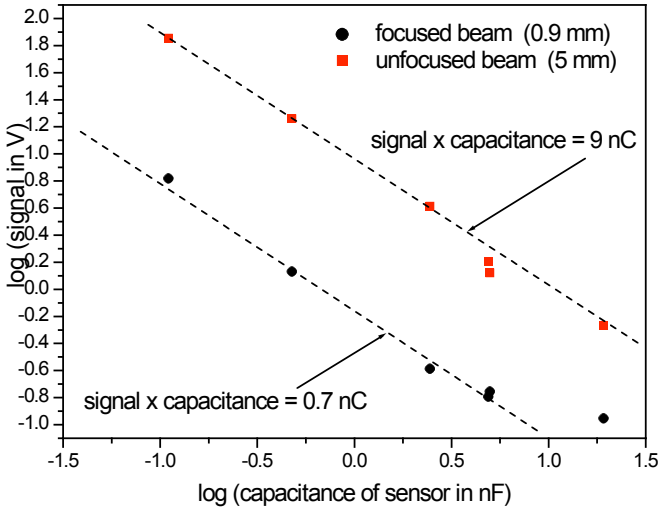

Figure A6: Maximum peak-to-peak signal resulting from on-sensor impacts, as a function of nominal PVDF sensor capacitance.

As indicated by the data of Figure A6 and in the following sub-section, the signal from the largest sensor (90 mm square) approached the noise floor when the focused laser beam was used. This will be discussed further below, but one possibility for improving the signal to noise ratio was explored, that of decreasing the capacitance of the sensor while keeping the sensor area constant. One way to do this is to segment the sensor into smaller parts and connect them in series. This requires electrically isolating the sensor from the aluminium sheet.

To investigate this technique, four square 30 mm x 30 mm sensors were fabricated and connected in series, forming a sensor area of approximately 60 mm x 60 mm square. A single square 60 mm x 60 mm sensor was also fabricated. Using Epotek epoxy these were adhered to a 1 mm-thick aluminium sheet that had been painted on one side so as to insulate all the sensors from the earthed aluminium sheet. Measurements of the on-sensor transient (see, e.g., Figure A5) of the 60 mm square sensor, of a 30 mm square sensor not connected to any of the other 30 mm sensors, and of the signal with the laser incident on the same 30 mm sensor from three 30 mm sensors connected in series. (One of the four 30 mm sensors showed an anomalously low capacitance and was omitted from further experiments.) The measured low frequency (1 kHz) capacitance of the 60 mm sensor was 7.25±0.10 nF, of the 30 mm sensor 2.10±0.10 nF, and of the three in series 0.75±0.10 nF. These experiments found that, using a focused laser beam, the maximum signal from the 60 mm sensor was about one third that of the 30 mm sensor, and that the signal from the three sensors in series did not differ significantly from that of the 30 mm sensor used alone.

While this might not at first glance appear to be consistent with the measured capacitances, two other factors need to be borne in mind. Firstly, as noted in the results comparing the focused and unfocused laser beam experiments (see also next sub-section), the output from the PVDF sensors is saturated at these laser power levels: this is a result of the generation mechanism rather than the sensor response.

Secondly, it will be the impedance of the electrical circuit formed by the oscilloscope probe and these capacitors at the frequencies involved here that will determine the transient voltage response, not the low frequency capacitance alone. Further experiments are planned to further investigate these results.

Some preliminary experiments investigating the effect of amplifiers on the signal-to-noise ratio of 'on-sensor' signals have been performed. A charge amplifier, based on the AD8065 (Analog Devices) wide-band, low-noise FET-input amplifier was used. Results from this experiment indicated several points. Firstly, the signal-to-noise ratio improved by a factor of about two. Secondly, the integrating capacitor across the amplifier needs to be chosen according to the capacitance of the sensor, as the gain of the charge amplifier is equal to the ratio of the sensor capacitance and the integrating capacitance. Finally, and most importantly, the gain-bandwidth product of these amplifier chips is ~ 120 (with the bandwidth given in MHz): the bandwidth at unity gain is ~ 120 MHz, while for a gain of 100, the bandwidth is only ~ 1.2 MHz. However, in the configuration used in these experiments the bandwidth at unity gain was only ~ 15 MHz, probably due to capacitive loading of the output. Even without this loading, a gain of no more than ~ 6 could be expected at 20 MHz. As a consequence the bandwidth of the charge amplifier used here, while broad enough to detect the reception of the initial compressive wave and the subsequent reverberations in the aluminium, was not sufficient to allow accurate resolution of these pulses which are themselves determined by the resonant frequency of the PVDF film (~ 21 MHz). Further work is required in this area, including improved charge amplifier design and development.

What may be concluded is that if insufficient signal amplitude proves to be a problem, then smaller sensors will certainly yield a larger voltage output. This would mean that many more sensors would be required to cover the area under measurement (four times, in the example discussed above), with commensurately more connections and data to process. It may be preferable to connect the smaller sensors in series and make fewer connections to the processor (by a factor of four in our example) without any loss in signal amplitude. The choice between these strategies may depend on the cell size and the spatial resolution required for impact location. The extreme cases are:

1) Use a larger number of smaller "direct impact" sensors, perhaps arranged as a matrix as proposed by Martin et al. (2002), and dispense with the need for the small acoustic emission sensors.
2) A combination of a large sensor and small AE sensors as shown schematically in Figure A1 above.

While strategy (1) might result in simplified impact location in appropriate circumstances (i.e. when the required spatial resolution is comparable with the cell size), it may not be as readily adaptable to impact location when individual sensors or whole cells have been damaged.

Sensitivity

As noted above, a pulsed laser was used to simulate impacts in these early experiments because of the availability and convenience of such a source for generating elastic waves, and thereby to allow testing of the processing and communications technologies in the Concept Demonstrator. Therefore, as the study

of impacts by particles is the goal of this demonstrator, the object of these experiments was not to understand the relationship between laser pulse parameters and the ultrasonic signals they generate when incident on an aluminium sheet. Nevertheless, it was thought useful to determine the limits of detectability of these simulated impacts by the PVDF sheets under these experimental circumstances. The maximum peak-to-peak signals of the various PVDF sensors as a function of incident laser energy using focused and unfocused laser beams are shown in Figure A7.

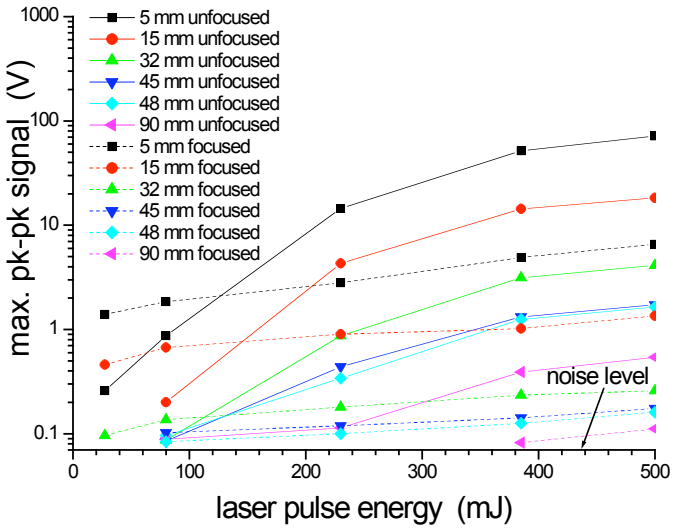

Figure A7: Maximum peak-to-peak signal as a function of laser pulse energy.

It appears from these results that the outputs of the PVDF sensors appear to saturate when the laser beam is focused, the outputs changing little with a change in laser pulse energy from 20 mJ to 500 mJ. On the other hand, saturation of the output of the sensors when the unfocused beam is incident on-sensor does not occur until pulse energies in excess of 400 mJ are reached. It is most likely that this apparent saturation is due primarily to saturation of the conversion of laser energy to elastic wave generation, referred to above (see also Scruby and Drain (1990), p.285). Thus it is probably not directly relevant to the detectability of particle impacts by these sensors even though it has significant "nuisance value" as far as our experiments are concerned. Again it may be seen that the largest sensor has an output barely above the noise level when the laser beam is focused, even at the highest pulse energies used here.

This noise problem was addressed further as it was found that the noise in the early part of the acoustic transient signal, the first microsecond or so where these reverberation signals in the aluminium sheet are found, was being caused by electromagnetic noise from the Q-switched laser power supply. Extensive shielding was applied to the coaxial cables that connected the probe to the oscilloscope, and earthing loops were eliminated as much as possible. The improvements in signal-to-noise of the 'noisiest' sensor (90 mm x 90 mm PVDF) subjected to an 'on-sensor' focused laser pulse are shown in Figure A8. These improvements, and the recognition that it is the laser source itself responsible for most of the present noise problems were

encouraging, indicating that it was the 'impact' source rather than any inherent noise in the PVDF as a result of 'impact' that is limiting the present experiments.

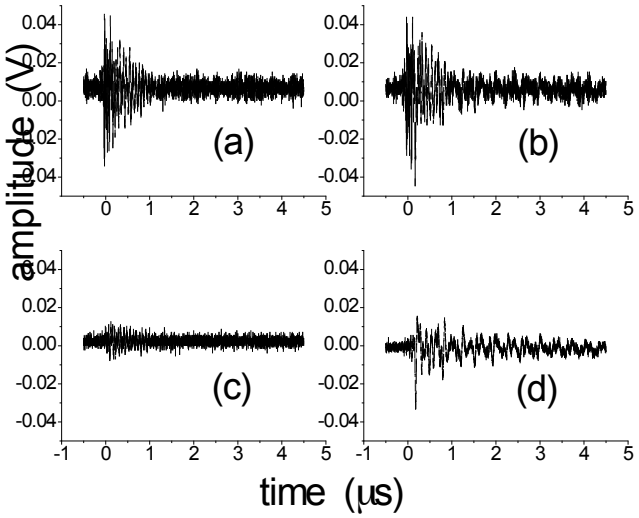

Figure A8: Improvements in signal-to-noise ratio of the 90 mm square PVDF sensor using a focused laser beam. (a) Signal from sensor as a result of laser firing, but with the beam blocked, so no pulse is incident on the aluminium sheet. (b) Signal with beam unblocked. (c) Signal with beam blocked, but with extensive earth shielding. (d) Signal with beam unblocked and shielding in place.

The results of Figure A8 emphasize the need for careful shielding of the sensors and connections from any noise from the impact source (whether it is a laser or some other electro-mechanical device that may propel particles into the CD in future tests), or from any other sources of EMI. When they are mounted within the CD structure, the sensors should be reasonably well shielded from external EMI, but the proximity of a number of fast digital processors inside the structure may present shielding problems that will need to be addressed. These results have also brought to our attention the possible interference that may arise from any plasma caused by a high-velocity impact, a problem that may need to be addressed at some future time.

The results presented here allow us to conclude with some confidence that the 90mm square PVDF sensors that we proposed to be an appropriate size for the 'direct impact' sensor will indeed allow the detection of an initial impact, though we don't yet know to what range of particle energies these experiments correspond. These conclusions are, of course, based on incident laser pulses as the source of elastic energy. We have yet to address the sensitivity of our sensor scheme to impacts from small particles of either high or low velocity. It is hoped that this will be possible in the near future.

Dependence on Δx

The suitability of a large-area direct impact sensor relies on, inter alia, the sensitivity of the sensor output to on-sensor and off-sensor hits. If the distinction between the two is not clear, for instance the signal from the sensor changes slowly as the impact

site is moved from on-sensor to off-sensor, then the usefulness of a large area sensor may be limited. To test this aspect of detectability, a medium sized PVDF sensor (32 mm square) was selected to ensure high signal-to-noise ratio, and its output was measured as the 'impact' site, the point where the focused laser beam pulse was incident, was moved from on-sensor to off-sensor in 1 mm increments. These results are shown in Figure A9.

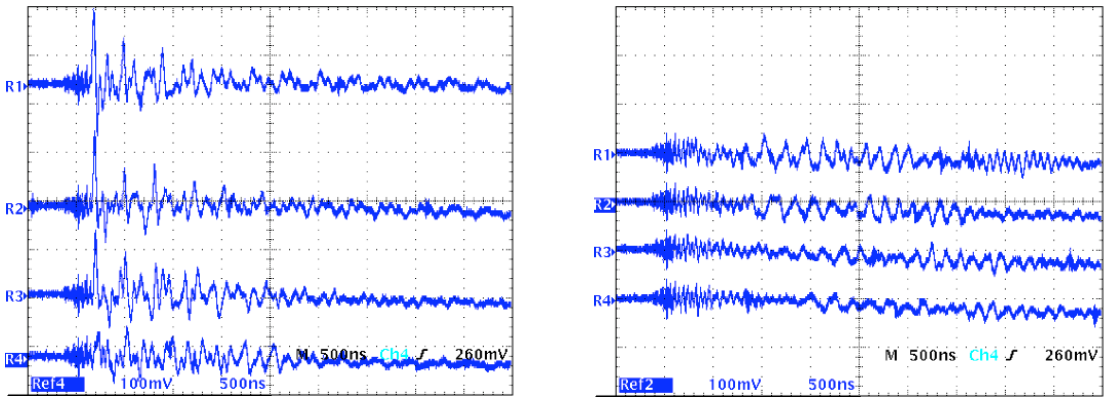

Figure A9: Change in the signal from a 32 mm square PVDF sensor as the 'impact' site of a focused laser beam moves from on-sensor to off-sensor. The oscilloscope traces on the left correspond to Δx = -2, -1, 0, and +1 mm from top to bottom respectively, and the traces on the right correspond to Δx = +2, +3, +4, and +5 mm from top to bottom respectively.

A strong on-sensor signal (corresponding to negative values of Δx) from the initial passage of a longitudinal wave through the aluminium sheet is seen on the transients up to and including a nominal '0 mm' position, but is absent for the '+1mm' and higher transients. (The signals that are evident later in the transients (for example, for $\Delta x > +2$ mm, after the first 500 ns) are the flexural waves being detected by the sensor and presumably subject to significant phase cancellation as the wave traverses the large area of the detector. A full understanding of these transients is an area of acoustic emission this project is seeking to avoid in order to facilitate rapid processing of signals.) It is clear from these results that this 32 mm square PVDF sensor, and from the improved signal-to-noise ratio of the 90 mm sensors, that these large area sensors have sufficient sensitivity to clearly distinguish on-sensor and off-sensor hits to better than 1 mm resolution.

While it is visually clear from the signals displayed in Figure A9 when a laser 'impact' is on the sensor or off the sensor, having the system determine the (relative) time of arrival and amplitude of the relevant signals may not be straightforward. Fourier transforms of the Δx = -2, -1 and 0 mm signals have indicated that there is a large component near 21 MHz (the through-thickness resonant frequency of the PVDF sensor) when the laser pulse is 'on-sensor'. As seen above, this component is associated with the reception of the first compressive wave through the aluminium and its subsequent reverberations. It is not present to any significant extent when the sensor signals are produced by plate waves propagating from 'off-sensor' impact locations.

Therefore, one possible means of distinguishing on- and off-sensor impacts may be to measure the amplitude of the 21 MHz component of the initial transient (numerically or electronically using a narrow-band filter), normalized to the amplitude of the transient. It will be preferable to avoid the need to digitize such high-frequency signals to reduce demands on the analogue-to-digital conversion rate of the processor (see also Section 5 and Appendix 2), so the use of narrow-band filtering will be investigated.

As mentioned previously, when studying simple plate geometries two possible methods of calculating the distance between the 'impact' site and the detecting transducer are (a) use a single-frequency component of a particular plate mode (whose velocity may be calculated) and whose time of arrival at the sensor is measured, and thus from the three different times of arrival of this particular component in the measured transients of the small sensors, the location of the impact may be determined, or (b) the difference in the time of arrival of two or more different frequency components (again, whose velocities may be known at the measured frequency) may also be used to determine distance, and hence triangulation again gives the location of the impact.

Both of these techniques require a time reference. This may be obtained from the arrival time of the direct compressional wave signal as measured by the direct impact sensor, or if this is not available due to sensor and/or communications failure, the fourth small-area sensor signal may be used. Whatever the operational state of the sensors, four are needed for the positional determination (in the event of sensor damage, the four need not be part of the same cell). Note that the propagation velocities of the single-frequency components used need not be known; the relative times of arrival of single-frequency components are sufficient to perform the triangulation.

The Δx dependence of the small AE sensors set within the large-area sensor was investigated. A 1.8 mm-diameter PVDF sensor was used for these experiments. The signals detected as a result of focused laser pulses incident a distance Δx from the centre of the detector are shown in Figure A10. These transients show that for small Δx ($\leq$ 20 mm) the relatively fast S_0 wave may be distinguished (at 0.95 μs, 1.9 μs and 3.8 μs for Δx = 5 mm, 10 mm and 20 mm respectively). For larger Δx this mode is difficult to distinguish in the raw, unprocessed data. The flexural modes, however, are clear, and so it seems more promising at present to use two or more selected frequencies of the low-order A_0 mode for distance measurement and subsequent triangulation to determine the impact location.

A high-pass filter (cut-off frequency ~ 50 – 100 kHz) might be used to distinguish the arrival of these flexural waves from later 'random' low-frequency signals caused by reflections from parts of the structure (panel edges, ribs, etc.) reaching the sensors. This is not an issue for single impacts, but it may be important to enable the detection of multiple impacts close in time.

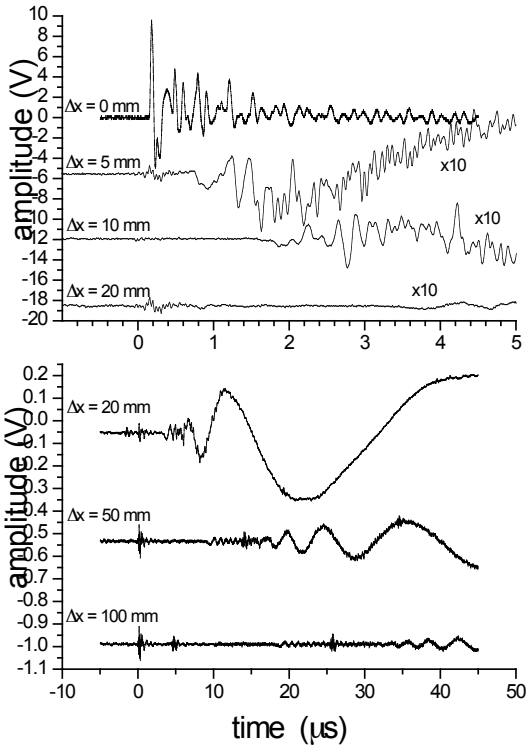

Figure A10: Signals from the 1.8 mm diameter PVDF sensor for different values of Δx. The upper traces show the 'direct hit' signal (Δx = 0 mm) and three other traces corresponding to Δx = 5, 10 and 20 mm. The voltages from the latter three have been multiplied by ten and displaced from each other for display purposes. The lower traces are for Δx = 20, 50 and 100 mm, on a longer time scale, and again displaced vertically

A1.4 Further work

The arrangement of large and small sensors discussed above was proposed to minimize the amount of data processing required to determine the location and energy of impacts. The experiments on sensors thus far have indicated that this appears to be a viable design. There is much yet to be understood about the form of the transients that have been measured, and clearly an understanding of the physics involved through modelling is necessary. Such an understanding is essential both to design the first level of signal processing to be applied to the measured transients, in order to provide concise information (such as the location and energy of the impact) to be transmitted to the system, and also to guide possible later active probing of the system to determine levels of damage and so on.

Several implementations of the basic sensor cell design are under evaluation at present, and the potential problem of EMI sensitivity has still to be examined in detail. A final decision on the appropriate design will be made in conjunction with a procedure for fabrication compatible with the production of hundreds of these sensor cells. One production procedure under consideration involves the purchase of poled PVDF sheet with metallized electrodes, followed by ion-beam etching of an electrode

pattern onto both faces of a sheet cut to the appropriate shape and size. Another is to trial different electrode patterns by screen-printing conducting paint onto poled but unmetallized PVDF sheet. After a final pattern has been decided, production of multiple copies by a commercial manufacturer may be the preferred option.

Each sensor cell would then be connected via a single connector and flexible ribbon cable (depending on EMI considerations) to the processing electronics. The possibility of using an anisotropic conductive polymer is also under consideration. The sensor cells will be affixed to the aluminium panels with epoxy. This provides a thin, relatively low-loss coupling medium between sensor and metal that is easy to apply in a uniform layer. Other possible sensors such as tape cast PZT, optical sensors, and so on, are also being investigated.

All of these preliminary experiments have used a pulsed laser to simulate the impact of small particles. Our conclusions regarding the suitability and adequate sensitivity of a 90 mm square PVDF sensor for the direct impact sensor, and the ~ 2 mm small locating sensors, is based on detection of a 500 mJ laser pulse focused to an area ~ 0.1-0.2 mm in diameter. The sensitivity of this system to particle impacts has not been determined. There is therefore a pressing need to move away from this simulated source and have an in-house source of fast, small particles, as discussed in Section 3.

References

Buttle, D. J. and Scruby, C. B., (1990) "Characterization of particle impact by quantitative acoustic emission", Wear, **137**, 63-90.

Christiansen, E.L., Kerr, J.H., De La Fuente, H.M. and Schneider, W.C., (1999) "Flexible and deployable meteoroid/debris shielding for spacecraft", Int. J. Impact Engng., **23**, 125-136.

Dewhurst, R. J. and Al'Rubai, W. S. A. R., (1989) "Generation of short acoustic pulses from an energetic picosecond laser", Ultrasonics, **27**, 262-269.

Dewhurst, R. J., Edwards, C., McKie, A. D. W. and Palmer, S. B., (1987) "Estimation of the thickness of thin metal sheet using laser generated ultrasound", Appl. Phys. Lett., 51(14), 1066-1068.

Fortunko, C. M. and Boltz, E. S., (1996) "Comparison of the Absolute Sensitivity Limits of Various Ultrasonic and Vibration Transducers", Materials Science Forum, Vols **210-213**, 471-478.

Greenspan, M., (1987) "The NBS conical transducer: Analysis", J. Acoust. Soc. Am., **81**(1), 173-183.

Hamstad, M. A. and Fortunko, C. M., (1995) "Development of practical wideband high-fidelity acoustic emission sensors", SPIE Vol. **2456**, 281-288.

Martin, W. M., Ghoshal, A., Sundaresan, M. J., Lebby, G. L., Schulz, M. J. and Pratap, P. R. (2002) "Artificial Nerve System for Structural Monitoring", SPIE Conference on Nondestructive Evaluation for Health Monitoring and Diagnostics (Conference 4702, paper 4702-6), San Diego, March 2002.

Proctor, T. M., (1982) "An improved piezoelectric acoustic emission transducer", J. Acoust. Soc. Am., **71**(5), 1163-1168.

Prosser, W. H., Seale, M. D. and Smith, B. T., (1999a) "Time-frequency analysis of the dispersion of Lamb modes", J. Acoust. Soc. Am., **105** (5), 2669-2676.

Prosser, W. H., Gorman, M. R. and Humes, D. H., (1999b) "Acoustic Emission Signals in Thin Plates Produced by Impact Damage", J. Acoust. Emission, **17** (1-2), 29-36.

Prosser, W. H., Hamstad, M. A., Gary, J. and O'Gallagher, A., (1999c) "Reflections of AE waves in Finite Plates: Finite Element Modeling and Experimental Measurements", J. Acoust. Emission, **17** (1-2), 37-47.

Sage, I., Badcock, R., Humberstone, L., Geddes, N., Kemp, M. and Bourhill, G., (1999) "Triboluminescent damage sensors", Smart Mater. Struct. **8**, 504-510.

Sage, Ian and Bourhill, Grant, (2001) “Triboluminescent materials for structural damage monitoring”, J. Mater. Chem. **11**, 231-245.

Scruby, C.B and Drain. L. E., (1990) **Laser Ultrasonics, Techniques and Applications**, Adam Hilger, Bristol.

Appendix 2: Details of the Electronics and Communications Protocols

This Appendix details the requirements for and the proposed implementation of the electronics hardware in the Concept Demonstrator, as outlined in Section 5.

While an eventual Robust Aerospace Vehicle would need to sense a wide range of system parameters and threats, the CD will be limited to a small subset of these parameters. This recognizes that the initial contribution of the CD is intended to be in the area of system architectural development and information gathering, rather than in developing novel sensing hardware.

While it is expected that later on the CD will use several sensor types, the initial system is being developed to detect micrometeoroid/debris impacts on the skin of a space-based vehicle, using piezoelectric sensors.

A2.1 Concept Demonstrator electronics requirements

General requirements

The ultimate application of the technology being developed is in a robust, or even ageless, aerospace vehicle. This requires that the vehicle perform its functions over its entire lifetime while continuing to meet all specifications. This requirement must be met in a potentially hostile environment, where parts of the vehicle will be damaged, perhaps on a frequent basis. Additionally this will probably occur in a changing environment, possibly even under unforeseen conditions. Consequently, some of the basic requirements for such a system are as follows.

- Robustness: the system must be durable and functional in a hostile environment.
- Redundancy: given that damage is inevitable, and that the vehicle must continue to operate with damaged components, some back-up is required.
- Reparability: the vehicle may operate over long time periods, in spite of ongoing damage. This requires some mechanism for repair or replacement of damaged systems.
- Reconfigurability: the optimum vehicle configuration may change considerably over the duration of the mission. Sensors and indeed even structures may have to be modified as the environment or task evolves. An important aspect of reconfigurability will be that necessary for a damaged system to continue functional operation prior to repair being effected. In this case, reconfiguration makes use of the inherent redundancy of the system.

While current aerospace vehicles are made from highly specialized subsystems, the constraints mentioned above favour a more modular approach. Currently the space station is composed of a number of large subsections, but the CD looks at a much smaller scale for the modularity of the sensing system, with a view that sees the size of the modules decreasing to more cellular entities over the extended life of the project.

Distributed and hierarchical options

The environment of the final vehicle is likely to be subject to occasional very high-energy impacts. Such impacts are unlikely to be completely avoidable, so that all sensing and processing systems must be redundant. In spite of this the vehicle will require a high degree of internal coordination, so internal communications are essential. Physically hierarchical systems provide the coordination required, but at the risk of having critical points where a major failure can result from damage to a relatively small part of the system. Such points might be command processors, communications trunks, or power supply trunks. This leads to a desire for a distributed architecture for the system. In such an architecture, the loss of any piece of the system results in a graceful, rather than catastrophic, degradation. The information contained is spread over many sub-systems, and communication and power can be easily re-routed around the damaged area. A valuable side effect of the distributed approach is the ability of the system to deal with simultaneous, real-time events.

Data sampling rates

Initial investigation of acoustic emission (AE) sensors suggested that the signal bandwidths of interest were in the low to medium MHz range. It is expected that additional lower bandwidth sensors may be also used (e.g. temperature, pressure sensors), but the system needs to be able to deal with the higher AE bandwidths. It is possible that future applications may require even higher bandwidths, but if such possibilities were to be pursued, a significant fraction of the project effort would be expended on high-speed sampling systems rather than the actual issues central to the project.

Computational requirements

Perhaps the area of greatest uncertainty is the eventual requirement for computational power. The desire for robustness, damage tolerance and flexibility of function, leads to a choice of having all sections of the distributed architecture having a potentially high level of computational power. This means that any element of the distributed structure can take over at least some of the functions of a damaged neighbour. There is also a need for distributed software and algorithms. This leads to the use of a multi-agent approach to the system software.

As for the sampling rate issues, some tolerance in the uncertainty of the requirements is possible. Firstly, if the units are over "powered" and use too much electrical power, it is possible to design systems which could slow their clocks or operate in burst mode to limit power dissipation[6]. Alternatively, if the units are computationally underpowered, the CD can be run in "pseudo real-time", and used to define more appropriate specifications for the next stage of development of the system.

If processor overload becomes a serious problem for a local processor, the agent-based software approach may permit load sharing with adjacent processors.

[6] There is no intent to implement this at this early stage of design of the CD. It is simply a recognition that the power costs of a high MIPS processor may be controlled if necessary.

Communication data rates

The first stage estimate for inter-processor data rates suggests a rate of a few Mbits/s. Until actual agent interactions and system loadings are understood, this is a sufficient estimate. The architectural decisions detailed later mean that higher rates[7] are possible with only minor system changes.

Number and distribution of processors

The system proposed here is only a concept demonstrator. It is not intended to be as extensive as the final application requires. At the same time it must deal with the expected increase in scale of the final application. An initial estimate was made that about 1000 sensors represented a large enough number to force the most likely issues of complexity to be confronted, while maintaining an affordable total system cost.

The desire to perform impact-positioning calculations on the sensor data suggests that a small set of sensors be attached to each data sampling and detection processor. Largely for simplicity and symmetry reasons each processor was intended to handle 4 sensors. The number of sensors and the number of sensors per processor result in a planned processor count of around 250. The sensing strategy described earlier suggested that a sensor array with 5 sensors might have some advantages. As a result the number of intended processors is reduced to ~ 200.

It is intended that the CD be a surface-sensing array so, at this stage, its local interconnection structure is "planar", even though the actual surface structure is three-dimensional.

A2.2 Overall design and architecture of the electronic system

System modularity and physical layout

The requirements for extension of the initial CD to cover much larger areas, the need for reparability, the need for flexibility, and suggestion of a distributed architecture, all argue strongly for a modular design. While in the short term the complexity and flexibility requirements of the design are increased, it is believed that over the longer term the modular design will have significant benefits in both function and cost of production.

The individual modules are known as "cells", partly because of their effective partition of a "skin" surface into sub-components, but also to recognise that in the future the modules are expected to be more compact and less obviously an array of technological objects. In the farther future they are expected to "evolve" into functionally flexible, self-repairing, almost biological entities.

While the final vehicle will have a complex surface structure, with intersecting surfaces, the CD is currently being implemented as a single closed surface. This has the topological features of a body section or a wing surface. The design of the CD electronics and computational hardware is capable of more complex spatial interactions, with intersecting surfaces, but this will not be implemented initially.

[7] up to 60 Mb/s with substitution of higher data rate serial hardware.

Partition of cells into layers

A significant effort has been expended considering what will be required of the sensing array hardware. A high level view of the overall outer structure of the vehicle shows a logical progression of layers as noted below.

1. The physical outer skin. This is at least protective, and possibly structural as well.
2. The sensor layer as described earlier in this Report. Note that in a generic sensing system, some types of optical, electromagnetic, tactile and chemical sensors would have to penetrate the outer skin to perform their functions. This has not been specifically addressed here as it has little direct impact on the following layers that form the core of the system.
3. Conditioning electronics. This layer converts the signals from the sensors to a form suitable for analogue to digital conversion (ADC). At its simplest this could involve nothing more than impedance conversion, gain control and level shifting. More complex functions might involve analogue processing, such as filter banks, and non-linear functions such as peak detection.
4. Sampling and data pre-processing. This includes both ADC, and retaining any digital signals and time stamps that are relevant. It extends as far as deriving consequential data, such as computed positions of impact, estimation of impact energy and many other similar values. It would also provide any self-calibration functions for the sensors.
5. Data analysis and system processing functions. While a sensor only generates data, a sensing system will be responsible for more complex tasks including: self and neighbour diagnostics; recognising patterns in the data streams; supervising a potentially dynamic collection of neighbouring cells to perform higher order functions. This is the layer in which the agent-based software will run, and is the source of the "intelligence" and adaptability in the cells.
6. Inter-cell communications functions. Each cell must communicate with its neighbours. In the simplest form this is just to allow data sharing and mutual functional checking. It also allows directed data transfers, from the sensing array back to whatever processes are going to use the sensor information. At its most complex it may allow agents to share processor resources, or move throughout the network.
7. Inter-cell physical connections. This permits transfer of both information and power between the individual cells of the array.

A schematic diagram of the layer structure is shown in Figure A11. It is important to recognise that the final system is likely to have bi-directional interactions between all layers, i.e. the system will provide actuation as well as sensing functions. While this is not implemented at this stage, the design allows for this bi-directional information transfer. Some plausible functions are opening of sensor protective screens, excitation of bi-directional sensors for active measurements, generation of sensor calibration signals, transmission of wireless signals, and even initiation of some types of repair.

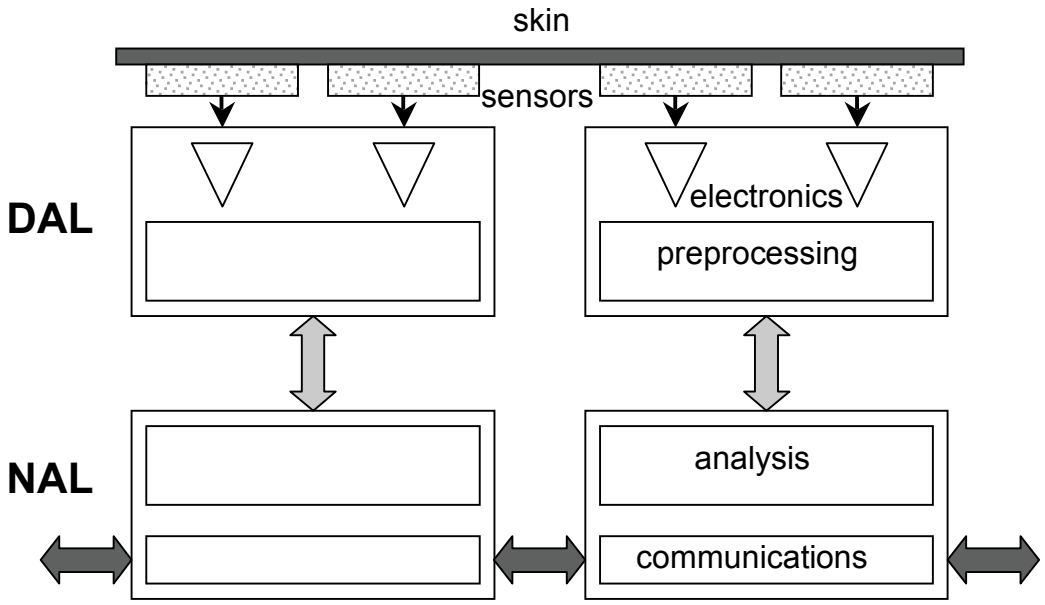

Figure A11: Layer structure of concept demonstrator.

In the earliest stages of the design, all the layers from 3-7 were regarded as an element of a single layered skin, with sensor connections at the top and communications links on the sides. As time progressed it became obvious that a cell consisting of a single hardware block would be relatively inflexible. The system was therefore partitioned into two sub-layers, a pre-processing layer and a post-processing and communications layer. The pre-processing layer performs the analogue electronic signal processing, the data sampling function, and the initial data pre-processing, i.e. the functions of layers 3 and 4 above. It has been named the data acquisition layer (DAL), and will be discussed in more detail below. The post processing and communications layer handles all the data interpretation functions, the system integrity and maintenance role and the inter-cell communications protocol functions, i.e. the remaining functions 5, 6 and 7 above. It is called the network and applications layer (NAL) and is discussed further following the discussion of the data acquisition layer.

One attractive consequence of this partition is that new or additional data acquisition hardware can be attached to the system without any changes to the underlying network. This makes it easy to add say a temperature sensor, a radio communications link, a digital camera, or even a local storage module to the system. In a way it mimics the structural layering of biological sensing systems.

Consideration of cell shapes and numbers

This cellular architecture evolved from the tiled surface concepts first presented in Report 2 (CTIP, 2002). While the discussion in that Report did not specifically define the shape of the tiles, most of the diagrams showed tiles that were triangular. Given that the CD is a functional system rather than an actual physical mock-up, it was felt that while the triangular tiles have some topological advantages, the fabrication of a system based on triangular tiles would add to the cost and complexity of creating the system. For this reason square tiles were selected as easier to manufacture and integrate.

This choice affects only one aspect of the electronic system design. While logically the number of neighbouring tiles is arbitrary (anywhere from 1 to N), in practice, hardware minimization has resulted in the use of chips that support communication with neighbours in groups of 4 ports at a time. This is not significant from a logical point of view, because the software will just ignore any unused ports.

A secondary issue relates to the mechanical fabrication of the electronic system. There may be practical advantages in terms of reliability in combining several of these cellular systems on each fabricated board. The change only involves the number of physically dismountable subsystems, not the number of sensors and processors. The word "tile" became rather confused at this stage, and was discarded. The word "cell" was used to describe the minimum logical partition of the system – a processor and attached sensing and communications functions. The word "module" describes the minimum physically removable chunk of the electronic system. A module may contain one or more cells. The only modules actively considered (either triangular or square) consist of 1, 4 or 16 cells. For the purposes of this Report the cell will be used as the structural element, as the system design is independent of the number of cells in a module.

The earlier discussion of processor and sensor numbers now combines with the architectural issues to define the intended system to have 192 cells. As discussed earlier, each cell will have 5 acoustic emission (AE) sensors, and possibly some additional temperature and pressure sensors, bringing the total planned sensor count to 960 or more.

Interconnection options for the cells

A major concern that relates to the modular approach to the system design is the issue of mechanical and electrical interconnection of the individual cells. A great deal of consideration has been given to these issues. The analysis will be split into 3 sections: power distribution, communications links, and mechanical integrity.

Power connections

The distribution of power could be done in several ways. Some of them are noted below.

- The simplest option is direct power coupling (AC or DC) between adjacent cells. The advantages are relatively high efficiency of power transfer, and ease of implementation. One disadvantage is that, in the simplest scenario, a cell far from a power source depends on connections via many other intermediate cells, which reduces the reliability of the connection. A second problem is the simple issue of voltage drop through many connections. It is important to recognize that while a remote cell requires many series power connections to work, in a practical system there are likely to be many parallel paths from a power source to the remote cell, i.e. the array is typically two dimensional rather than one dimensional. It is fairly clear that in a real system there must be multiple coordinated power supplies distributed about the vehicle, or there will be the potential for single point failures in the power supply.
- It is possible to distribute power without direct contact, via EM radiation, either at microwave, or optical frequencies. While the removal of the need for

a direct power link is attractive, there are serious issues of increased complexity, reduced power efficiency and vulnerability of the EM sources to be dealt with.

- A sort of intermediate EM transmission mechanism using split core transformers (primary winding and half of the core in one cell, with the secondary and the other half core in the neighbouring cell) is also possible, but it is not clear whether the increased physical complexity produces any significant advantages.
- Isolated local power sources for each cell. In the simplest version these would be standard high capacity electrical storage devices, such as batteries. The attractive feature of this is that power interconnections are not needed. The problem is simply one of limited lifetime, and the cost of "battery" replacement or recharging.
- Some type of refuelable local power cell, such as a fuel cell. There are some advantages in terms of distributed power generation in this idea, but the connection of the "fuel" lines (continuous or packetized) has similar difficulties to the direct electrical power connection.

While many of these options have important advantages and disadvantages, the decision has been made to go with simple DC power interconnections. Partly this is because power distribution is not seen as the core contribution of this stage of the project, but mostly it is because of the simplicity and efficiency of power distribution that results.

Some additional factors that make this option more sensible are as follows.

- It is easy to distribute higher voltages than required to each cell on the power bus, and then to switch-mode regulate them to the desired voltage. This allows high efficiency as well as a tolerance for voltage drops.
- In the long term it is expected that the real power source will be distributed throughout the vehicle, in the form of solar/nuclear/fuel cells, so the serial connection issue is likely to be balanced by the parallel paths issue.
- It is plausible for the final power interfaces to be capable of both sourcing and sinking current, and to boost and buck voltages, and to use this to control power flows in the array.

Signal connections

As with the requirements for power links, the issue of data connections is quite complex. Some obvious options are as follows.

- Broadcast EM connections, either using RF or free space optical transmission. At first consideration this seems a very attractive option. There is no need for any physical contact between systems, and in theory any cell can communicate with any other cell. The serious limitation of this type of link is that the "ether" is a shared resource, requiring some mechanism for multiple access (MA). While many MA techniques exist, all require relatively complex techniques for domain division (TDMA/FDMA/CDMA/SDMA[8]) and for coordination of the division process (slot/code/direction allocation etc.). Each division process trades off bandwidth and communication range. At one end are ALOHA-like systems where anyone can broadcast to everyone, but only

[8] Time Division, Frequency Division, Code Division, Spatial Division Multiple Access.

when the channel is available; at the other are pico-cellular networks, where the "broadcast" range is very short, but the total throughput is much larger[9]. In some of these systems there is the additional problem of directional control. If the system used sectored cells to maximize domain reuse, there would be a need for complex antennae structures, possibly even steerable structures. There is also a serious risk that high-level EM interference might block the main communications channels. Free space optical communication links are also of interest. Their shorter EM wavelengths permit tighter directional control of transmission, and thus easier SDMA, but the down-side is the need for more precise orientation of the transmission and reception elements.

- An alternative approach is to use a nearest neighbour, direct link system. Each cell can talk only to its neighbours, via a direct electrical or optical connection. In this case longer-range connections must be created as a chain of inter-cell links. While there are no longer problems of domain sharing, as each transmit-receive pair has a unique channel, there are potentially problems with channel capacity saturation. A second class of problems is related to message routing: to get a message from cell "A" to cell "B" requires either bandwidth-inefficient flooding algorithms or creation and maintenance of routing tables. This approach is somewhat like a miniature version of the Internet.

There are obvious advantages to both types of systems presented above. After significant discussion, the latter approach has been adopted as the normal mechanism of communications, at least for the initial development. Details on the hardware and protocols will be given later. In the first instance the transmissions will be direct digital as the inter-cell distances are expected to be small. It is possible that future systems will use either LVDS[10] electrical, or even fibre-based optical links for the normal communication channels.

Future plans allow for the evolution of dynamic hierarchies among the cells, and the possibility of special communication facilities being allocated to such cells. In such a case a "supervisor" cell might be given the right to control special or emergency RF communications between itself and individual cells, or to operate the RF channel as a broadcast facility. This facility requires extra functions of some or all of the cells, but provides some valuable additional communications features.

A subdivision of the direct connection issue is the use of serial or parallel data interfaces. The availability of high bandwidth serial interface hardware and standards, and the increased costs and risk of connection failures in parallel systems, have resulted in a decision to use high-speed serial links for intercellular and interlayer communications.

Mechanical interconnection issues

The type of connection from the sensor to the DAL has not yet been decided. Two options that have been considered are the use of a strip of flexible conducting material (possibly metallized PVDF) as a ribbon cable to contact the DAL board, or the use of a compliant layer, with embedded contacts through it, directly between the sensor

[9] A proposed variation of this was to use deliberate range attenuation through an absorbing sheet, which allowed broadcast transmission to nearby cells, but severely attenuated long-range transmission.
[10] Low voltage differential signalling.

elements and the DAL board. This issue of EMI sensitivity of the sensors is likely to have an impact on this decision.

Some debate was held on the best method to make the connections (power and signal) between the cells. Perhaps the most promising candidate for long-term implementation is the use of channelled directional conductive strips, which would be bonded as ribbons and trimmed to fit the spacing between the cells. For simplicity it has been decided to use basic IDC ribbon cables to mimic the conductive strips. This allows a relatively cheap and well-defined commercial solution, rather than the investigation of a less well understood technology. Again, this will have to be investigated in relation to possible EMI effects.

Perhaps in the future the cells will have connection ports on their edges that respond to the attachment of the contact strip, by learning the function of each line and configuring power and communication links as necessary[11].

Controlling complexity and cost of the system

It is very clear that there are significant risks associated with the highly distributed CD design. Some of these are listed below, with the strategies used to control the risks.

1. The (relatively) large number of cells in the array will amplify any design cost changes. A large task has been the selection of hardware that minimizes parts counts, and cell internal connections, to lower the cost and (external) complexity of the cells. Where possible, bus interface chips and peripheral chips have been avoided by the choice of processors that have embedded peripheral features. The relatively large number of cells also allows some limited economies of scale and the use of commercial automated assembly equipment.

2. The complexity of such a large system may be too great for the limited time and resources available. The modular architecture and the staged development process are both designed to limit many problems to a local cell. The intention is to debug the concepts using a few development systems before proceeding to a small (say) 4 x 4 array of cells, and moving to the complete system once the smaller unit is functional. The deliberate partitioning of the cells into two layers allows the acquisition and network processing to be separated, and the two layers to be tested independently.

3. The central elements of the array are distant from the edges where access is intended. The intention is that testing and debugging of the system will be controlled and observed by an external "host" computer that can plug into any of the cell's free communication ports. One benefit of the modular architecture is the ability of the "host" computer to be plugged into any port in the array. All edge ports are immediately available. The "internal" ports can be unplugged from neighbours and directly connected to the "host". The in-

[11] In the more distant future maybe the strips will be grown into place by electrical or chemical gradients!

built fault tolerance, and auto-configuration, is intended to make this a simple activity.

There are also other problems related to the software, especially issues of distributed control, but these are the issues that the CD is designed to explore. A major part of the design process for the underlying hardware is controlling the known risks of the system and buying or creating tools that help in the control of these risks.

A2.3 Data acquisition layer design

The data acquisition layer (DAL) is designed to interface with sensor inputs[12] on the outer surface, and a digital interface to the network and applications layer (NAL) on the inner surface (see Figure A11).

Sensor specifications

As mentioned in Section 4 and Appendix 1, the first-generation sensors are piezoelectric sensors, which generate signal voltages as a result of direct mechanical distortion of the sensor, or as a result of elastic waves travelling laterally from the impact point to the sensor element. Some of the sensor elements will be small area units, which will be used for time-delay impact location measurements, while others will be large area sensors used to guarantee a direct signal from an impact almost anywhere on the surface of the cell.

Initial testing of the sensor and skin structures being considered suggests a signal bandwidth of several MHz. Each cell needs to sample the data from five or more sensors, in real time. The strategy to be used in acquiring data from the sensors has not yet been finalized. It is expected at this stage that it will not be necessary to record extended full bandwidth data from all sensors. Most practical proposals suggest the recording of data from each sensor at a few MSPS. Ideally all the analogue sampling should be performed with the minimum requirement of additional hardware, but it will be necessary to reach a compromise between the use of some external components (e.g. for filtering and/or level detection), and higher data sampling rates. The selection of processors for the data acquisition layer (see below) suggests that five analogue channels can each be sampled at over 3 MSPS in a simple integrated DSP unit.

It is likely that additional low-bandwidth sensors will be used to sense other parameters such as temperature, pressure etc., but this is unlikely to limit performance in the system.

Data acquisition electronics

Some sort of sensor signal pre-processing is likely to be required in order to condition the signal prior to sampling. The minimum processing is probably impedance matching, signal gain and anti-aliasing. Other types of processing may be required, either to reduce the necessary data bandwidth, or to reduce the subsequent computational load on the processor. Some examples include filtering to select one or

[12] as well as probable signal and actuator outputs in later versions.

more frequency bands containing information of interest, and logarithmic scaling to expand the dynamic range. The actual hardware required is very dependent on the nature of the signal being recovered.

Any analogue pre-processing hardware is likely to add significantly to the system cost, so its complexity must be minimized. Wherever possible signal pre-processing will be performed inside the processor, for maximum flexibility and for cost reduction.

Processor functions

The major reason for having some kind of processing for the sensor/actuator signals is to provide a simple and consistent interface for the processing and network hardware. The sensors are likely to increase in number and function over time, and it is not desirable to have to rebuild all the processing and network circuits every time such a change is required. The presence of a pre-processor will allow a wide range of sensor types to communicate using a well-defined protocol.

The data acquisition processor (DAP) thus acts as a flexible interface between the particular set of sensors embedded in the cell, and the higher-level intelligent processing and communications of the network. With appropriate software, the DAP and the network and applications processor (NAP) can negotiate the functions and signals that will be transferred between them, even if the sensor function is entirely new.

DSP pre-processing

The presence of the DAP allows a decrease in loading on the NAP, and real-time processing of the input signals even under extreme loading of the network. In addition, it allows for independent processor integrity tests between the two different types of processors used in the acquisition and networking layers.

The DAP will be used for both simple and complex signal processing. At the simplest end of this range it will make any required corrections (such as calibration) to the raw sampled data. Two possible mechanisms can be used. One is that the DAP and attached sensors can be connected to a calibration system that uses the DAP to measure known signals, and determines a correction function to produce a calibrated standard output from the sensors. A more desirable possibility is to enable the system to self-calibrate. If either a known local signal can be induced in the sensors, or a globally (or at least broadly) distributed signal can be supplied to all the DAPs, this can be used to generate calibration information without needing to dismantle the units during use.

At the next level the DAP allows compensation of the sensor data, e.g. temperature and pressure corrections for the local piezoelectric sensors. It can also be used to deduce local information from multiple sensor measurements, such as the processing required to estimate the impact location from the time delays in the signals from the small AE sensors.

In essence the DAP will carry out the first stage of the necessary role of the cells: data reduction and interpretation in terms of local events. The presence of the DAP means

that the information content of its outputs is much higher per bit of data transferred than that of its inputs. A meaningful output of "S severity impact at position (X,Y)" is much more useful than 4 or 5 sampled signal sequences.

Another potentially valuable feature of the DAP is that it is capable of returning logged samples of any raw data with which it is supplied, for diagnostic purposes. While the "host" computer (referred to in the previous sub-section) may not be able to read all data from all processors in real time continuously, the individual cells could be programmed to log certain types of data for diagnostic analysis. It is even possible that the system may be programmed to record certain types of data for later analysis.

A facility that would be valuable for the DAP, but which requires the facilities of the network processor and communications links as well, is some kind of distributed absolute time stamp. It may be possible to generate this in a distributed way using high priority inter-cell communication messages, and stable local cell clocks.

Processor selection

The original intention was for the electronics of each CD cell to consist of one DSP chip with built-in multi-channel A/D conversion hardware, FLASH memory and multiple high-speed communications ports. Despite a detailed search, no single processor was found with all the required features. Quite a number of DSP chips have attractive configurations, but none have all the features with sufficiently high performance on the sampling and communications interfaces.

The split into acquisition (DAL) and networking (NAL) sub-units reduces the breadth of demands on the processors. The requirements for the DAP are now:

- multiple (five +) high-speed (few MSPS) analogue sampling channels;
- built-in FLASH memory to store code for data pre-processing; and
- a standard high-performance communication link to the NAP to allow data transfer and inter-processor communications.

Despite the reduction in the demands, the number of potential processors is still quite small. A variation on the architecture, using a number of slightly slower sampling DSP devices[13], was considered but added to the complexity of the system. It would have required more interconnections and made time delay calculations more complex.

A number of potential processors have been considered. The processor that most closely matches the specification is the TMS320F2810/2812 from Texas Instruments[14]. Some abbreviated specifications for the device are noted below.

- 150 MHz, 150 MIPS processor – which allows for quite complex pre-processing.
- 64/128 kword FLASH memory (2810/2812), providing a reasonable amount of space for software without the need for external memory.
- 16 multiplexed analogue input channels sharing 2 sample and hold circuits and a single 12 bit, 16.6 MSPS, pipelined ADC.

[13] The TMS320LF2401.

[14] Some close competitors were the Analog Devices ADSP2199x processors with slightly higher sampling rates, but no FLASH memory, and the Motorola 56F8xx DSP devices with FLASH but slower sampling rates.

- High-speed serial (McBSP[15]) interface, to allow rapid communications throughput to the NAP.
- Many other memory, timer and interface facilities, which permit the system to run with very little additional logic.

A schematic diagram of the proposed DAL is shown in Figure A12. Perhaps the greatest potential limitation is that the ADC sampling rate is a little low, given that it must be shared by five inputs. The resulting 3.3 MSPS average per input is expected to be acceptable. A more minor limitation is that only two of the inputs can be sampled at the same time, as there are only 2 sample and hold circuits. This will have to be compensated for by either: the external electronics, and digital "time of arrival" detection, or by time-delay compensation in the processing of the interleaved data samples.

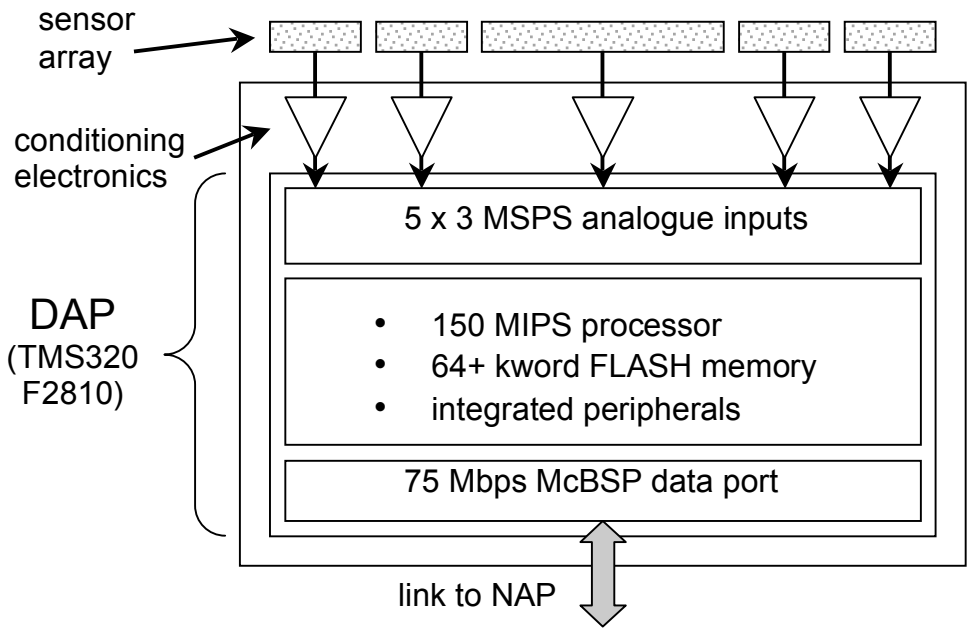

Figure A12: Block diagram of the data acquisition layer (DAL) for one cell.

Another important selection feature of the DAP (and similarly the NAP which will be described below) is the ready availability of low-cost DSP Starter Kits (DSKs) to aid the initial development process. A total of 6 DSKs have been purchased to allow different hardware and software users to develop the system hardware and software. It is expected that the software for the DAL can be generated using the simple environment provided for in the DSK, without the need for a full emulator system.

Interlayer communications

In an earlier sub-section it was noted that interlayer communications would be implemented by high-speed serial links. One of the attractive features of some of the TMS family of DSP devices is the use of a flexible high-speed serial bus known as the Multichannel Buffered Serial Port (McBSP). This bus can support up to 75 Mb/s data

[15] Some limited information is provided in the next sub-section.

rates, as well as allowing multiple devices to share the bus. The presence of a McBSP controller on both the DAP and the NAP greatly simplifies the design of inter-processor communications.

At this stage the link between the DAP and NAP is a point-to-point link, but one attractive option is the ability to attach multiple DAPs to the same McBSP bus. This would allow the DAL to support additional sampling bandwidth, via multiple DAPs. It would also allow specialized sensing units to be paralleled into this bus.

A2.4 Network and application layer

Layer functions

As was explained earlier, there is one Network and Application Processor (NAP) in each cell, and this communicates with the attached Data Acquisition Processor (DAP) and with adjacent NAPs in the Network and Application Layer (NAL). Besides facilitating the communication of data, it is anticipated that much of the data processing will be performed in the NAL processors, and this will be done in a robust and distributed fashion through the use of software agents, which are explained in more detail in other sections of this Report.

The requirements of each NAL cell can be summarized as follows.

- Communication with the Data Acquisition Processor. This requires a standardized hardware and software interface so that DAP modules can be interchanged.
- Communications with adjacent Network and Application Processors. As the processors in the NAL will be configured in a mesh, high-speed serial ports are required for the physical interface to each NAP. To allow communication between arbitrary NAPs (for maximum flexibility of the CD) the communications software must not only implement point-to-point communication, but must also perform routing of data, and there must be the flexibility to experiment with networking protocols. This will require the implementation of a flexible and layered communications stack software.
- Data Processing. Each NAP, besides running the communications software for the high-speed ports, must also have the processing capability for implementing the agent-based data processing algorithms. As implementation, debugging and continuous development of this software will require frequent updates of code, it is essential that software can be readily and rapidly distributed to each NAP.

Processor selection

Based on the requirements given above for each NAP, the required capabilities of the processor have been estimated. Some of these estimates are very rough at this stage, but better figures will not be known until a section of the CD has been implemented. The desirable characteristics used to select a processor and its support components were as follows.

- Processing capability in 100's of MIPS (with 4 ports operating at 1 Mbps the aggregate data rate is about 400 kbytes/sec, and a 400 MIPS processor can execute 1000 instructions per byte received).

- FLASH memory of at least a few hundred kbytes from which the processor boots. This does not need to contain all NAP software, but just enough to enable the processor to obtain the rest of its software using the network.
  - Desirable: If this resides in the processor it reduces the external component count.
- Fast RAM of at least a couple of Mbytes for software and data. This is too large to be found in the processor, so will be required to be external. For low cost, low power consumption and small footprint this will need to be some type of dynamic RAM (e.g. SDRAM or its DDR variant).
  - Desirable: If the processor supports a glueless interface to such memory the external component count is reduced.
- NAL communications hardware supporting four UARTs with data rates of at least 1 Mbps.
  - Desirable: If this resides in the processor it reduces the external component count.
- NAP communications hardware supporting a standard high-speed serial interface.
- Desirable characteristics of the processor include:
  - low power consumption,
  - watchdog timer,
  - hardware timers,
  - unique identifier in each processor,
  - low cost.

Based on these criteria a number of processors were considered, but none were ideal. The major problem was that there were no processors containing four homogeneous high-speed serial communications ports at reasonable cost, so an early decision was that this requirement would have to be implemented in external hardware. The processor selected for the best compromise of the remaining criteria was the Texas Instruments TMS320C5509 digital signal processor. Its capabilities against the requirements are listed below.

- Processing capability up to 400 MIPS.
- FLASH memory: none on the processor, but a glueless external interface to FLASH.
- RAM: 256 kbytes in the processor and glueless external interface to SDRAM.
- DAP communications: McBSP hardware supporting high-speed serial communications.
- Low power consumption: C55x family claims to be most power efficient DSP, down to 0.05 mW/MIP.
- Watchdog timer: available.
- Hardware timers: two 20-bit timers.
- Unique identifier in each processor: 64-bit unique identifier in silicon.
- Low cost: approximate cost US$25 each.

Other factors that also influenced the decision were the fact that the C55x family has available good software development tools (Code Composer Studio), Real-Time Operating System (RTOS, included with Code Composer Studio), low cost evaluation systems (C5510 DSK for US$395) and a wide range of third-party software available to reduce development times.

Communications software architecture

Communications requirements

The NAL communications software needs to implement not only communications to each port, but also a four-port router for passing data between NAPs. This must also be done in a flexible manner so that we can use the CD to experiment with networking protocols. The types of communications required are as follows.

- Initialization. Code and data need to be able to be sent to each NAP using the NAL, and loaded in RAM or programmed into FLASH, then executed. Entering code and data using the JTAG on each processor is far too slow, so using the NAL is the best way to distribute code updates. This requires that each NAP has enough functionality when locally booted to use the NAL. This networking functionality would not be used operationally, and it is reasonable to assume that no hardware faults or reconfiguration will occur during the initialization phase, so this does not need to be as robust or as sophisticated as the operational protocols.

- Diagnostics. As the CD will be used as a tool for experimenting with agents and sensing technologies, it will be useful to have the ability to obtain information that would not be sent by the operational protocols. This might include information about the configuration during initialization, and the ability to determine the status of arbitrary hardware and software during operation. Although this type of communication needs to be robust to hardware faults and reconfiguration, it is not intended to be used operationally so can use information specific to the CD to simplify its implementation.

- Agent Communication. This is the type of communication that would occur in the real application in a space vehicle. This will consist of the communications between software agents running on the processors. It is expected that there will be frequent changes to the operational communications protocols, so this must be able to be updated via software download during initialization. It is also possible that multiple protocols will be running simultaneously to allow communications between different types of software agents.

- Packet Routing. This type of communication would also occur in the real application. Where agent communication is not just between adjacent processors with a direct communication path, there will be a need for routing of communications packets. Different protocols, or experiments with different network topologies, may also require different routing algorithms. This level of communications software will need to be capable of being downloaded during initialization.

To support these functions, a basic level of communication must be available to each NAP, coded in its local FLASH memory. As reprogramming this software may use the JTAG, and hence be very slow, the software should be as simple as possible so that it is reliable and stable. Also, the software should be small, so that it can be loaded into the internal FLASH of a processor.

Overview of communications architecture

The communications software architecture to be used is a layered communications stack. The Data Link Layer (DLL) controls communications between two processors across a physical link and forms the lowest level in the stack. This protocol is fixed and is not intended to be changed. In the next level are the network protocols, and the data link protocol can support multiple simultaneous network protocols. To allow network protocols downloaded during initialization to be used, the data link uses the concept of registering a network protocol. Therefore, some network protocols (e.g. for initialization) can reside in the processor FLASH memory, and some are downloaded during initialization (e.g. agent communication). When a network protocol registers itself with the data link, a software interface between the two is established. When a packet from a registered protocol is received by the data link it is passed to the relevant network protocol, but packets from unregistered protocols are discarded.

A diagram showing the type of communications stack that will be implemented is given in Figure A13. This illustrates the protocols that need to be implemented in the NAP FLASH, and those that can be downloaded during initialization. Many of the protocols are indicative only, as not all have yet been defined. From the network layer up the stack is not fixed, as new protocols can be transferred through the network and registered with the Data Link Layer. The transport layer (like TCP for the internet) provides reliable end-to-end communications based on the unreliable transport of packets at the network layer, but it is not needed for all applications. The agent protocols are indicative only of what could be done, and will not be further described in this document.

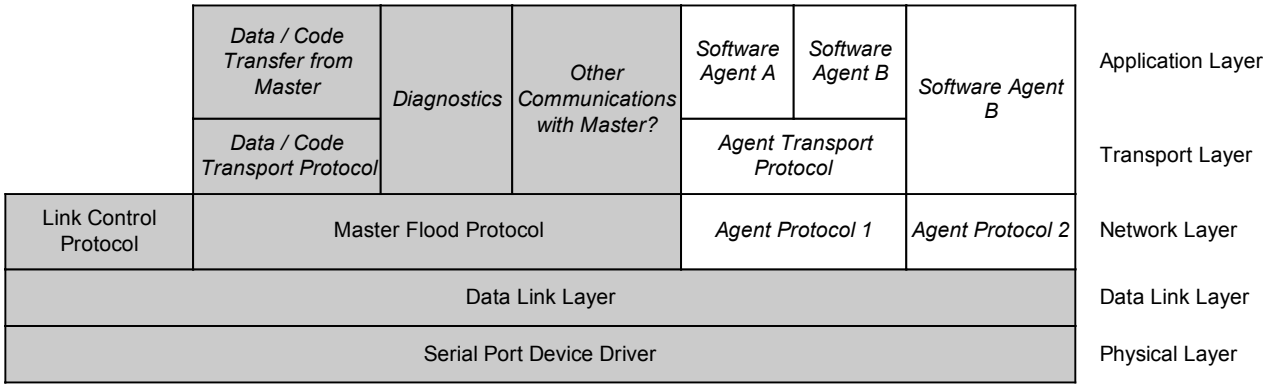

Figure A13: The communications stack to be implemented on the concept demonstrator. The protocols in italics are indicative only and have not yet been defined. The protocols with a grey background will be implemented in the NAP FLASH; the others may be downloaded during initialization.

The serial port driver is responsible for controlling the physical communications hardware, and the data link layer passes data through the serial port driver.

The data link layer provides the basic data transport between the two processors on a physical data link, and also provides the mechanism for registering network protocols. This is described in more detail below.

The network protocols provide packet communication through the NAL. The currently defined protocols are:

- Link Control Protocol (LCP) – this is a special protocol to control the data links and is described in the next sub-section.
- Master Flood Protocol (MFP) – this protocol is intended for use communicating between one master computer (probably a PC) and all the processors in the NAL. Routing is based on flooding so that routing tables do not need to be constructed, hence this is simpler to implement. The applications that use this protocol include software distribution during CD initialization and communications with the master for diagnostics and status information. This is described below.

Data Link Layer

Overall, the purpose of the Data Link Layer (DLL) of the NAL communications is to:

- allow network protocols to register themselves with the data link layer;
- send packets from registered network protocols to a selected physical data link;
- pass received packets from a physical data link to the corresponding network protocol;
- format network packets for transmission and reception over the physical data link;
- monitor the physical data link and determine when connection and disconnection occur;
- when connection is detected, negotiate a physical link data rate; and
- control the physical data link (e.g. adjust serial port speed).

The last three of these are handled by a special network protocol called the Link Control Protocol (LCP). For each physical data port there is an instantiation of the Data Link Layer software and a corresponding LCP. The LCP will be discussed in the next sub-section.

The packet format used by the DLL is similar to the widely used Point-to-Point Protocol (PPP) that is described in RFC1661 (http://www.faqs.org/rfcs/rfc1661.html) and RFC1662 (http://www.faqs.org/rfcs/rfc1662.html), and is shown in Figure A14. The protocol byte specifies a protocol number, the maximum size of the payload is 1500 bytes (the usual maximum packet size for the internet), and the checksum is a 16-bit cyclic redundancy code (CRC). Byte-stuffing is used to prevent the occurrence of the flag character in the payload.

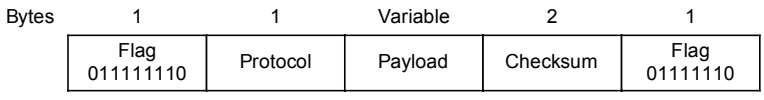

Figure A14: Data Link Layer packet format for concept demonstrator.

The software class that allows for the registration of network protocols and passing of packets between the network protocol and DLL will be described in another document.

Link Control Protocol (LCP)
The purpose of the LCP is to monitor the data link and determine when a processor is connected at the other end. When this is detected there is a capability exchange (where the only capability currently exchanged is supported serial communication speeds) that occurs at a base communication speed (currently 9600 baud). Once a speed has been agreed, both ends of the link change their port speeds, and then check that they can communicate. If all is well the DLL is then declared open for other protocols to use. The state transition diagram for the LCP is given in Figure A15, but details about the state transitions will not be given in this document.

There are only four commands for the LCP, which are:

- CapReq – send local capabilities to remote end,
- CapAck – reply to received CapReq with selected capabilities common to both ends,
- EchoReq – request an echo from the remote end, and
- EchoAck – reply to EchoReq.

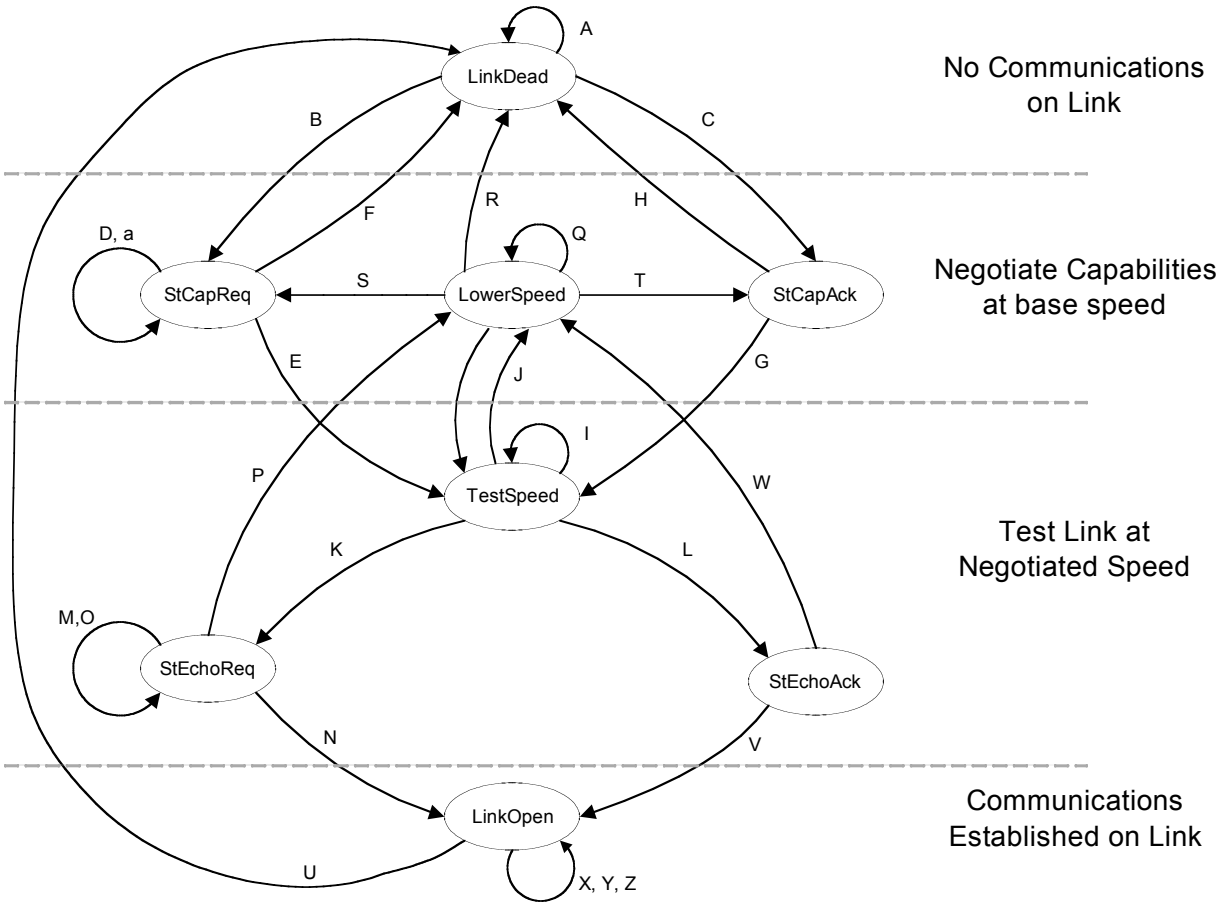

Figure A15: State flow diagram for link control protocol.

The packet format for the LCP is given in Figure A16.

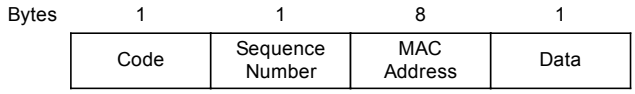

Figure A16: Packet format for link control protocol.

The Code byte encodes the command. The sequence number is incremented for each CapReq and EchoReq packet, and CapAck and EchoAck contain the sequence number of the packet to which they are replying. The MAC address is the 64-bit unique identifier for the NAP, and the Data byte is used for the capability exchange.

Master Flood Protocol (MFP)
The Master Flood Protocol (MFP) is intended to provide simple but reliable communication between a "master" processor (probably a PC used to monitor and control the CD during non-operational functions) and all processors in the NAL. It is not intended for use for inter-processor communication. It should be emphasized that such a master processor would only have this status during non-operational functions: the agent-based operational system of the CD will operate without external hierarchical control. The master processor can send packets either to all processors or to a single processor, and the other processors can send packets either to all processors or to the master processor. These functions will permit the network protocol to be used for applications including software distribution, initialization of the CD and obtaining diagnostic information.

The protocol has not yet been fully defined, and so far the specifications are as follows.

- Routing will be based on flooding, to keep the protocol simple and so that routing tables do not need to be built.

- All packets will contain the following information.
  - Source Processor identifier, which will be the same 64-bit identifier used by the LCP.
  - Destination Processor. This can indicate all processors, the master processor, or the master can send to a particular NAL processor.
  - Sequence Number, which is used to control the flooding.
  - Hops-to-Live, which is a value that is decremented each time a packet is passed to another processor. When this reaches zero the packet is discarded.

The flooding based routing is quite simple. When a processor receives a packet, unless the destination is only that processor, the packet is passed out all communications ports except the one on which the packet was received, and the Hops-to-Live counter is decremented before the packet is passed on. If a received packet has an error it is simply discarded. When a processor receives a packet that it has previously received without error, and it knows this by examining the source processor and sequence number in the packet, then the packet is discarded. Only a limited memory of past packets needs to be kept, and if an old packet is received more

than once and not remembered, then the Hops-to-Live counter will ensure that it is not passed around indefinitely.

Communications hardware

The choice of serial communications as the preferred data transmission mechanism between the NAPs was justified earlier on the grounds of reduced interconnection complexity. There are still some issues to be resolved relating to the timing of the data transfers. One option is the use of a global clock that is distributed throughout the system. This has some advantages that are quite attractive in that the data transfer rates can be higher and global time synchronization is possible. Some serious consequences of a synchronous communications system include the difficulty in defining reference causality in a complex or irregular mesh-connected structure, and the problem of losing and regaining lock if sections of the array are damaged or repaired.

Quite a number of serial interface standards were considered including I^2C, SPI, SCI, USB1.1, USB2.0 and even Ethernet. The inter-cellular links have some requirements that remove some of these options.

- The interface must handle high priority messages with low latency and overheads.
- Given the distributed nature of the cell array, communications must be peer-to-peer rather than master/slave.
- The multiple links (typically 4) must be identical.
- The links must all be bi-directional.
- The links are all point-to-point, so there is no need for contention or arbitration or physical address recognition.

Some consideration was given to designing "custom" FPGA devices. With the added time and cost constraints the decision was made to use high-speed universal asynchronous receiver transmitter devices (UARTs)[16]. While most UART-based communication systems are fairly slow, this is largely due to the length of the cables. For the short-range systems that are being contemplated here, the data rate is likely to be limited by the hardware rather than the cabling. Quite a number of UARTs are able to operate at the > 1Mb/s rates which are estimated to be required. Another advantage associated with the use of UARTs is that they come in multiples. It is easy to get double, quadruple and even octuple UART chips.

The decision was made to use a standard pinout quad UART from TI, the TL16C754BFN. This particular part is a little faster than some of the similar pinout devices, and has slightly deeper buffering. The specific characteristics of the selected part include:

- 4 independent UART devices,
- high-speed performance up to 3.3 Mb/s,
- 64 byte transmit and receive FIFOs for each channel, and
- a simple interface to microprocessors.

[16] A potential future candidate is USB2.0, which has many attractive features including the availability of many existing peripherals. The present problems with USB2.0 are software complexity, and lack of low cost multi-port integrated hardware.

During the hunt for UARTs an even faster alternative was discovered from Oxford Semiconductor. Their part is the OX16C954, and in at least one package it is pin compatible with the TI (and other) parts. The OX16C954 has deeper FIFOs (128 bytes) and faster operation. It can support 15 Mb/s in normal mode and 60 Mb/s in isochronous mode. The plug compatibility of these devices, and significant delays in their availability, led to the selection of the TL16C754BFN as the intended chip, but samples of the faster OX16C954 are being sought.

For the moment, the UARTs will simply operate directly from one to another. If distances ever exceed the safe limits for driverless operation, appropriate driver/receivers will be added to the system.

Mechanical node interconnections

The physical interconnection between NAL modules is used for the following functions.

- Serial Communications Signals: Transmit and Receive Data signals. The handshaking that will be used is yet to be determined.
- Power Distribution: probably distributed at a higher voltage (12V?) with switching regulators on the NAL modules providing power for both the NAP and DAP.
- A few parallel port bits that could be used for diagnostic purposes
- Clock Distribution? This could be for synchronising clocks on the processors.

A few possibilities were considered for the interconnection, and the use of ribbon cable or directional conductive polymers were the main contenders, but in the end it was decided that for simplicity and flexibility, ribbon cable would be the best choice. The exact signals on the cable have yet to be determined.

A2.5 Current status and ongoing plans

The concept demonstrator is a complex system, and design and implementation has been divided into a number of stages. The major stages of electronic development and their sub-tasks are listed below, with the sub-tasks in italics the ones that have commenced.

- Design of NAL Hardware and Basic Software.
  - *Design of NAL communications protocols.*
  - *Implement basic communications software on PC.*
  - *Build hardware to implement communications ports on C5510 DSK.*
  - Implement basic communications software on DSK.
  - Design and build hardware for C5509 prototype module (build about 16).
  - Construct network of prototype modules, test and extend basic communications software using simple sensing (switches on NAP used as inputs, DAP not used).
  - Design and build hardware for C5509 final module (build about 200).

- Design of DAL Hardware and Software.
  - *Determine processing required by sensors, test algorithms using MATLAB.*

  - Implement basic processing software on F2812 DSK.
  - Design and build hardware (including analogue interface to sensors) for F2810 prototype module (build a few).
  - Implement processing software on F2810 prototype module.
  - Design (if revision required) and build hardware for F2810 final module (build about 200).

- Integration of NAL and DAL.
  - Write software for communication between NAP and DAP.
  - Test hardware and software communications between NAP and DAP.

- Implementation into the Concept Demonstrator.

Reference

CTIP (2002). *Development and Evaluation of Sensor Concepts for Ageless Aerospace Vehicles. Development of Concepts for an Intelligent Sensing System*. CSIRO Telecommunications and Industrial Physics. Confidential Report No. TIPP 1517. May 2002. Also published as NASA technical report NASA/CR-2002-211773, Langley Research Center, Hampton, Virginia.

Appendix 3: Simulation of Self-Reconfigurable Sensor Networks in Ageless Aerospace Vehicles

A3.1 Introduction

Self-monitoring, self-repairing aerospace vehicles require modular, flexible and adaptive sensing and communication networks. In general, a modular (multi-cellular) sensing and communication network is expected to detect, evaluate and react to impact location, energy and damage over a wide range of impact energies (CTIP, 2002).

In this Appendix we describe the underlying principles, methodology, preliminary results, and future directions for modelling and simulating a multi-agent system made of units that will be referred to as "cells". These cells will not only form a physical shell for an aerospace vehicle, but will also have sensors, logic, and communications. Other cells may be mobile, carrying their physical and logical capabilities to wherever they are needed, perhaps performing active measurements using in-built sensors, or other functions. Single cells may need to make fast and automatic responses to sudden damage, while collections of cells may solve more complex tasks, for example, create an impact boundary with desired characteristics. The following sequence of responses may illustrate our ultimate intentions.

- Cells re-configure their connections by seeking or activating new communication links, and disabling or downgrading some old links.
- Cells self-organize into new groups (e.g., impact boundaries or impact clusters) in response to new information obtained from their sensors and communication ports.
- Appropriate short-term repairs (possibly temporary) are made with appropriate urgency.
- Subsequently, cells monitor repairs and run series of self-tests confirming the new coordination ability.
- Cells cooperate, or refer to a higher-level supervisory system, to develop a long-term strategy for permanent repair or replacement of damaged parts, if necessary, and avoidance of similar damage in the future.

At this stage work will be focused on the first two of these responses.

The present work is aimed at investigating the use of a non-hierarchical system of agents, from which a global response emerges from purely local information and interactions. Such a system contains no supervisor and no central intelligence to direct agents' behaviour and responses. A major benefit of this approach in the context of an ageless vehicle is that there is no single point of vulnerability and no explicitly provided redundancy. The inherent redundancy of a multi-agent system is utilized to enable the system to continue operating when individual agents are damaged.

This Appendix describes the development, within the Simulator, of two algorithms that will form the basis of the intelligent response of the stage 1 development of the CD. These two algorithms embody the following strategies.

1. A strategy appropriate for the case where major damage is inflicted on one or more cells by one or more impacts. This would include damage in which the skin is penetrated and/or the functionality of the cell is impaired (listed as "serious" or "heavy" impacts in Section 1). The initial aim of this strategy is the formation of "impact boundaries" that enclose critically damaged areas.

2. A strategy appropriate for the case of minor damage to the vehicle skin produced by one or more impacts. This would include impacts that did not penetrate the skin and resulted in no damage to the cell functionality (listed as "light" or "moderate" impacts in Section 1). Such impacts may require repair of skin damage. Even if repair is not required, the system needs to be aware of the occurrence, rate and spatial clustering of impacts.

It is intended that a hybrid version of these algorithms will be implemented in the initial development stage of the CD, while further development and evaluation of these algorithms and others will continue using the computer simulator (CS).

A3.2 Methodology

The primary principle that is followed in this work is that a *global response emerges* as a result of interactions involving transfer of information embedded locally. This method (relying on *emergent system behaviour*) attempts to completely avoid or reduce the number of single points-of-failure. The second important principle is *economy of information* – the behaviour of each cell should be as simple as possible, in terms of both the internal logic and the communication policies. The information economy principle is directly related to the ability to manufacture new cells and to repair or replace damaged cells: the simpler the cell, the easier it should be to repair or replace it.

Recent advances in sensor networks and micro-electro-mechanical systems (MEMS) and devices led to the idea of *localized algorithms*, in which simple local node behaviours achieve a desired global objective (Estrin et al., 1999), while communicating only with nodes within some neighbourhood. Estrin et al. proposed a simple communication model for describing localized algorithms – *directed diffusion*. According to this approach, network nodes propagate interests that establish gradients directing the diffusion of data. As it propagates, data may be locally cached and/or transformed at each node. However, despite some progress, there is a lack of a unifying methodology underlying *design* of localized algorithms. The main question that has to be solved is how to constrain the emergent behaviour, or, in other words, how to produce and retain desirable emergent behaviour while avoiding potentially damaging patterns of agents' interaction.

The problem of systematically transforming the global task to individual behaviour models is yet to be resolved, although some promising results have been reported by Nagpal (2002), in the context of *amorphous computing*, where programmable self-assembly was demonstrated using biologically-inspired multi-agent control. The contribution of Nagpal's work is in defining a small class of primitives (e.g., gradients, neighbourhood query, polarity inversion, cell-to-cell contact, etc.), a set of global operations, and a translation implementing the global operations as localized

algorithms using the set of primitives. However, the question of how to obtain and inter-connect global operations themselves is left unanswered. Moreover, the task of discovering the most effective primitives and translating them into localized agent programs would have to be repeated for each domain, in the absence of generic techniques and guidelines.

Thus, the problem of global response engineering in multi-agent networks is of central importance to this project, and motivates our search for patterns and invariants in self-organization of multi-agent systems for monitoring and repairing impacts on the AAV.

Our proposed methodology is based on an iterative process that includes the following steps:

a) forward simulation (for a class of localized algorithms dealing with impacts of various strengths), leading to emergent behaviour;
b) measurement of emergent behaviour (based on information-theoretic metrics for bounded emergent behaviour);
c) evolutionary modelling of the desired global emergent behaviour, where the fitness functions correspond to the metrics obtained at step (b).

Another, final, step would involve development of *design primitives* suitable for self-reconfigurable sensor networks in Ageless Aerospace Vehicles.

This methodology is reflected in the work done so far, which has been oriented to designing and prototyping representative algorithms, while development of the information-theoretic metrics for bounded emergent behaviour will follow. Evolutionary modelling would not only verify the results obtained in the previous stages, but may shed more light on the design primitives.

The following sub-sections present the proposed cell structure and the reactive agent architecture for the cell logical block. A description of the developed software simulator and the results obtained for a class of localized algorithms follow.

A3.3 Localized algorithms for impact inspection

Computational modelling at the cellular level in the context of space exploration is not new – a few biological analogies have been investigated in the literature (Mjolsness and Tavormina, 2000). The information-gathering process embedded in a modular multi-cellular vehicle skin assumes that the skin can determine the impact boundaries and their extent in the presence of connectivity disruptions and cell failures – analogous to the initial clotting of a wound on a mammal.

One of the immediate tasks is the formation of *impact boundaries* that enclose the critically damaged areas. It is highly desirable that such boundaries form a continuously connected closed contour, and are robust to fluctuations caused by proximity to the impact. In short, the aim is to achieve spatio-temporal stability in impact boundaries.

The second important task is forming a flexible network among cells that registered non-critical impacts, in such a way that the obtained *impact network* (a cluster) can facilitate fast impact area inspection and routing of the repair resources.

We selected these two problems (impact boundaries and impact networks) to investigate self-organization potential and feasibility, and to provide a test-bed for the information-theoretic metrics measuring bounded emergent behaviour.

A3.4 Cell structure and agent architecture

The fundamental components of an autonomous agent (or *cell*) were decided to be:

- Structure – physical shape of the cell;
- Sensors – obtain data readings from the environment;
- Logic and memory – ability to process sensed data, interpret the data (to the extent local interpretation is possible), make decisions and perform useful tasks;
- Communications – read and write message values for interaction with neighbouring cells;
- Energy – a source of energy to enable the cell to perform tasks such as processing logic or moving;
- Mobility – actuators enabling movement (changing surface shape, movement of mobile cells, cell replacement, etc.) within the environment.

A cell has a physical shape and can be damaged – when random damage occurs, the cell's physical appearance can be altered and all attached components may be randomly damaged also.

Typically, additional physical factors determine how an agent reacts to external stimuli. Cells in the human body can be considered as autonomous agents in the sense that their actions appear relatively autonomous (i.e. each response is not directly controlled by some external entity). Interestingly, external influences such as radiation, viruses, extraneous environmental conditions and the like can cause damage to the physical structure of the cells and in some cases cause the cells to become cancerous. A cancerous cell does not perform the functions of a normal cell, and by this inaction, further damage to the system or other cells can be caused. Even more hazardous is the situation when the cell performs malicious actions such as attacking good cells and inducing further cancerous cells. It is possible that their non-biological counterparts could be susceptible to similar dangers (Bradley and Tyrrell, 2002). Regardless of whether cancerous behaviours emerge, at the very least physical damage will alter the agent's internal representation of the external environment, and would have to be investigated.

A *logic unit* executes a code sequence, and stores values in the local agent RAM. Before the logic code is executed, the sensor readings are updated and communication buffers are read. The reading may be affected by noise or be incorrect, depending on the damage levels of the particular sensor or buffer. As a result of code execution, the logic unit can write to communications buffers. The implemented logic units have varying degrees of reactive behaviour, described later in this sub-section.

Sensors produce a reading (a real number) that may be affected by noise – the noise is simulated as a product of an ambient noise level, the maximum reading value and a random function of unit amplitude. Other sensor implementations may require other definitions of noise to match the sensor type.

The method for propagation of information throughout the system requires a protocol and medium. Inter-agent communication in an AAV could be realized in many forms and the communications unit has been left reasonably abstract. One function (*Transmit Data*) places a string of values on the transmit buffer which can then be propagated to receiving cells by the simulator. The *Receive Data* function places a string of values from a predetermined source on the receive buffer, which can be read by the receiving cell's logic unit. This enables any communications system to be implemented, ranging from direct connections to wireless communications.

Each cell has a source of energy contained in the energy unit. Each operation such as processing logic, reading sensor values or moving mechanisms on the cell will deplete the energy unit by a certain amount. When the energy source is fully depleted, these actions can no longer be performed. The energy source has a maximum storage value. Damage to the energy unit will always result in a decrease of available energy and may also reduce the maximum storage value.

An agent may have a number of methods for moving within the environment. Typically, movement is achieved through actuators and so the *mobility* unit attempts to encapsulate this hardware. Damage to the mobility unit can result in arriving at an incorrect location within the environment. Figure A17 shows a square cell.

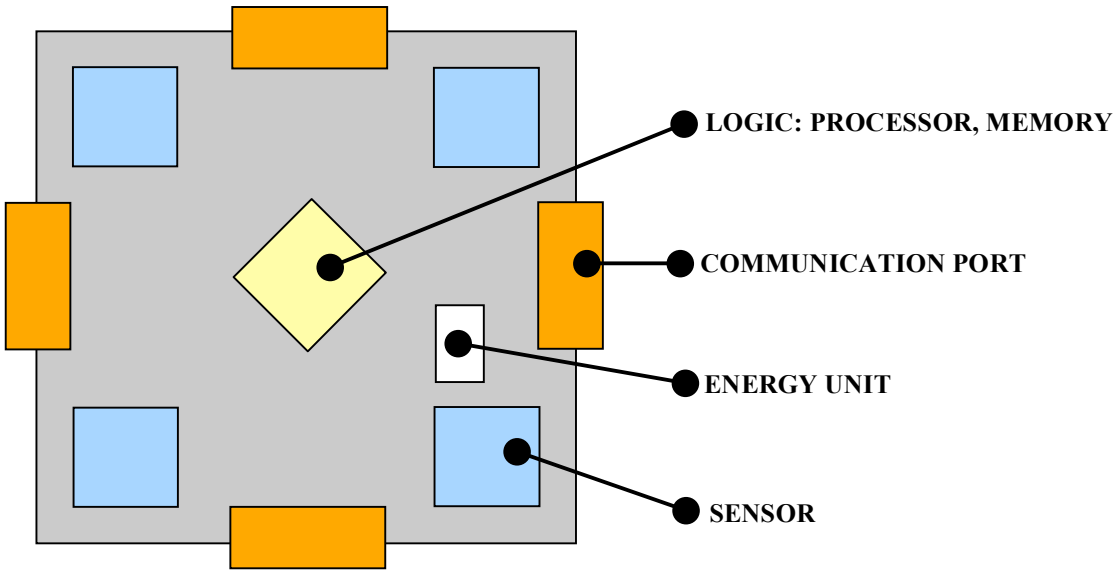

Figure A17: A square cell with 4 communication ports.

As mentioned above, cells may have varying reactive behaviour embedded in their logic unit. We followed the Deep Behaviour Projection (DBP) framework (Prokopenko et al., 2001; Prokopenko and Wang, 2002) in representing increasing levels of agent reasoning abilities, where every new level can be projected onto a deeper (more basic) behaviour. Put simply, a DBP behaviour can be present in the architecture in two forms: implicit (emergent) and explicit (embedded). What the

DBP approach suggests in particular is that the reactive/cognitive distinction is always relative in a hierarchical architecture. The behaviour produced by the level $\mathbf{l_k}$ may appear reactive with respect to the level $\mathbf{l_{k-1}}$ but, at the same time, may look deliberate with respect to the level $\mathbf{l_{k+1}}$. Let us exemplify this with the following three levels of the DBP agents:

- tropistic behaviour: Sensors → Effectors,
- hysteretic behaviour: Sensors & Memory → Effectors,
- tactical behaviour: Sensors & Memory & Task → Effectors.

The Deep Behaviour Projection framework underlies this hierarchy and ensures that more advanced levels capture relevant behaviour more concisely than their deeper (simpler) projections. The hysteretic behaviour is definitely more reactive when compared with the tactical behaviour, because the latter uses the task states in choosing the effectors. However, contrasted with a very basic tropistic behaviour, the hysteresis provided by (internal) memory states ensures a *degree* of cognition. More precisely, the hysteretic behaviour addresses some lagging of an effect behind its cause, providing a (temporary) resistance to change that occurred previously. For instance, in order to detect a persistent failure in communication with an adjacent cell, the agent needs to filter away spurious occasional miscommunications. Thus, the hysteretic behaviour is slightly more deliberate than the tropistic one (exemplified by a simple detection of a missed acknowledgement) – it better situates the agent in time (not only in space) and allows it to better respond to changes. Continuing with the example, we re-iterate that the hysteretic detection of a communication failure is a behaviour embedded explicitly (by specifying a filter of a given length), while the persistent tropistic detection is only possible as a result of the recurring pattern.

Importantly, for any pair of behaviours realised at two different levels of the architecture, it is possible to replicate one in terms of another, trading off the elaboration and high performance produced by the deeper and more automatic level for conciseness and control presented by the other.

A3.5 AAV Simulator

More often than not, multi-agent systems show "emergent behaviour", which is not explicitly programmed. Several algorithms for spatial self-organization exemplifying the use of emergent behaviour are given by Unsal and Bay (1994): self-organising agents can arrange themselves geometrically in two- and three-dimensional space using only local information, obtained by their own sensors. A quite sophisticated multi-layered hierarchical motion planning strategy, for a class of self-reconfigurable modular robotic systems, is described by Prevas et al. (2002).

In general, tasks could be managed more easily and reliably if emergent behaviour is engineered by programming (situated) agents locally, without reference to the knowledge of the global task structure (bottom-up approach). Moreover, in this case, failure or partial malfunction of agents would not critically endanger the vehicle. Thus, programming and maintaining relatively simple distributed agents reduces the complexity of control, which would otherwise have to be globally imposed on all components.

In general, the process of self-organization (e.g. self-reconfiguration) is not random but emerges as a result of interactions involving the transfer of information that is embedded locally.

A flexible architecture was developed for simulating the modular surface or skin of the vehicle, being comprised of cells with sensing and computing capabilities. Furthermore, it has the ability to simulate simple environmental effects, such as the incidence of small impacts. The initial aim of the simulator is to study the effects produced by different communications strategies and locally embedded behaviours. As mentioned earlier, our main focus so far has been the study of self-organizing impact boundaries and impact networks that enclose the damaged areas, and in particular, conditions enabling formations of robust, stable and continuously connected (a) closed boundaries and (b) spanning trees.

In general, many events occur in parallel, so the simulation has a (non-real time) clock, and all events have a defined duration. The simulation is, essentially, a state machine that sweeps through the elements (cells) of the system and updates their current state $\mathbf{S_i(t)}$ at time point **t** on a regular basis. Cells are represented as (mobile) objects (polygons) on a two-dimensional plane (Figure A18) where they interact with their immediate neighbours through connected (geometrically overlapping) communication ports.

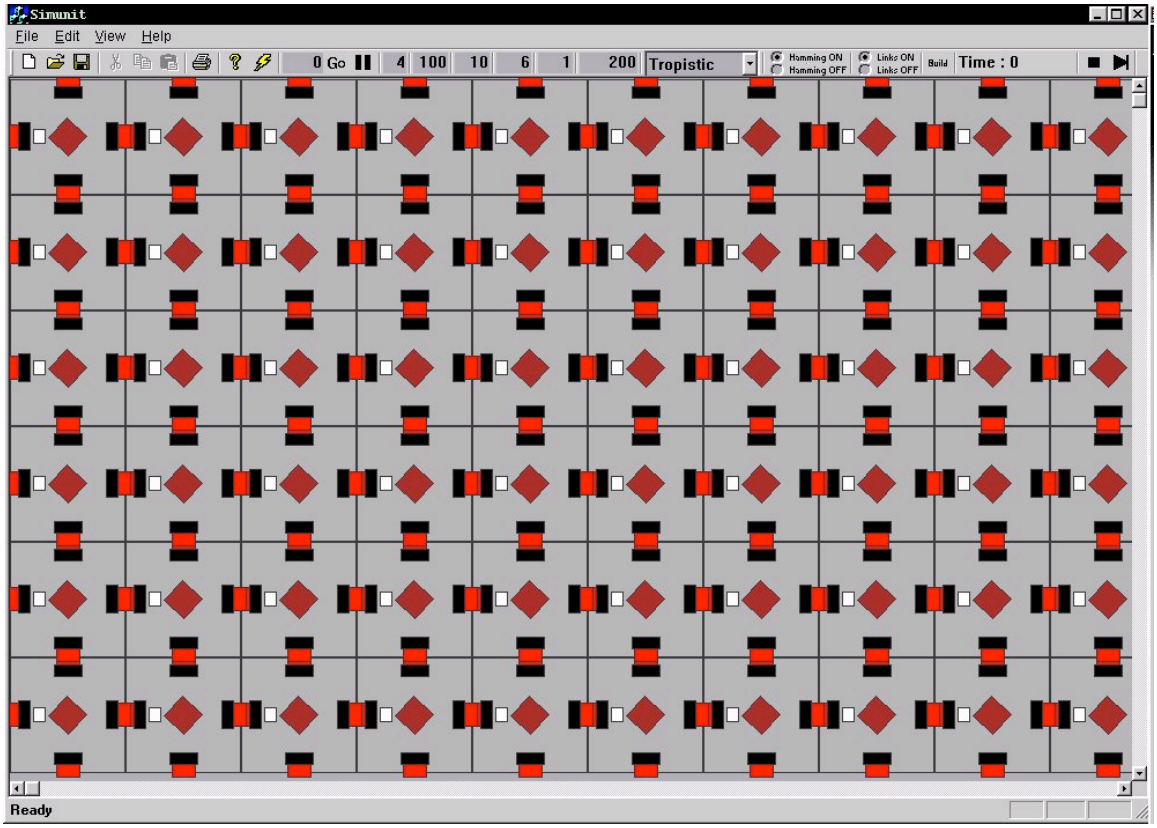

Figure A18: An initial configuration of 10x6 square cells.

The next state is, generally, dependent only upon the current state and current inputs, so the next state is a result of interactions with immediate neighbours. The decision

about what is the next state of each element depends upon a possibly complicated algorithm embedded in the cell logic.

A3.6 Self-organizing impact boundaries: algorithms and simulation results

This sub-section describes the development and performance of an algorithm for the creation of self-organizing impact boundaries, to apply to situations where damage to the structure and functionality of one or more cells is produced by one or more impacts. In studying conditions leading to robust, stable and regular self-organizing impact boundaries, we followed an incremental approach, trying to impose as few requirements as possible.

An important characteristic of a critical impact is that, typically, the energy of the impact dissipates throughout some neighbourhood, destroying cells close to the point of the impact and affecting other cells. Communication ability is among those that suffer most. The basic assumption made is that communication damage can be simulated by a "bit-by-bit" corruption – by assigning a probability of a bit error dependent on proximity of the affected communication port to the epicentre. The proximity dependency underlying the probability distribution can be modelled in many ways, and we investigated a range of functions, from linear to exponential decreases. We also simulated a basic error correction mechanism embedded in each communication port, based on a typical Hamming error correction code. It should be noted, however, that this code cannot generally recover from error rates exceeding 15% of the message, while in many cases even cells relatively remote from an epicentre may suffer communication damage exceeding this threshold.

Frame boundary

Our first target was formation of a boundary that is not necessarily continuously connected as a closed circuit, but is well placed in separating the cells that suffered unrecoverable communication damage (including those that were completely destroyed) from the cells that are able to communicate to their normal functional capacity. Such a *preliminary* border, it was hoped, would form a "frame" of the desired closed boundary, regardless of cell shape (triangular or square). To achieve this, one of the most basic communication strategies was employed:

(C1) *every cycle each cell sends an "OK" message to all its neighbours,*

together with one of the most basic tropistic behaviours embedded in each cell's logic unit:

(B1) *if at least one neighbour cell failed to communicate the "OK" message this cycle, switch to the frame boundary state* $\boldsymbol{S_f}$.

While (B1)-(C1) combination worked reasonably well, a common problem was the formation of a "thick" boundary surrounding the damaged region. Figure A19 illustrates this situation: white cells are crippled by the impact; normal cells

(background colour) do not detect any damage, while blue cells self-organise in the frame boundary.

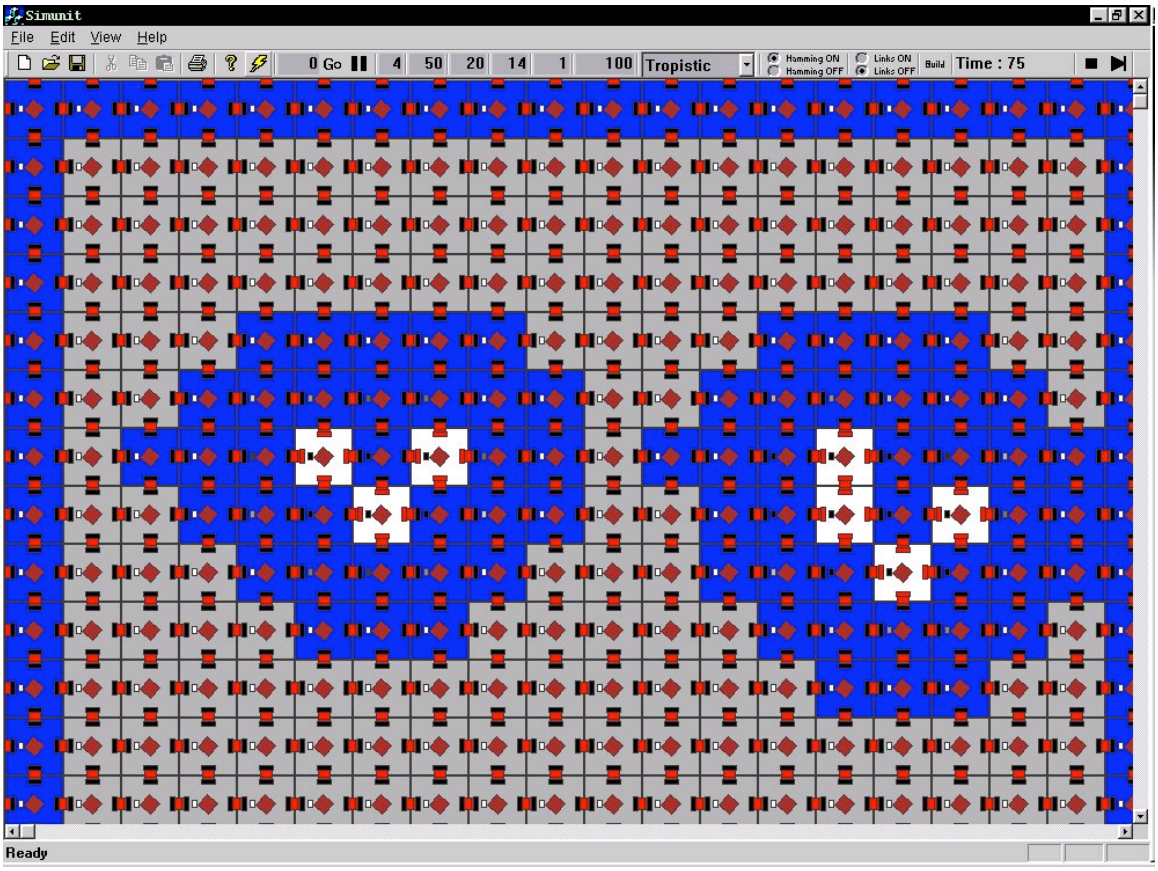

Figure A19: A thick frame boundary produced by the (B1)-(C1) algorithm. In this case each of the white cells was hit and suffered critical impact damage. Cells surrounding the impact sites were also damaged, but not critically. These partially damaged cells are not distinguished from the undamaged frame boundary cells in this algorithm.

The thick frame boundary problem can be easily corrected by segmenting the boundary region into two regions: the proper frame and internal "scaffolding". The scaffolding cells are not critically damaged but have probably suffered some damage. They may be damaged cells adjacent to them. This segmentation is achieved by a change in logic to (B2):

(B2-1) *if all neighbour cells failed to communicate the "OK" message this cycle, switch to the scaffolding state* $\boldsymbol{S_s}$*;*

(B2-2) *if at least one neighbour cell failed to communicate the "OK" message this cycle and at least one neighbour cell did communicate the "OK" message this cycle, switch to the frame boundary state* $\boldsymbol{S_f}$*.*

While the (B2)-(C1) combination avoided thick frame boundaries (Figure A20, where red cells indicate scaffolding state), it still produced some irregularities in the frame. Two types of undesirable feature are present in Figure A20, and explanations for these are as follows.

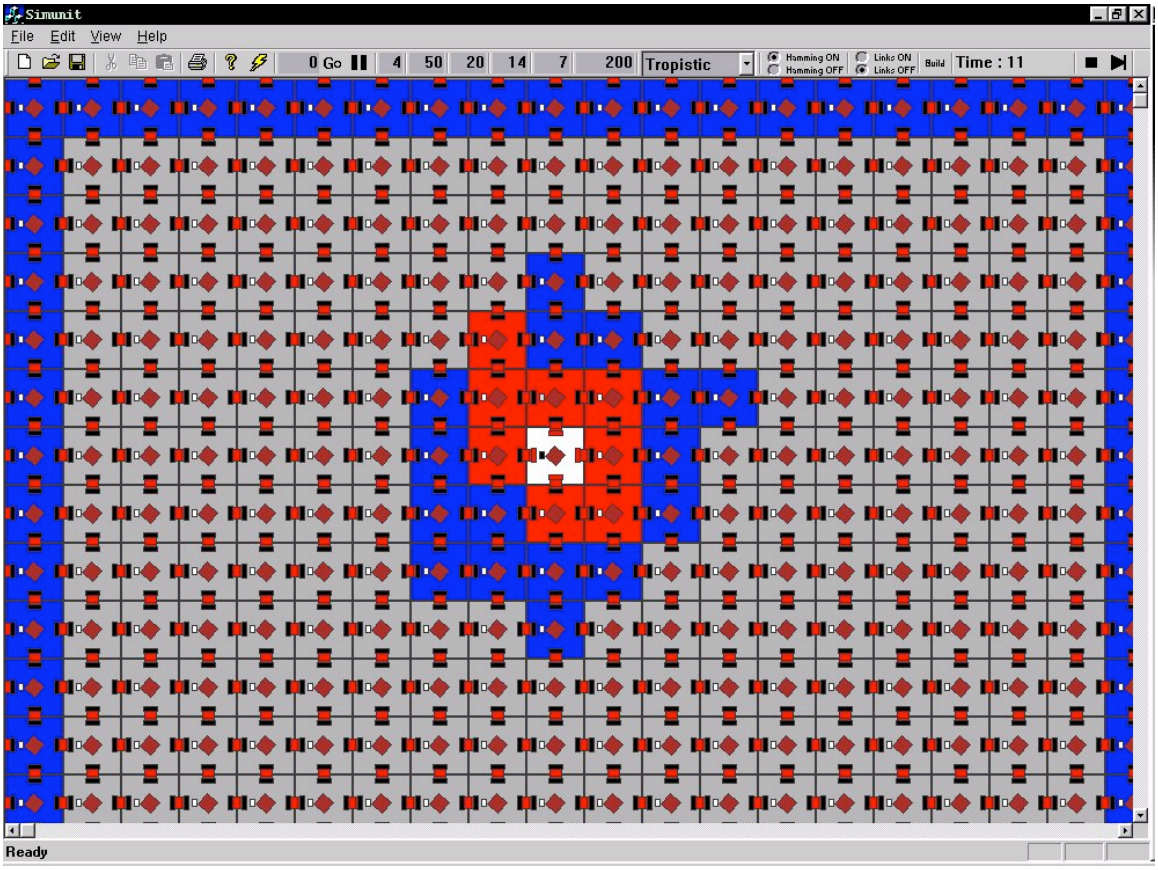

Figure A20: An irregular frame boundary produced by the (B2)-(C1) algorithm.

Firstly, there is a situation that occurs quite commonly for this algorithm in which two frame cells A and B are adjacent, while cell A is between B and the impact epicentre (Figure A20). This occurs because both cells A and B received at least one "OK" message and failed to receive at least one "OK" message from their neighbours, satisfying the condition of the behaviour (B2-2). In this case cell A has sustained some damage: A received the "OK" message from cell B, but could not transmit its "OK" to the cell B.

A second undesirable scenario (common to exponential damage functions) involves a scaffolding cell A being directly adjacent to a normal cell B, and again the cell A was strictly closer to the impact epicentre than B (Figure A20). In this case cell B has sustained some damage: cell A did not receive the "OK" message from any of its neighbours including B, while cell B received the "OK" message from all its neighbours including cell A, but could not transmit the "OK" message to cell A (essentially, a reversal of the first scenario).

These situations emphasize a feature of the communications assumptions made in the simulator, which is that communications faults in a link are not necessarily symmetric. In general, if a message from cell B reaches cell A then the reverse need not be the case. To resolve irregularities illustrated by the first scenario, we needed to augment the communication strategy by acknowledgement messages:

(C2-1) *every cycle each cell sends an "OK" message to all its neighbours;*
(C2-2) *upon receiving the "OK" message each cell replies with an "Acknowledgement" message.*

The (B2)-(C2) policy not only handled the first undesirable scenario above, but also provided grounds to address the second problem. A principled way to deal with the second scenario is for each cell to go into "silent mode", in which it may receive but chooses not transmit if it detects that its own communication channel has been compromised:

(B3) *if all neighbour cells failed to communicate the "OK" message this cycle or there is no "Acknowledgement" message from any neighbour cell, stop sending messages.*

The result of the (B2)-(B3)-(C2) strategy was an emergent regular boundary surrounding the scaffolding region. This boundary was however, erratic and unstable – some frame boundary cells frequently changed their states to scaffolding or normal and back. This occurred because until this point only tropistic algorithms were used. Hysteretic algorithms for (B2)-(B3), employing simple filters for detection of miscommunication, complemented the communication policy (C1) quite nicely. This resulted in a stable self-organizing boundary around the damaged area (Figure A21).

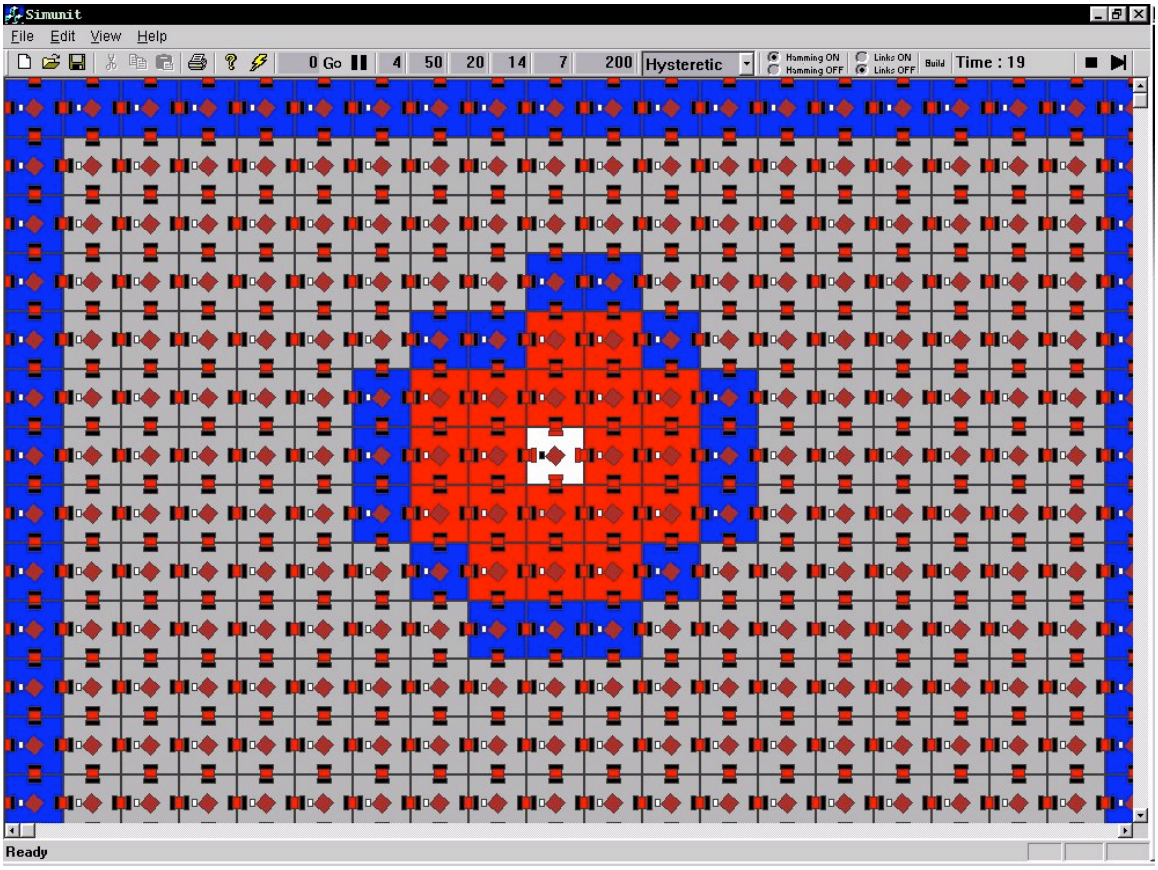

Figure A21: A regular frame boundary produced by the hysteretic (B2)-(B3)-(C2) algorithm.

Closed boundary

Creation of the frame boundary is the first stage leading to the desired continuously connected (closed) boundaries. In fact, it can be safely postulated that

(B4) *if the cell state is* $\boldsymbol{S}_f$*, and there are at least two communicating neighbours, switch to the closed state* $\boldsymbol{S}_c$.

In order to generate links between disconnected cells on the frame boundary, it was necessary to introduce the following communication rules and behaviours:

(C3-1) *if the cell state is* $\boldsymbol{S}_c$*, (1) determine a (the) cell X that failed to communicate, (2) determine two communicating neighbour cells nearest to the cell X, and (3) send a "Connect(*τ*)" message to these neighbours with a "time-to-live" parameter* τ *;*

(C3-2) *upon receiving the "Connect(*τ*)" message, if the cell state is not* $\boldsymbol{S}_c$*, (1) switch to the state* $\boldsymbol{S}_c$*, (2) if* $\tau > 0$*, determine two communicating neighbour cells nearest to the cell that communicated the "Connect(*τ*)" message and (3) send a "Connect(*τ*-1)" message to these neighbours.*

The "time-to-live" parameter τ prevents spurious links from persisting. When cell A determines its own neighbour cells that are nearest to some other neighbour cell B, it chooses the cells on opposite sides (clockwise and counter-clockwise) relative to B. However, this is not sufficient to avoid some redundant connections, especially with triangular cells. Figure A22 illustrates the case with redundant links forming on the edges of frame boundaries (white links indicate the closed state $\mathbf{S}_c$).

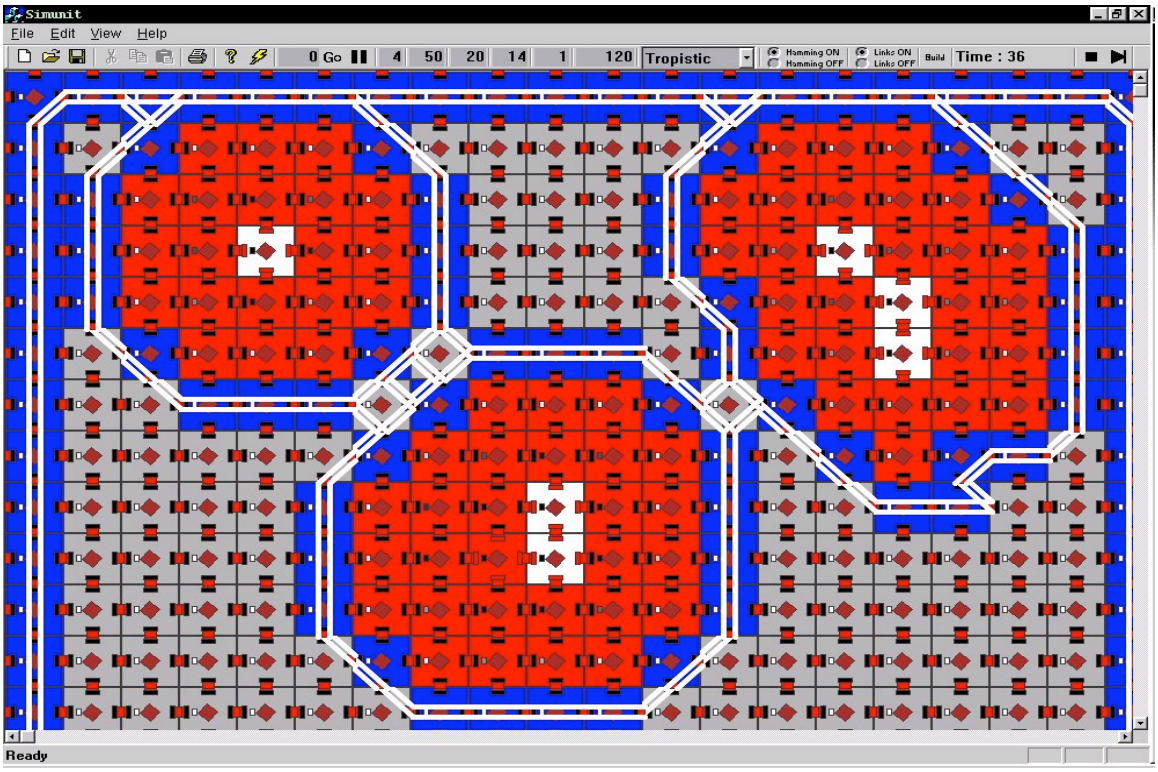

Figure A22: An ambiguous closed boundary: square cells using "Connect(τ)" messaging .

To prevent such redundant links, the simple "Connect(τ)" message had to be replaced by a more complex "Connect(τ, γ)" message, where γ is the relative direction of a desired connection, resulting in the (C3γ) policy. This required a simple behaviour rule (Bγ) mapping the relative direction α of the neighbour cell that failed to communicate and the relative direction β of the neighbour cell receiving the "Connect(τ , γ)" message onto the argument γ.

The (B2)-(B3)-(B4)-(Bγ)-(C2)-(C3γ) policy achieves the desired robustness and continuity of self-organizing impact boundaries for a variety of cell shapes, impact energy dissipation profiles and communication damage probability models. An example of triangular cells with hysteretic behaviour handling exponential damage decrease is shown in Figure A24, while Figure A23 shows that tropistic behaviour cannot cope with this case. Triangular cells are shown in these examples because for this case convergence was more difficult than for square cells.

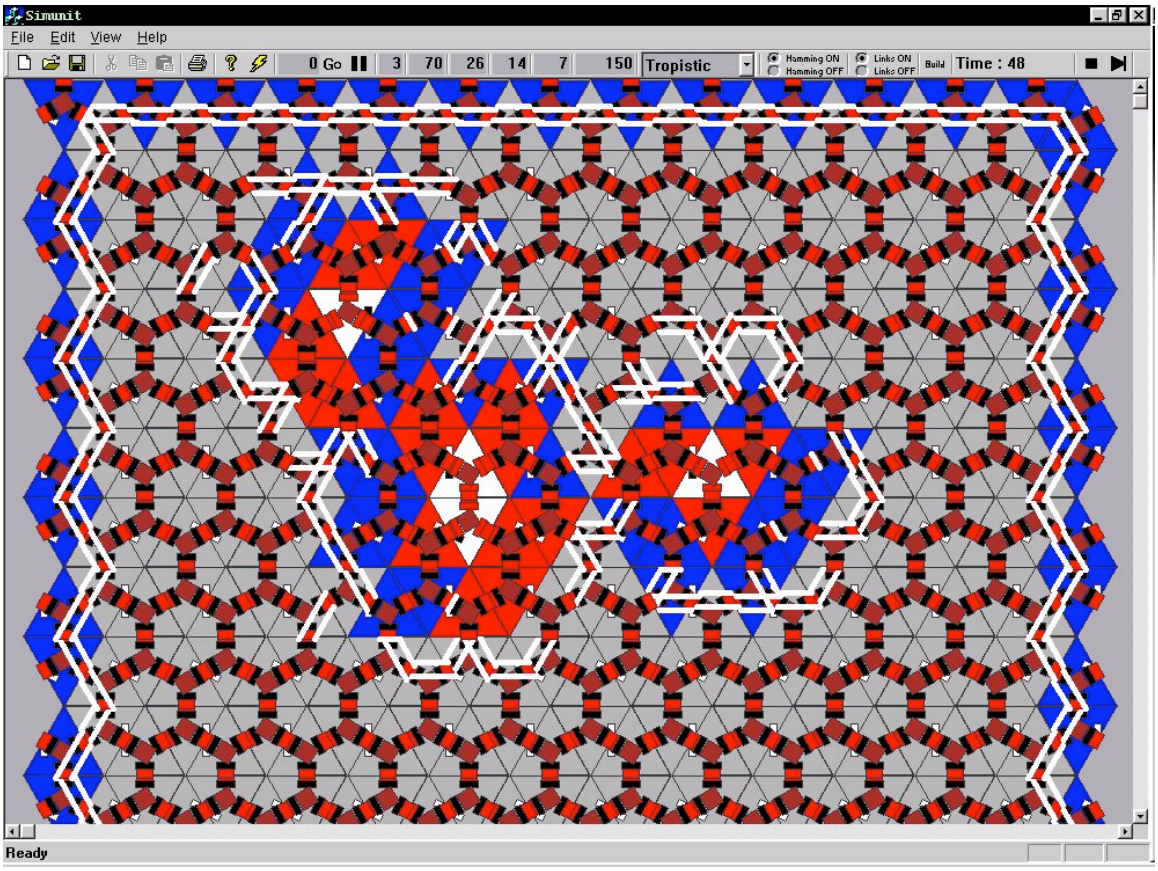

Figure A23: An irregular "closed" boundary: triangular cells with tropistic behaviour.

Figure A24 demonstrates a strategy for constructing a stable, closed boundary around a damaged region using only the local information obtained by the cells on the boundary from their immediate neighbours. It is a structure that emerges from the local interactions between the cells, and requires no hierarchical overview.

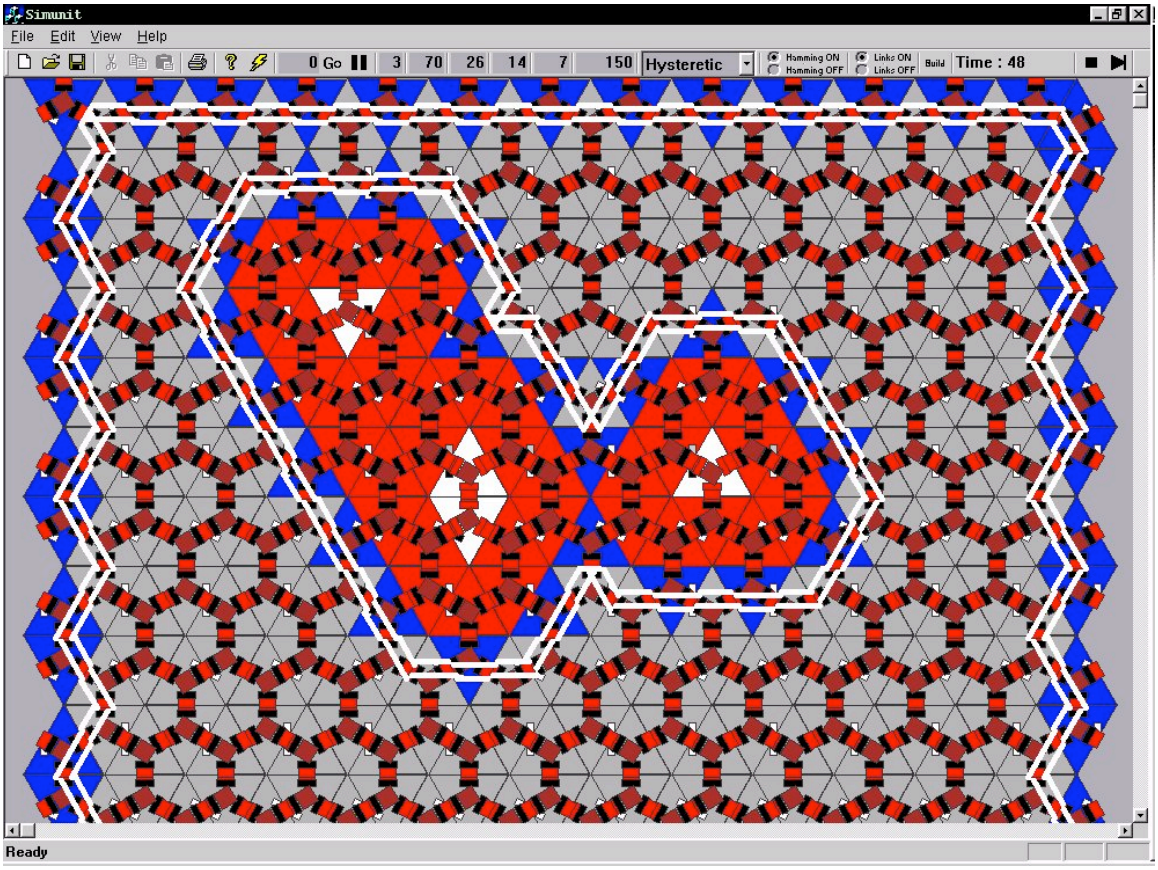

Figure A24: A robust closed boundary: triangular cells with hysteretic behaviour.

A3.7 Self-organizing impact spanning trees: algorithms and simulation results

Self-organizing impact boundaries are useful when the cells very close to (or right on) the impact points are destroyed, and the communication links between the cells in a certain impact neighbourhood are damaged.

However, when dealing with non-critical impacts, which do not damage the functionality of the cell, it is possible to extract information directly from the cells that register the impact. Moreover, in these cases the communication links between the cells that are close to the impact point are likely to remain intact. This suggests the use of the impact points (detected by the individual cells) as nodes in an *impact network*. As mentioned earlier, such impact networks may be needed to conduct a fast inspection of the impact area, to determine impact densities and to route the repair resources.

The concept of the impact network introduced here makes it possible to apply some fairly well-known algorithms, such as Ant Colony Systems (ACS) algorithms proposed by Dorigo et al. (1991), to the problem of impact analysis in the AAV. ACS algorithms use the ability of agents to indirectly interact through changes in their environment (*stigmergy*) by depositing *pheromones* and forming a pheromone trail. They also employ a form of *autocatalytic* behaviour – *allelomimesis*: the probability

with which an ant chooses a trail increases with the number of ants that chose the same path in the past. The process is thus characterized by a positive feedback loop (Colorni et al., 1991). The most interesting aspect of this autocatalytic process is that finding the shortest path around an obstacle is an emergent property of the interaction between the obstacle shape and the distributed behaviour of the ants.

There are, however, a few differences between this application and others to which ACS algorithms have been successfully applied that make the direct application of ACS algorithms less than straightforward. First of all, the impact nodes are not known in advance. This rules out a set of "bootstrapping" and reinforcement learning techniques heavily used in a sub-class of ACS algorithms developed for optimization problems, such as the Travelling Salesman Problem (TSP) and Minimum Power Broadcast (MPB). Secondly, the impact nodes may appear at a much greater rate than *towns* in the TSP (Dorigo and Gambardella, 1997), or wireless/wired sensor network *nodes* in MPB (Das et al., 2002; Subramanian et al., 1997). This means that it is much harder to maintain so-called distance-vectors or gradient fields that correspond to the food scent field used by ants. The distance-vectors are a very important component in the ACS algorithms.

The canonical form for the transition probability from node **i** to node **j** at time **t** (which corresponds to the probability of an ant at node **i** moving to node **j**) is given by the following expression:

$$P_{i,j} = [\varphi_{i,j}(t)]^{\alpha} [\eta_{i,j}(t)]^{\beta} / \sum_j ([\varphi_{i,j}(t)]^{\alpha} [\eta_{i,j}(t)]^{\beta}),$$

where:

$\varphi_{i,j}(t)$ is the intensity of trail on the path between nodes **i** and **j;**
$\eta_{i,j}(t)$ is the visibility, determined as the inverse distance between nodes **i** and **j;**
α and β are parameters.

The intensity $\varphi_{i,j}(t)$ gives information on how many ants have chosen the path in the recent past, while the visibility $\eta_{i,j}(t)$ indicates that closer nodes are more strongly preferred. The trail intensity is updated each time an ant agent passes through the node:

$$\varphi_{i,j}(t+1) = \rho \varphi_{i,j}(t) + \Delta\varphi_{i,j}(t, t+1),$$

where ρ is an evaporation coefficient. There are different ways to choose the quantity $\Delta\varphi_{i,j}(t, t+1)$ to update the trail intensity. According to the simplest scheme (ANT-density), this additional quantity is always constant, while the ANT-quantity scheme makes $\Delta\varphi_{i,j}(t,t+1)$ inversely proportional to the distance between nodes **i** and **j**, further reinforcing the visibility factor. Other variants (ANT-cycle) and the most recent and popular AntNet algorithm (Di Caro and Dorigo, 1998) use, in addition, the information collected during past simulations to direct the search for better solutions. In particular, in the AntNet scheme, the ants collect information about the time length of the path followed, and use this information in future runs. This additional feedback improves the convergence properties of the algorithm.

The parameters α and β determine the relative importance of the effects of intensity and visibility. For example, setting $\alpha = 0$ results in classical stochastic search algorithms, while the choice $\beta = 0$ ignores the gradient information and leads to a pure autocatalytic process. These two extreme options exhibit convergence to sub-optimal solutions. In other words, trail intensity needs to be balanced against some distance-based (gradient) field.

A major difficulty in applying ACS algorithms to a multi-cellular aerospace vehicle skin is the highly dynamic nature of the impact networks. In particular, it would be impractical to employ a distance-based visibility measure because absolute coordinates of individual cells are not maintained: a cell does not know where it is. In order to address this difficulty we need to employ an efficient method of maintaining distance-based gradient field(s), where the share of static information is negligible, while information on new impacts can be easily integrated.

There are a few approaches employing gradient fields in the context of packet routing and querying algorithms in sensor networks, based on distance-vectors and link-costs. The work of Ye et al. (2001) covers some background material, and introduces the *cost field* concept: at each node, the value of the cost field is defined as the minimum cost of sending a message from that node to the event node (called a *sink*). The cost field is established in a single pass – by choosing a minimal value between the broadcast cost and the currently held value. More precisely, let us consider two nodes A and B, with the cost of messaging between them pre-set as $\mathbf{c_{A,B}}$. Assume that the node B currently holds value $\mathbf{l_B}$, and receives a message from the node A with the cost $\mathbf{l_A}$, (this is the cost of reaching the sink from A; initially all costs to the sink are set to infinity). The new value of $\mathbf{l_B}$ is then set to $\mathbf{min}(\mathbf{l_B}, \mathbf{l_A} + \mathbf{c_{A,B}})$. This algorithm (GRAdient Broadcast) essentially forms gradients toward the event (sink). In order to reduce the flooding overhead of the required broadcast, the approach includes a timing mechanism to control the propagation. GRAdient Broadcast attempts to capitalize on the similarity between the cost field and the natural gravity field "that drives water flowing from a high post to a low post" (Ye et al., 2001). The crucial difference, however, is that, unlike gravity, the cost field is specific to each sink – there is no superposition among the fields established by different sinks. This feature, of course, makes the cost field concept less practical, especially with multiple sinks: each node would have to keep (and propagate) costs to each sink. Besides, the static costs $\mathbf{c_{A,B}}$ need to be maintained for each pair of nodes.

Another approach, Rumor Routing, described by Braginsky and Estrin (2002), avoids establishing the cost field, and tries to balance propagation of queries and events by extending the content of each propagated packet with a table that stores distances and directions to multiple events. At each newly reached node this table is synchronized (merged) with a local table, and the merged table is propagated further. Again, as with GRAdient Broadcast or visibility-employing ACS algorithms, this procedure essentially creates and maintains *multiple* fields, unlike the single natural gravity field.

The hybrid method of establishing *impact networks* proposed in this report is based on a single *impact gradient field (IGF)*, used to complement the autocatalytic process of ant-like agents. This gradient field is created by *all* impacts in a given spatio-temporal neighbourhood. Obviously, by superposing all impacts we lose optimal

routes between an individual cell and a given impact node, but we gain in economy of information: each cell needs to keep only a single IGF value. The IGF values are initialized to infinity and then established by propagating messages from impact nodes as follows:

(G1) *each impact node sets its IGF value to 0 and sends an IGF(0) message to all its neighbours (every T cycles);*

(G2) *if a cell i receives an IGF(n) message, it compares its own current IGF value m_i with (n+1), and sets $m_i = min(m_i , n+1)$; if the new value m_i is smaller than the old, the cell sends an IGF(n+1) message to all the neighbours except the sender of the IGF(n) message.*

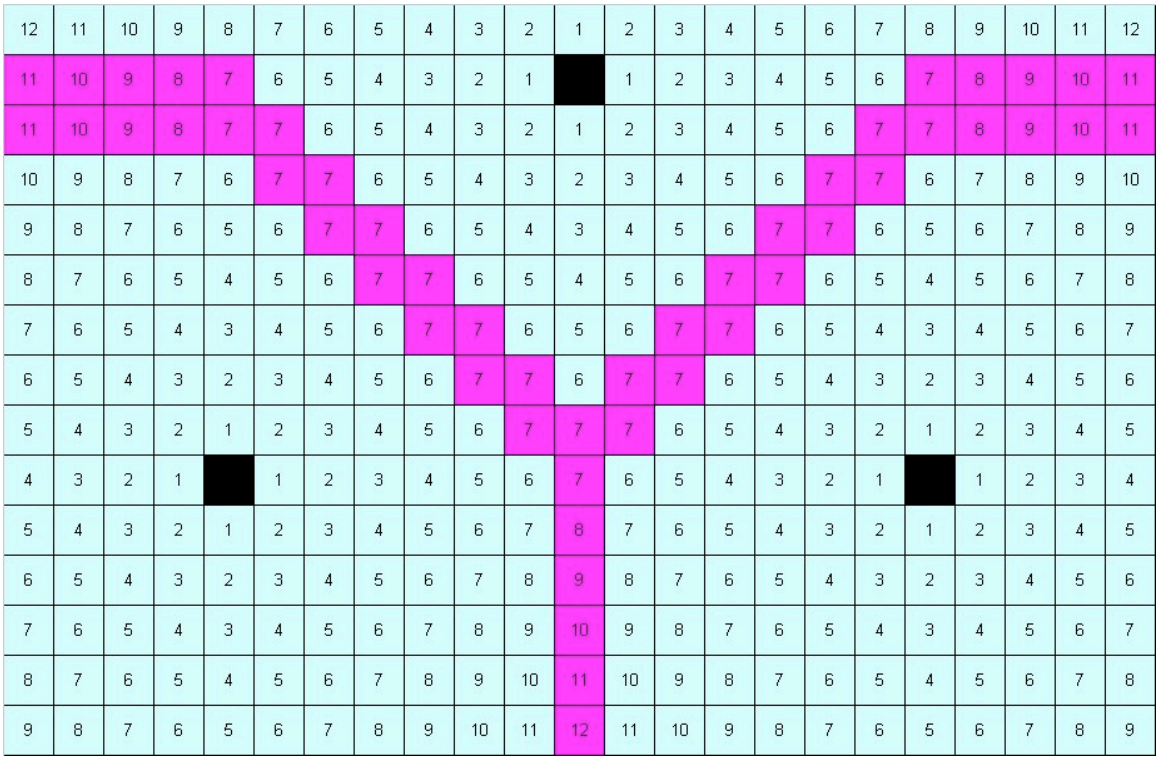

Figure A25: An example of an Impact Gradient Field: black cells are impact nodes; purple (dark) cells form the ridge (weightless) region.

The (G1)-(G2) strategy is essentially that adopted by the GRAdient Broadcast method, but it establishes a single IGF because each cell minimizes gradients to all impact nodes. The minimization scheme approximates vector superposition used in gravity field calculations. An important aspect of the (G1)-(G2) strategy is that propagation of IGF values from each impact node does not result in message flooding: eventually the propagation waves meet each other and stop along the ridge regions, which are said to correspond to regions of "weightlessness" in a gravity field (Figure A25). In order to maintain the IGF and account for the possibility that some impact cells are repaired, each impact node repeats the step (G1) every T cycles.

The IGF helps to guide ant-like agents, especially during the initial *exploration* phase. In other words, rather than explore the area randomly the agents may ascend along the gradient until they reach a ridge region, and only then switch to random exploration:

(E1) *each impact node generates a number of exploring ants every A cycles;*

(E2) *if not performing a random walk, each exploring ant located at the cell i determines which neighbour cell j has a highest IGF value* m_j*, and moves there if* $m_j > m_i$*; otherwise it switches to random walk*;

(E3) *an exploring ant performs a random walk until either (a) another impact node is found, or (b) the ant has returned to the home impact node; or (c) the ant can move to a cell with a non-zero trail intensity (this is set by returning ants as will be described below);*

(E4) *if an exploring ant can move to a cell with a non-zero trail intensity, the transition probabilities are calculated and the destination cell is selected accordingly.*

While performing a random walk (E3), exploring ants exclude the cell where they were at the previous cycle. Similarly, the transition probabilities used on the "follow-trail" step (E4) are set to 0 for the cell where the ant came from.

The ants are implemented as communication message packets, so the policies are implemented via appropriate message passing, in which the cells are responsible for unpacking the packets, interpreting them, and sending updated packets further if necessary. Thus, ants cannot move into the cells with damaged (or shutdown) communication links. Therefore, the regions enclosed by self-organising boundaries described in the previous sub-section form obstacles, and the ants are supposed to find the shortest paths around them using positively reinforced pheromone trails.

The investigated method also involves a *dead reckoning* scheme enabling the agents to return home when another impact node is located. The scheme is implemented as follows:

(R1) *at each step from cell i to cell j, an exploring ant updates the x- and y-shift coordinates from the home node (initially set to 0);*

(R2) *when another impact node is found, the exploring ant switches to a return state and starts moving back to the home node – moving to cells that reduce the x- and/or y-shift coordinate; if both x- and y-shift are zero (the home node is found), the returning ant stops;*

(R3) *if the ant cannot move to the cell suggested by the dead reckoning scheme (the minimization of x- and/or y-shift) because of a communication failure in that cell (an obstacle), the ant moves according to the transition probabilities* $\mathbf{P}_{i,j}$*;*

(R4) *each cycle, a returning ant deposits pheromone in the quantity that is inversely proportional to the traversed return distance d (d is incremented by 1 each cycle), thus setting the trail intensity.*

In general, the ants proceeding along a shorter return path deposit more pheromone than the ants that selected (due to transition probabilities) a longer path around an obstacle, simply because the deposited quantity is inversely proportional to the traversed distance. A higher quantity of pheromone attracts more ants. Eventually, a trail is established between a pair of impact nodes. It is important to realise that for any such pair, both impact nodes generate exploring ants that potentially find the other impact node and return back. The shortest trail is therefore reinforced by *returning ants* going in opposite directions (Figure A26).

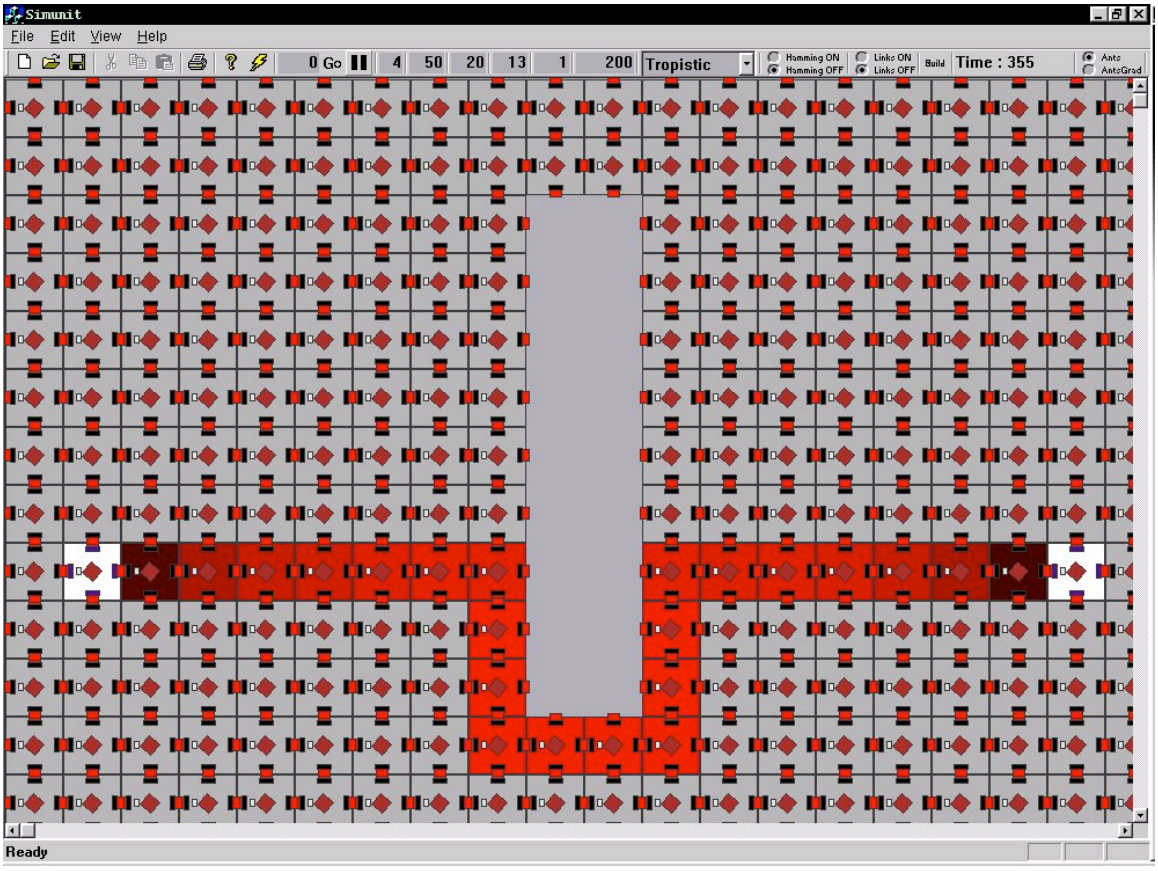

Figure A26: An example of a shortest path between two impact nodes (white cells) around an obstacle. Different shades of red (dark) colour represent the trail intensity, which is greater for darker cells.

At this stage two strategies have been investigated. The first "ants" strategy (E1)-(E3)-(E4)-(R1)-(R2)-(R3)-(R4) did not employ an IGF at all, while the second "IGF-ants" strategy (G1)-(G2)-(E1)-(E2)-(E3)-(E4)-(R1)-(R2)-(R3)-(R4) used all the described rules. The transition probabilities were calculated using $\alpha = 1$ and $\beta = 0$, resulting in

$$P_{i,j} = \varphi_{i,j}(t) \; / \; \sum_j \varphi_{i,j}(t) \, ,$$

The visibility factor was discarded because the IGF subsumes its role in the initial exploration stage of the second "IGF-ants" strategy.

The strategies were investigated with the aim of observing the emergence of shortest paths and spanning trees in impact networks (Figure A27). The "IGF-ants" strategy performs slightly better (as expected), but only a formal evaluation that will be carried out later will show if its benefits are worth the additional time cost.

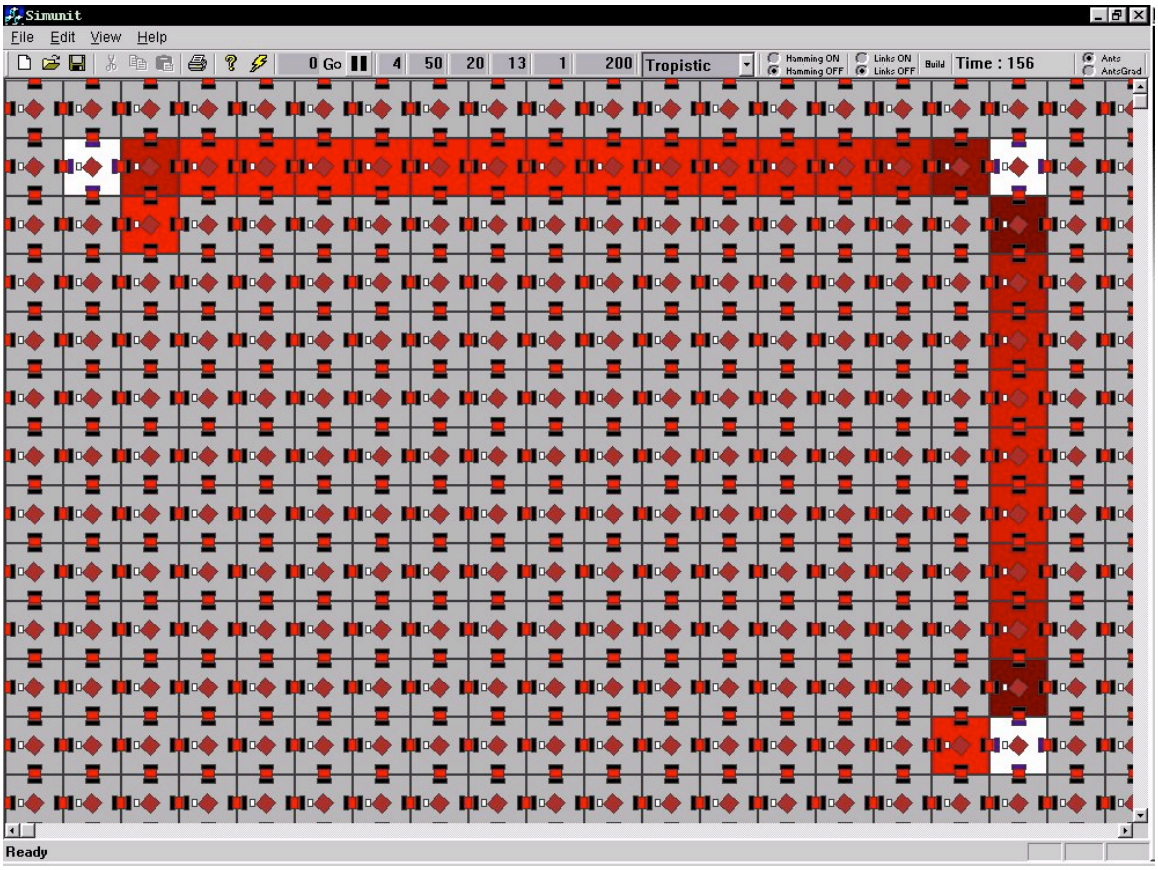

Figure A27: An example of a spanning tree in a simple impact network (impact nodes are white cells). A diagonal trail is present but is much weaker: its trail intensity is below a visualization threshold.

A3.8 Future directions

The described communication strategies, behaviours and emergent patterns of impact boundaries and impact networks demonstrate the potential of self-organizing multi-agent networks for detecting and containing critically damaged sections of the modular multi-cellular aerospace vehicle skin.

The main challenge in the immediate future will be to investigate information-theoretic complexity of various communication strategies, and relate it to the coordination of the agents.

References

CTIP (2002). *Development and Evaluation of Sensor Concepts for Ageless Aerospace Vehicles. Development of Concepts for an Intelligent Sensing System.* CSIRO Telecommunications and Industrial Physics. Confidential Report No. TIPP

1517. May 2002. Also published as NASA technical report NASA/CR-2002-211773, Langley Research Center, Hampton, Virginia.

Bradley, D. W. and Tyrrell, A. M. (2002). "Immunotronics: Novel Finite-State-Machine Architectures With Built-In Self-Test Using Self-Nonself Differentiation." IEEE Transactions on Evolutionary Computing, Vol. 6., No. 3., June 2002.

Braginsky, D. and Estrin, D. (2002). "Rumor Routing Algorithm For Sensor Networks." In Proceedings of the First ACM International Workshop on Wireless Sensor Networks and Applications, Atlanta, Georgia, 2002.

Colorni, A., Dorigo, M. and Maniezzo, V. (1991). "Distributed optimization by ant colonies." In Proceedings of the First European Conference on Artificial Life, Paris. MIT Press/Bradford Book.

Das, A. ,Marks II, R.J., El-Sharkawi, M.A., Arabshahi, P. and Gray, A. (2002). "The minimum power broadcast problem in wireless networks: an ant colony system approach." *Proceedings IEEE CAS Workshop on Wireless Communications and Networking*, Pasadena, CA, Sept. 5-6, 2002.

Di Caro, G. and Dorigo, M. (1998). "AntNet: Distributed Stigmergetic Control for Communications Networks", Journal of Artificial Intelligence Research, volume 9, 317-365, 1998.

Dorigo M. and Gambardella, L. M. (1997). "Ant Colonies for the Traveling Salesman Problem." *BioSystems.*

Dorigo M., Maniezzo, V. and Colorni, A. (1991). "The Ant System: An Autocatalytic Optimizing Process." *Technical Report No. 91-016 Revised*, Politecnico di Milano, Italy.

Estrin, D., Govindan, R., Heidemann, J. and Kumar, S. (1999). "Next Century Challenges: Scalable Coordination in Sensor Networks." In Proceedings of the Fifth Annual International Conference on Mobile Computing and Networks (MobiCOM '99), August 1999, Seattle, Washington (Mobicom'99), Seattle, USA.

Mjolsness, E. and Tavormina, A. (2000). "The Synergy of biology, intelligent systems, and space exploration." In IEEE Intelligent Systems - AI in Space, 3/4 2000.

Nagpal, R. (2002). "Programmable self-assembly using biologically-inspired multiagent control." In Proceedings of the First International Joint Conference on Autonomous Agents and Multi-Agent Systems (AAMAS'02), Bologna, Italy, July 2002.

Prevas, K. C., Unsal, C., Efe. M. O. and Khosla, P. K. (2002). "A Hierarchical Motion Planning Strategy for a Uniform Self-Reconfigurable Modular Robotic System." In the Proceedings of IEEE International Conference on Robotics and Automation, 2002.

Prokopenko, M. and Wang, P. (2002). “Relating the Entropy of Joint Beliefs to Multi-Agent Coordination.” In Proceedings of the 6th International Symposium on RoboCup, 2002.

Prokopenko, M., Wang, P. and Howard, T. (2001). “Cyberoos '01: 'Deep Behaviour Projection' Agent Architecture.” In RoboCup-2001: Robot Soccer World Cup V, Springer, 2001.

Subramanian, D., Druschel, P. and Chen, J. (1997). “Ants and Reinforcement Learning: A Case Study in Routing in Dynamic Data Networks.” In Proceedings of IJCAI-97, 1997.

Unsal, C. and Bay, J. S. (1994). “Spatial Self-Organization in Large Populations of Mobile Robots.” In Proceedings of 1994 IEEE International Symposium on Intelligent Control, Columbus, Ohio, 1994.

Ye, F., Chen, A., Lu, S. and Zhang, L. (2001). “A Scalable Solution to Minimum Cost Forwarding in Large Scale Sensor Networks.” In Proceedings of the International Conference on Computer Communications and Networks, Dallas, Texas, 2001.

REPORT DOCUMENTATION PAGE

Form Approved
OMB No. 0704-0188

1. REPORT DATE *(DD-MM-YYYY)*	2. REPORT TYPE	3. DATES COVERED *(From - To)*
01- 05 - 2008	Contractor Report	

4. TITLE AND SUBTITLE

Development and Evaluation of Sensor Concepts for Ageless Aerospace Vehicles: Report 3 - Design of the Concept Demonstrator

5a. CONTRACT NUMBER

5b. GRANT NUMBER

5c. PROGRAM ELEMENT NUMBER

6. AUTHOR(S)

David Abbott, Jon Ables, Adam Batten, David Carpenter, Tony Collings, Briony Doyle, John Dunlop, Graeme Edwards, Tony Farmer, Bruce Gaffney, Mark Hedley, Peter Isaacs, Mark Johnson, Bhautik Joshi, Chris Lewis, Geoff Poulton, Don Price, Mikhail Prokopenko, Torsten Reda, David Rees, Andrew Scott, Sarath Seneviratne, Philip Valencia, Peter Wang, Denis Whitnall, and John Winter

5d. PROJECT NUMBER

PO L-71346D

5e. TASK NUMBER

5f. WORK UNIT NUMBER

7. PERFORMING ORGANIZATION NAME(S) AND ADDRESS(ES)

NASA Langley Research Center
Hampton, VA 23681-2199

8. PERFORMING ORGANIZATION REPORT NUMBER

Report No. TIPP 1628

9. SPONSORING/MONITORING AGENCY NAME(S) AND ADDRESS(ES)

National Aeronautics and Space Administration
Washington, DC 20546-0001

10. SPONSOR/MONITOR'S ACRONYM(S)

NASA

11. SPONSOR/MONITOR'S REPORT NUMBER(S)

NASA/CR-2008-215307

12. DISTRIBUTION/AVAILABILITY STATEMENT

Unclassified - Unlimited
Subject Category 38
Availability: NASA CASI (301) 621-0390

13. SUPPLEMENTARY NOTES

Langley Technical Monitor: Edward R. Generazio

14. ABSTRACT

This report provides an outline of the essential features of a Structural Health Monitoring Concept Demonstrator (CD) that will be constructed during the next eight months. It is emphasized that the design cannot be considered to be complete, and that design work will continue in parallel with construction and testing. A major advantage of the modular design is that small modules of the system can be developed, tested and modified before a commitment is made to full system development.
The CD is expected to develop and evolve for a number of years after its initial construction. This first stage will, of necessity, be relatively simple and have limited capabilities. Later developments will improve all aspects of the functionality of the system, including sensing, processing, communications, intelligence and response. The report indicates the directions this later development will take.

15. SUBJECT TERMS

Concept demonstrator; NDE; NDI; NDT; Structural health monitoring; Vehicle health monitoring

16. SECURITY CLASSIFICATION OF:			17. LIMITATION OF ABSTRACT	18. NUMBER OF PAGES	19a. NAME OF RESPONSIBLE PERSON
a. REPORT	b. ABSTRACT	c. THIS PAGE			STI Help Desk (email: help@sti.nasa.gov)
					19b. TELEPHONE NUMBER *(Include area code)*
U	U	U	UU	114	(301) 621-0390